

NASA TECHNICAL NOTE



NASA TN D-6629

2.1

NASA TN D-6629

LOAN COPY: RETURN TO
AFWL (DOW) 100
KIRTLAND AFB,

0133150



TECH LIBRARY KAFB, NM

DEFINITION AND APPLICATION OF
LONGITUDINAL STABILITY DERIVATIVES
FOR ELASTIC AIRPLANES

by William B. Kemp, Jr.

Langley Research Center

Hampton, Va. 23365





0133150

1. Report No. NASA TN D-6629		2. Government Accession No.		3. Re... 0133150	
4. Title and Subtitle DEFINITION AND APPLICATION OF LONGITUDINAL STABILITY DERIVATIVES FOR ELASTIC AIRPLANES				5. Report Date March 1972	
				6. Performing Organization Code	
7. Author(s) William B. Kemp, Jr.				8. Performing Organization Report No. L-8050	
9. Performing Organization Name and Address NASA Langley Research Center Hampton, Va. 23365				10. Work Unit No. 136-13-01-02	
				11. Contract or Grant No.	
12. Sponsoring Agency Name and Address National Aeronautics and Space Administration Washington, D.C. 20546				13. Type of Report and Period Covered Technical Note	
				14. Sponsoring Agency Code	
15. Supplementary Notes					
16. Abstract A set of longitudinal stability derivatives for elastic airplanes is defined from fundamental principles allowing perturbations in forward speed. Application of these derivatives to longitudinal stability analysis by use of approximate expressions for static stability and control parameters as well as the dynamic equations of motion is illustrated. One commonly used alternative formulation for elastic airplanes is shown to yield significant inaccuracies because of inappropriate interpretation of inertial effects.					
17. Key Words (Suggested by Author(s)) Aeroelasticity Longitudinal stability and control			18. Distribution Statement Unclassified - Unlimited		
19. Security Classif. (of this report) Unclassified		20. Security Classif. (of this page) Unclassified		21. No. of Pages 119	22. Price* \$3.00



CONTENTS

	Page
SUMMARY	1
INTRODUCTION	1
SYMBOLS	3
DEVELOPMENT OF FORMULATION	8
Fundamental Assumptions	8
Formulation of Stability Derivatives	9
Formulation of Equations of Motion	21
Calculation of Stability Derivatives	29
Effect of Structural Fixity Point Location	34
ILLUSTRATIVE ANALYSIS	35
The Example Airplane	35
Aerodynamic Derivatives	37
The Characteristic Stability Roots	37
Static-Stability Considerations	40
Effect of Dynamic-Pressure Derivatives	46
Alternative Formulations for Normal-Acceleration Contribution	46
CONCLUDING REMARKS	49
APPENDIX – A FORTRAN PROGRAM FOR CALCULATING LONGITUDINAL STABILITY DERIVATIVES OF ELASTIC OR RIGID AIRPLANES	51
Input Data	51
Output Data	54
Sample Cases	55
Program Listing	65
REFERENCES	76
FIGURES	77

DEFINITION AND APPLICATION OF LONGITUDINAL STABILITY DERIVATIVES FOR ELASTIC AIRPLANES

By William B. Kemp, Jr.
Langley Research Center

SUMMARY

A review of past practices in the analysis of longitudinal stability of elastic airplanes has revealed some inconsistencies arising from an inappropriate constraint on airplane speed. These inconsistencies lead to ambiguous definitions of stability derivatives and inaccurate prediction of some stability characteristics and, possibly, even performance characteristics.

A single, consistent set of longitudinal stability derivatives for elastic airplanes is defined in this paper. Unlike past practice, the aeroelastic contributions of dynamic-pressure perturbations are included, and the aeroelastic contributions of normal acceleration appear primarily in the derivatives with respect to pitching velocity and angle-of-attack rate.

Approximate expressions for static stability and control parameters in terms of these derivatives are shown to correlate well with results of more complete dynamic solutions. Some results of an illustrative analysis cast doubt on the general existence of a neutral point or maneuver point and indicate the possibility of a strongly divergent phugoid oscillation at relatively high frequency, particularly when the variation of atmospheric properties with altitude are considered. One commonly used alternative formulation of the stability derivatives is shown to yield significantly inaccurate predictions of not only the speed stability and phugoid characteristics, but also the short-period frequency and damping.

INTRODUCTION

The overall flight performance of many aircraft designs of current interest is strongly influenced by the effects of elastic deformation of the aircraft structure under the action of the flight loads. These aeroelastic effects are particularly important for aircraft having large size, low structural design load factor, low structural weight fraction, and high operating dynamic pressure. Aeroelastic effects are manifested not only in the area of structural dynamics (flutter, landing loads, etc.) but also in the quasi-steady areas of stability and control and trimmed flight performance.

Two different approaches are widely used for analysis of quasi-steady aeroelastic effects: the modal technique and the influence-coefficient technique. As pointed out in reference 1, both techniques can utilize the same description of aerodynamic, elastic, and mass properties but differ in the form of the perturbation variables whose effects are superimposed to describe the structural deformation. In the modal technique, a relatively complete dynamic formulation involving the normal modes of free vibration is reduced to a quasi-steady formulation by assuming that the velocities and accelerations in these vibration modes are negligible. The influence-coefficient technique applies steady-state solutions for structural deformation to the relatively low frequency rigid-body motions. Both techniques are developed in some depth in reference 2, which points out that from either technique, the quasi-steady (termed "equivalent elastic" in ref. 2) formulation embodies the implicit assumption that the structural deformation is in phase with the applied loads and therefore the dynamic analysis requires no more degrees of freedom than are needed for analysis of a rigid airplane. The quasi-steady effects of aeroelasticity are then represented completely by changes in the aerodynamic stability derivatives and by new derivatives which are either nonexistent or negligible for a rigid airplane.

A review of the procedures outlined in references 1, 2, and 3 for calculating the longitudinal stability and control characteristics of elastic airplanes reveals some disturbing inconsistencies. For example, in reference 1 the forward-speed degree of freedom is omitted from the basic dynamic formulation, yet a static stability parameter for 1g level flight is developed. This omission of the speed degree of freedom is believed to be typical of many applications of the modal technique. In reference 2, aerodynamic derivatives with respect to dynamic pressure are included in the expression for longitudinal static speed stability but are omitted in the dynamic stability analysis. Moreover, all the derivatives recommended for use in the dynamic analysis are derived under a constraint which is valid only at constant dynamic pressure. Reference 3 makes use of the same constraint but suggests the use of two neutral-point locations, one applicable to constant-speed maneuvers and the other applicable to constant-load-factor maneuvers. These inconsistencies can lead to errors not only in the predicted stability and control characteristics, but also in the predicted trimmed drag coefficient through use of inappropriate aerodynamic derivatives related to lift-curve slope and static stability.

When it is considered that meaningful indices of static stability during perturbations in either speed or load factor can be obtained from control response transfer functions resulting from a single solution of the dynamic longitudinal equations of motion, it is apparent that a single set of aerodynamic stability derivatives must exist for a given flight condition. These stability derivatives are then applicable, within the limitations of linear dynamic analysis and the quasi-steady aeroelastic assumptions, to the prediction of all the pertinent static and dynamic stability and control characteristics as well as aerodynamic

performance characteristics. In this paper, an attempt to define such a set of derivatives is described and the significance of certain of the derivatives to the longitudinal stability and control problem is examined by means of illustrative calculations.

SYMBOLS

a	aerodynamic operator
[A]	aerodynamic influence-coefficient matrix
a	velocity of sound, meters/second
[B]	aeroelastic correction matrix
[B $_{\dot{q}}$]	matrix used in calculating dynamic-pressure contributions to stability derivatives
[B $_{MA_m}$]	matrix used in calculating Mach number contributions to stability derivatives
b	reference span, meters
C_A	axial-force coefficient, $-\frac{F_{X,A}}{\bar{q}S}$
C_D	drag coefficient, $\frac{\text{Drag}}{\bar{q}S}$
C_L	lift coefficient, $\frac{\text{Lift}}{\bar{q}S}$
C_m	pitching-moment coefficient, $\frac{M_{Y,A}}{\bar{q}Sc}$
C_N	normal-force coefficient, $-\frac{F_{Z,A}}{\bar{q}S}$
C_X	local X-force coefficient, $\frac{F_{X,A}}{\bar{q}S_l}$
C_Z	local Z-force coefficient, $\frac{F_{Z,A}}{\bar{q}S_l}$
c	reference chord, meters
F	force, newtons

F_X, F_Y, F_Z	force components along reference axes, newtons
g	gravity acceleration, meters/second ²
g_0	gravity acceleration at sea level, meters/second ²
H	angular momentum, kilogram-meters ² /second
h	altitude, meters
\bar{I}	inertia dyadic
I_X, I_Y, I_Z	moments of inertia about reference axes, kilogram-meters ²
I_{XZ}	product of inertia about X- and Z-axes, kilogram-meters ²
$\bar{i}, \bar{j}, \bar{k}$	unit vectors along reference axes
M	Mach number; or $\frac{M_{Y,A} + M_{Y,T}}{I_Y}$, 1/second ²
M_X, M_Y, M_Z	moment components about reference axes, newton-meters
m	mass, kilograms; or any motion variable
n	component of combined kinetic and gravity acceleration in negative Z-direction, normalized by g_0
p, q, r	angular velocities about reference axes, radians/second
p	any physical variable
\bar{q}	dynamic pressure, $\frac{\rho V^2}{2}$, newtons/meter ²
R	Reynolds number, $\frac{\rho V c}{\mu}$
S	reference wing area, meters ²
S_l	local panel area, meters ²

\mathcal{L}	structural operator
[S]	structural slope influence-coefficient matrix
s	Laplace variable
T	displacement of propulsive thrust control
t	time, seconds
u,v,w	velocity components along reference axes, meters/second
\hat{u}	normalized velocity perturbation, $\frac{V - V_1}{V_1}$
V	velocity, meters/second
W	airplane weight, newtons
X,Y,Z	orthogonal reference axes
$X = \frac{F_{X,A} + F_{X,T}}{mV_1}$	1/second
x,y,z	coordinates relative to reference axes, meters
$\frac{x}{c}$	distance behind leading edge of reference chord, fraction of reference chord
$Z = \frac{F_{Z,A} + F_{Z,T}}{mV_1}$	1/second
α	angle of attack, radians
β	angle of sideslip, radians
δ	angular displacement of aerodynamic control surface, radians
ϵ	local slope of mean camber surface, $-\frac{dz}{dx}$
ϵ_δ	weighted value of mean-camber-surface slope used to represent unit δ
ζ_p	damping ratio of phugoid mode

ζ_{sp}	damping ratio of short-period mode
θ, ϕ, ψ	Euler attitude angles in pitch, roll, and yaw, respectively, taken in order of ψ, θ, ϕ from earth reference to airplane reference, radians
μ	air viscosity, newton-seconds/meter ²
ρ	air density, kilograms/meter ³
σ	induced downwash angle used as boundary condition, radians
ω	angular velocity, radians/second; or circular frequency, radians/second
ω_p	undamped natural frequency of phugoid mode, radians/second
ω_{sp}	undamped natural frequency of short-period mode, radians/second

Subscripts:

A	from aerodynamic sources
a	value at aerodynamic control point
c.g.	value at center of gravity
des	value at airplane design condition
F	increment due to flexibility
f	value at force application point
I	from inertial sources
i,j,k	index indicating a member of a set
jig	value corresponding to jig shape
l	local value

p	perturbation from reference flight condition
S	steady state
s	referred to stability axes
T	from propulsive sources
U	unsteady
1	value at reference flight condition

Mathematical notation:

($\dot{\quad}$)	derivative with respect to time
($\ddot{\quad}$)	second derivative with respect to time
($\vec{\quad}$)	vector quantity
{ }	column matrix
{ } ^T	row matrix
[]	matrix
[\nearrow] [\searrow]	diagonal matrix

Stability derivative notation:

Any of the following variables:

$$\delta, \alpha, \dot{\alpha}, \theta, q, \dot{q}, \hat{u}, \dot{\hat{u}}, T, h$$

when used as a subscript on any of the following quantities:

$$X, Z, M, C_A, C_N, C_m$$

denotes the stability derivative of the indicated quantity with respect to the indicated variable.

DEVELOPMENT OF FORMULATION

Fundamental Assumptions

As indicated in the introduction, it is desired to define a self-consistent set of aerodynamic stability derivatives applicable to the calculation of the longitudinal static and dynamic stability and control and trimmed flight characteristics of an elastic airplane. These derivatives will be defined in the context of their role as constant coefficients in the dynamic equations of airplane motion. Since the aerodynamic processes involved are not necessarily linear with the motion variables, the concept of local linearization will be used so that the aerodynamic derivatives can be considered constant for small motion perturbations from a reference flight condition. The linearized small-perturbation equations of motion then constitute an appropriate form for use of the derivatives.

The basic assumption of quasi-steady aeroelasticity will be made, namely, the structural deflection is assumed to be in phase with the applied loads. This assumption is equivalent to ignoring the velocities and accelerations in the elastic degrees of freedom. One result of this assumption, stated in reference 2, is that the set of equations of motion is reduced to include only those governing motion of the airplane center of gravity (abbreviated c.g.). The quasi-steady aeroelastic effects are then embodied completely in the aerodynamic characteristics, and the equations of motion are otherwise identical to those for a rigid airplane. The related assumption that the aerodynamic load change arising from structural deformation is in phase with the structural deflection is also made. In other words, the unsteady aerodynamic effects related to structural deformation are neglected. However, this does not preclude the existence of aerodynamic derivatives with respect to the rate of change of angle of attack.

Although use of the quasi-steady assumptions clearly introduces no error in the prediction of steady-state flight characteristics, some inaccuracy can occur in the characteristic stability (rigid body) modes because dynamic coupling between these modes and the elastic modes of structural vibration is neglected. This coupling can become increasingly significant as the frequency of any structural mode approaches that of any rigid-body mode. In spite of the possible inaccuracy, the quasi-steady assumptions are frequently made, particularly in preliminary aircraft design studies, because of the simplified dynamic formulation that results from their use.

To describe the elastic properties of the airplane structure, a structural reference plane is assumed to exist and to be oriented in such a way that the in-plane flexibility is negligible relative to that normal to the reference plane. Furthermore, the longitudinal aerodynamic characteristics are assumed to be unaffected by elastic distortion of either vertical fins or fuselage cross sections. All remaining structural deflections are constrained to the direction normal to a single plane chosen to lie as nearly as possible

parallel to the mean camber surfaces of the wing, body, and horizontal tail. It is appropriate, then, to choose an orthogonal system of reference coordinate axes, as shown in figure 1, so that the Z-axis is parallel to the direction of allowed structural deflections and the X-axis lies in the plane of symmetry. For small perturbations from the deflections existing in a reference flight condition, the center-of-gravity location, the pitching moment of inertia, and the aerodynamic and structural influence coefficients can be considered to be constant. In practice, these quantities, determined for a given reference condition, are frequently used over a set of flight conditions to be analyzed.

Formulation of Stability Derivatives

In airplane longitudinal stability analysis, one is concerned with the motion of the airplane as a whole in three degrees of freedom, including two components of translational freedom and one of pitch rotation. An additional degree of freedom exists for each independent control system. In the present development, two such control systems will be assumed, one aerodynamic and one propulsive, having control displacements denoted by δ and T , respectively. The conditions for dynamic equilibrium in the three airplane degrees of freedom are

$$F_{X,A} + F_{X,T} + F_{X,I} = 0 \quad (1a)$$

$$F_{Z,A} + F_{Z,T} + F_{Z,I} = 0 \quad (1b)$$

$$M_{Y,A} + M_{Y,T} + M_{Y,I} = 0 \quad (1c)$$

where the nine force and moment components may vary with time. Conditions for dynamic equilibrium in the two control degrees of freedom are assumed to exist and be satisfied although they will not be specified.

Equations of motion are formed from the equilibrium equations when the forces and moments are expressed as functions of a set of motion variables. The fundamental set of motion variables consists of the displacement and its successive time derivatives in each degree of freedom. Alternative sets of motion variables can be derived from the fundamental set by transformation. The total number of motion variables is somewhat arbitrary and depends on the maximum and minimum order of differentiation of each displacement needed to express the forces and moments with sufficient accuracy for the problem at hand. Second derivatives of the airplane displacements are needed to define the inertial contributions and are believed to be of sufficiently high order to describe the aerodynamic and propulsive contributions at frequencies compatible with the quasi-steady assumption made in the present problem. At the low-order end, one or more of the displacements themselves may be omitted from the set of motion variables. Under the frequently made

assumption of a uniform atmosphere, the forces and moments do not depend on the location of the airplane, and even if atmospheric variations with altitude are considered, the horizontal displacement is of no significance.

Alternative sets of motion variables can be derived by transformation from the fundamental set. Common practice in the analysis of longitudinal aircraft motions has resulted in the use of variables such as (V, α, θ) as the set of lowest order motion variables in the three airplane degrees of freedom. These variables must be supplemented by the control displacements δ and T for the five-degree-of-freedom problem at hand. These five variables and their time derivatives constitute an appropriate set of motion variables only if a locally uniform atmosphere is assumed. If the variation of atmospheric properties with altitude is to participate in the dynamic problem, a more appropriate set will be $(V, h, \alpha, \theta, \delta, T)$, but because these variables are not mutually independent, the equations of motion must include a kinematic equation relating \dot{h} to V , α , and θ . This scheme is retained in the present development.

Common practice in dynamic stability analysis has led to the use of stability derivatives expressed in either coefficient form or a dimensional form having units of negative powers of time. The coefficient form is usually applied only to aerodynamic forces and moments, whereas the dimensional form includes both aerodynamic and thrust contributions. To define these derivatives, equations (1) may be restated as

$$X = \frac{1}{mV_1} (F_{X,A} + F_{X,T}) = -\frac{F_{X,I}}{mV_1} \quad (2a)$$

$$Z = \frac{1}{mV_1} (F_{Z,A} + F_{Z,T}) = -\frac{F_{Z,I}}{mV_1} \quad (2b)$$

$$M = \frac{1}{I_Y} (M_{Y,A} + M_{Y,T}) = -\frac{M_{Y,I}}{I_Y} \quad (2c)$$

Expressing X , Z , and M as functions of the motion variables and applying the principle of linear superposition of small perturbations give

$$X(m_1 \dots m_j \dots m_J) = X(m_{1,1} \dots m_{j,1} \dots m_{J,1}) + \sum_{j=1}^J m_{p,j} \left(\frac{\partial X}{\partial m_j} \right)_1 \quad (3a)$$

$$Z(m_1 \dots m_j \dots m_J) = Z(m_{1,1} \dots m_{j,1} \dots m_{J,1}) + \sum_{j=1}^J m_{p,j} \left(\frac{\partial Z}{\partial m_j} \right)_1 \quad (3b)$$

$$M(m_1 \dots m_j \dots m_J) = M(m_{1,1} \dots m_{j,1} \dots m_{J,1}) + \sum_{j=1}^J m_{p,j} \left(\frac{\partial M}{\partial m_j} \right)_1 \quad (3c)$$

where $m_{j,1}$ is the value of the j th motion variable in the reference flight condition and $m_{p,j}$ is the perturbation of the j th motion variable from its reference value. The partial derivatives appearing in equations (3) are defined as the complete set of stability derivatives in dimensional form. The stability derivatives in coefficient form are similarly defined as the partial derivatives of the coefficients C_A , C_N , and C_m with respect to motion perturbations where

$$C_A = -\frac{F_{X,A}}{\bar{q}S} \quad (4a)$$

$$C_N = -\frac{F_{Z,A}}{\bar{q}S} \quad (4b)$$

$$C_m = \frac{M_{Y,A}}{\bar{q}Sc} \quad (4c)$$

In determining the values of the stability derivatives by theoretical, experimental, or combined means, the set of motion variables is not necessarily the most appropriate set for isolating and understanding all the contributions to the stability derivatives. A more appropriate set might be those variables describing the physical processes involved in the production of aerodynamic and propulsive loads. In general, any change in the shape of an airplane surface will produce a change in the aerodynamic load distribution. Therefore, any process capable of deforming the structure of an elastic airplane will contribute to one or more stability derivatives. Conversely, for an elastic airplane, a change in aerodynamic or thrust loading will, in general, change the structural deformation. Consequently, all stability derivatives reflect contributions from one or more processes capable of deforming the structure. Therefore, a set of physical variables capable of defining the structural deformation is a suitable set for determining the stability derivatives of an elastic airplane.

If it is assumed that such a set of physical variables p_k exists and that it can be functionally related to the set of motion variables, then a stability derivative, $\partial X / \partial m_j$ for example, can be expressed as

$$\left(\frac{\partial X}{\partial m_j} \right)_1 = \sum_{k=1}^K \left(\frac{\partial X}{\partial p_k} \right)_1 \left(\frac{\partial p_k}{\partial m_j} \right)_1 \quad (5)$$

The number of physical variables K need not equal the number of motion variables J and the physical variables need not be mutually independent under the constraints of the airplane dynamic problem.

Under the concept described, the distribution of structural deflection can be considered as the linear superposition of a number of deflection distributions, each identified

with a particular physical variable. For small perturbations from a given reference flight condition, the shape of each distribution is invariant and its amplitude is proportional to the perturbation of its physical variable.

An appropriate set of physical variables may now be determined. Consider an airplane configuration represented by a nearly planar mean camber surface divided into a large number of elemental panels. In symmetric flight, the configuration shape is defined for aerodynamic purposes by the paneling geometry and the set of chordwise slopes $\{\epsilon\} = \{-dz/dx\}$ at all panels. The configuration is flying in an aerodynamic environment defined globally by Mach number, Reynolds number, and dynamic pressure, and locally by the set of local angles of attack $\{\alpha_l\}$ and angle-of-attack rates $\{\dot{\alpha}_l\}$ acting on each panel and arising from aircraft motion and induced effects of the propulsion system. The sets of X- and Z-components of the aerodynamic force coefficients acting on the panels can be expressed by

$$\{C_{X,A}\} = A_{X,S} \{\alpha_l + \epsilon\} + A_{X,U} \{\dot{\alpha}_l\} \quad (6a)$$

$$\{C_{Z,A}\} = A_{Z,S} \{\alpha_l + \epsilon\} + A_{Z,U} \{\dot{\alpha}_l\} \quad (6b)$$

where A represents an aerodynamic operator dependent on paneling geometry, Mach number, and Reynolds number. The subscripts S and U refer, respectively, to steady-state and first-order unsteady aerodynamic processes. The corresponding sets of force components are

$$\{F_{X,A}\} = \bar{q} \{C_{X,A} S_l\} \quad (7a)$$

$$\{F_{Z,A}\} = \bar{q} \{C_{Z,A} S_l\} \quad (7b)$$

The distributions of local angle of attack, angle-of-attack rate, and surface slope are represented by the superposition of specifically identifiable contributions as follows:

$$\{\alpha_l\} = \alpha \{1\} - \frac{q}{V} \{x_a\} + \{\alpha_l, T\} \quad (8a)$$

$$\{\dot{\alpha}_l\} = \dot{\alpha} \{1\} - \frac{\dot{q}}{V} \{x_a\} \quad (8b)$$

$$\{\epsilon\} = \{\epsilon_{jig}\} + \delta \{\epsilon_\delta\} + \{\epsilon_F\} \quad (9)$$

The contributions to α_l and $\dot{\alpha}_l$ arise from the time-dependent airplane angle of attack and pitch rate and the thrust-induced flow perturbations. The set $\{x_a\}$ consists of the

x-coordinates of points (one per panel) at which the aerodynamic boundary condition of no flow through the surface is satisfied. The contributions to local surface slope, defined at the same points as x_a , arise from the jig shape (mean camber surface of the completely unloaded structure), control-surface deflection, and structural flexibility.

The flexible contribution to surface slopes can be expressed as the influence of a structural operator \mathcal{S} operating on the Z-component of the forces acting on each panel arising from aerodynamic, inertial, and propulsive sources as follows:

$$\{\epsilon_F\} = \mathcal{S}\{F_{Z,A} + F_{Z,I} + F_{Z,T}\} \quad (10)$$

The aerodynamic-force set $\{F_{Z,A}\}$ has been defined by equation (7b). The inertial-force set $\{F_{Z,I}\}$ results from the action on the mass distribution of the set of Z-components of linear acceleration arising from gravity and airplane motion. By using a lumped parameter concept, let m_i be the mass assigned to the i th panel, assumed to be located at the point $(x_{f,i}, y_{f,i}, 0)$. The effect of this mass can be replaced by the inertial-force vector

$$\vec{F}_{I,i} = m_i \left(\vec{g} - \frac{d\vec{V}_i}{dt} \right)$$

where V_i is the velocity of m_i in inertial space. Under the quasi-steady assumption, the velocity and acceleration of m_i relative to the airplane as a whole are neglected, and the Z-component of inertial force can be written (ref. 4) as

$$F_{Z,I,i} = m_i \left[g \cos \theta \cos \phi - \dot{w} - pv + qu + x_{f,i}(\dot{q} - pr) - y_{f,i}(\dot{p} + qr) \right]$$

In the following section, equations of motion applicable to analysis of longitudinal motions in a banked turn are developed. For this case, the bank angle ϕ and the rolling and yawing velocities p and r are nonzero but are considered to be constants. In equation (30) the first four terms in the above equation are related to n , the normal acceleration sensed at the airplane center of gravity. The last term gives rise to an antisymmetric distribution of inertial force whose effect on the longitudinal stability derivatives should be negligible and will be neglected. With these considerations, the inertial-force set can be written as

$$\{F_{Z,I}\} = ng_0 [m] \{1\} + (\dot{q} - pr) [m] \{x_f\} \quad (11)$$

where $[m]$ is the diagonal matrix of masses assigned to the individual panels and $\{x_f\}$ is the set of x-coordinates of points at which loads are applied to the panels and is not necessarily identical with $\{x_a\}$. The relationship of x_a and x_f to panel geometry is,

of course, involved in the processes represented by both the aerodynamic and the structural operators, \mathcal{A} and \mathcal{S} .

The propulsive-force set $\{F_{Z,T}\}$ is the set of Z-components of panel forces statically equivalent to the direct thrust reactions at the engine mounts.

The quantities X, Z, and M and the coefficients C_A , C_N , and C_m can be obtained by summation over the set of panels lying on one side of the plane of symmetry. Thus,

$$X = \frac{2}{mV_1} \{1\}^T \{F_{X,A} + F_{X,T}\} \quad (12a)$$

$$Z = \frac{2}{mV_1} \{1\}^T \{F_{Z,A} + F_{Z,T}\} \quad (12b)$$

$$M = -\frac{2}{I_y} \{x_f\}^T \{F_{Z,A} + F_{Z,T}\} \quad (12c)$$

$$C_A = -\frac{2}{S} \{S_l\}^T \{C_{X,A}\} \quad (13a)$$

$$C_N = -\frac{2}{S} \{S_l\}^T \{C_{Z,A}\} \quad (13b)$$

$$C_m = -\frac{2}{S c} \{S_l x_f\}^T \{C_{Z,A}\} \quad (13c)$$

It is now possible to identify the set of physical variables with which structural deflection modes can be associated and aerodynamic and thrust loads can be determined. Table I lists these variables and the symbols used for each value in a steady reference

TABLE I. - THE PHYSICAL VARIABLES

Physical variable	Value in reference condition	Perturbation from reference condition	Equation
Control deflection	δ_1	δ_p	(9)
Angle of attack	α_1	α_p	(8a)
Angle-of-attack rate	0	$\dot{\alpha}$	(8b)
Pitch rate	q_1	q_p	(8a)
Pitch acceleration	0	\dot{q}	(8b), (11)
Normal acceleration	n_1	n_p	(11)
Mach number	M_1	M_p	(6a), (6b)
Reynolds number	R_1	R_p	(6a), (6b)
Dynamic pressure	\bar{q}_1	\bar{q}_p	(7a), (7b)
Thrust command	T_1	T_p	(8a), (10)

flight condition and for the perturbation of each from the reference condition. The equations through which their effects enter the aeroelastic problem are also identified.

In the foregoing discussion, the propulsive process was not described in detail. To define the form of stability derivatives, the assumption is made that the propulsion system outputs, $\{F_X, T\}$, $\{F_Z, T\}$, and $\{\alpha_L, T\}$ can be described in terms of the physical variables listed in table I.

In concept, the partial derivatives of X , Z , and M or of C_A , C_N , and C_m with respect to each physical perturbation variable can be obtained through application of equations (6) to (13). The desired stability derivatives are then defined by relations such as equation (5) once the partial derivatives $\partial p_k / \partial m_j$ have been determined. Because a mutually dependent set of motion variables has been adopted, the partial derivatives will be evaluated from expressions for each physical variable in terms of a mutually independent set of motion variables obtained by omitting either h or α from the set $(V, h, \alpha, \theta, \delta, T)$. Thus, the physical variables δ , α , $\dot{\alpha}$, and T appear without change in the set of motion variables. The variables q and \dot{q} will also appear unchanged in the motion variables, replacing $\dot{\theta}$ and $\ddot{\theta}$ since, for longitudinal motions, $\dot{\theta}$ is a linear function of q , as shown in the following section. The normal acceleration n is expressed as a function of V , α , and θ and their time derivatives in equation (34) of the following section. The remaining physical variables are expressed as functions of V and h as follows:

$$M = \frac{V}{a(h)} \quad (14)$$

$$R = \frac{\rho(h)Vc}{\mu(h)} \quad (15)$$

$$\bar{q} = \frac{\rho(h)V^2}{2} \quad (16)$$

In applying the principle of small perturbations, it is convenient to define a non-dimensional perturbation in velocity magnitude as

$$\hat{u} = \frac{V - V_1}{V_1} \quad (17)$$

where the perturbation velocity component $\hat{u}V_1$ is directed along the unperturbed velocity vector and is orthogonal to the component $\alpha_p V_1$, as shown in figure 1.

After expressing each motion variable as the sum of a reference value and a perturbation value, the partial derivatives $(\partial p_k / \partial m_j)_1$ can be derived and are given in table II.

TABLE II. - THE PARTIAL DERIVATIVES $\left(\frac{\partial p_k}{\partial m_j}\right)_1$

m_j	p_k									
	M	R	\bar{q}	α	$\dot{\alpha}$	q	\dot{q}	n	δ	T
\hat{u}	M_1	R_1	$2\bar{q}_1$	0	0	0	0	$\frac{V_1}{g_0} q_1 \cos \alpha_1$	0	0
$\dot{\hat{u}}$	0	0	0	0	0	0	0	$-\frac{V_1}{g_0} \sin \alpha_1$	0	0
α	0	0	0	1	0	0	0	$-\frac{V_1}{g_0} q_1 \sin \alpha_1$	0	0
$\dot{\alpha}$	0	0	0	0	1	0	0	$-\frac{V_1}{g_0} \cos \alpha_1$	0	0
θ	0	0	0	0	0	0	0	$-\frac{g}{g_0} \sin \theta_1 \cos \phi$	0	0
q	0	0	0	0	0	1	0	$\frac{V_1}{g_0} \cos \alpha_1$	0	0
\dot{q}	0	0	0	0	0	0	1	0	0	0
h	$-\frac{M_1}{a_1} \left(\frac{\partial a}{\partial h}\right)_1$	$\frac{R_1}{\rho_1} \left(\frac{\partial \rho}{\partial h}\right)_1 - \frac{R_1}{\mu_1} \left(\frac{\partial \mu}{\partial h}\right)_1$	$\bar{q}_1 \left(\frac{\partial \rho}{\partial h}\right)_1$	0	0	0	0	0	0	0
δ	0	0	0	0	0	0	0	0	1	0
T	0	0	0	0	0	0	0	0	0	1

The desired stability derivatives can now be defined by using equation (5) and table II. In dimensional form,

$$X_\delta = \left(\frac{\partial X}{\partial \delta}\right)_1 \quad (18a)$$

$$X_\alpha = \left(\frac{\partial X}{\partial \alpha}\right)_1 - \frac{V_1}{g_0} q_1 \sin \alpha_1 \left(\frac{\partial X}{\partial n}\right)_1 \quad (18b)$$

$$X_{\dot{\alpha}} = \left(\frac{\partial X}{\partial \dot{\alpha}}\right)_1 - \frac{V_1}{g_0} \cos \alpha_1 \left(\frac{\partial X}{\partial n}\right)_1 \quad (18c)$$

$$X_\theta = -\frac{g}{g_0} \sin \theta_1 \cos \phi \left(\frac{\partial X}{\partial n}\right)_1 \quad (18d)$$

$$\mathbf{X}_{\dot{q}} = \left(\frac{\partial \mathbf{X}}{\partial \dot{q}} \right)_1 + \frac{V_1}{g_0} \cos \alpha_1 \left(\frac{\partial \mathbf{X}}{\partial n} \right)_1 \quad (18e)$$

$$\mathbf{X}_{\dot{q}} = \left(\frac{\partial \mathbf{X}}{\partial \dot{q}} \right)_1 \quad (18f)$$

$$\mathbf{X}_{\hat{u}} = \frac{V_1}{g_0} q_1 \cos \alpha_1 \left(\frac{\partial \mathbf{X}}{\partial n} \right)_1 + M_1 \left(\frac{\partial \mathbf{X}}{\partial M} \right)_1 + R_1 \left(\frac{\partial \mathbf{X}}{\partial R} \right)_1 + 2\bar{q} \left(\frac{\partial \mathbf{X}}{\partial \bar{q}} \right)_1 \quad (18g)$$

$$\mathbf{X}_{\hat{u}} = -\frac{V_1}{g_0} \sin \alpha_1 \left(\frac{\partial \mathbf{X}}{\partial n} \right)_1 \quad (18h)$$

$$\mathbf{X}_T = \left(\frac{\partial \mathbf{X}}{\partial T} \right)_1 \quad (18i)$$

$$\mathbf{X}_h = -\frac{M_1}{a_1} \left(\frac{\partial a}{\partial h} \right)_1 \left(\frac{\partial \mathbf{X}}{\partial M} \right)_1 + \left[\frac{R_1}{\rho_1} \left(\frac{\partial \rho}{\partial h} \right)_1 - \frac{R_1}{\mu_1} \left(\frac{\partial \mu}{\partial h} \right)_1 \right] \left(\frac{\partial \mathbf{X}}{\partial R} \right)_1 + \frac{\bar{q}_1}{\rho_1} \left(\frac{\partial \rho}{\partial h} \right)_1 \left(\frac{\partial \mathbf{X}}{\partial \bar{q}} \right)_1 \quad (18j)$$

where the subscript 1 denotes a quantity evaluated at the reference flight condition or, more specifically, at the reference condition values of the physical variables as noted in table I. The Z and M stability derivatives are defined by the expressions obtained by replacing X in equations (18) by Z or M. The defining expressions for the coefficient stability derivatives are equivalent to those for the dimensional derivatives but may include constant factors as appropriate to render each motion variable dimensionless; thus

$$\left. \begin{aligned} C_{A\dot{\alpha}} &= \frac{2V_1}{c} \left(\frac{\partial C_A}{\partial \dot{\alpha}} \right)_1 - \frac{2V_1^2}{g_0 c} \cos \alpha_1 \left(\frac{\partial C_A}{\partial n} \right)_1 \\ C_{Aq} &= \frac{2V_1}{c} \left(\frac{\partial C_A}{\partial \dot{q}} \right)_1 + \frac{2V_1^2}{g_0 c} \cos \alpha_1 \left(\frac{\partial C_A}{\partial n} \right)_1 \end{aligned} \right\} \quad (19)$$

The motion variables δ , α , θ , \hat{u} , and possibly T are already dimensionless. The stability derivatives of C_A , C_N , and C_m with respect to \dot{q} , \hat{u} , and h are considered herein to retain units reciprocal to those of the respective motion variables.

In evaluating the stability derivatives from wind-tunnel experiments and/or theory, it is anticipated that the coefficient form will be evaluated first and then converted to the dimensional form for use in stability analysis. Expressions for the dimensional deriva-

tives in terms of the coefficient derivatives are needed therefore. Combining equations (2) and (4) gives

$$\mathbf{X} = -\frac{\bar{q}SC_A}{mV_1} + \frac{F_{X,T}}{mV_1} \quad (20a)$$

$$\mathbf{Z} = -\frac{\bar{q}SC_N}{mV_1} + \frac{F_{Z,T}}{mV_1} \quad (20b)$$

$$\mathbf{M} = \frac{\bar{q}ScC_m}{I_Y} + \frac{M_{Y,T}}{I_Y} \quad (20c)$$

The partial derivatives with respect to the physical variables are

$$\frac{\partial \mathbf{X}}{\partial p_k} = -\frac{SC_A}{mV_1} \frac{\partial \bar{q}}{\partial p_k} - \frac{\bar{q}S}{mV_1} \frac{\partial C_A}{\partial p_k} + \frac{1}{mV_1} \frac{\partial F_{X,T}}{\partial p_k} \quad (21a)$$

$$\frac{\partial \mathbf{Z}}{\partial p_k} = -\frac{SC_N}{mV_1} \frac{\partial \bar{q}}{\partial p_k} - \frac{\bar{q}S}{mV_1} \frac{\partial C_N}{\partial p_k} + \frac{1}{mV_1} \frac{\partial F_{Z,T}}{\partial p_k} \quad (21b)$$

$$\frac{\partial \mathbf{M}}{\partial p_k} = \frac{ScC_m}{I_Y} \frac{\partial \bar{q}}{\partial p_k} + \frac{\bar{q}Sc}{I_Y} \frac{\partial C_m}{\partial p_k} + \frac{1}{I_Y} \frac{\partial M_{Y,T}}{\partial p_k} \quad (21c)$$

Note that

$$\frac{\partial \bar{q}}{\partial p_k} = \begin{cases} 1 & \text{for } p_k = \bar{q} \\ 0 & \text{for } p_k \neq \bar{q} \end{cases}$$

Substituting equation (21a) into each of equations (18) in sequence results in

$$\mathbf{X}_\delta = -\frac{\bar{q}_1 S}{mV_1} \left(\frac{\partial C_A}{\partial \delta} \right)_1 + \frac{1}{mV_1} \left(\frac{\partial F_{X,T}}{\partial \delta} \right)_1 \quad (22a)$$

$$\mathbf{X}_\alpha = -\frac{\bar{q}_1 S}{mV_1} \left[\left(\frac{\partial C_A}{\partial \alpha} \right)_1 - \frac{V_1}{g_0} q_1 \sin \alpha_1 \left(\frac{\partial C_A}{\partial n} \right)_1 \right] + \frac{1}{mV_1} \left[\left(\frac{\partial F_{X,T}}{\partial \alpha} \right)_1 - \frac{V_1}{g_0} q_1 \sin \alpha_1 \left(\frac{\partial F_{X,T}}{\partial n} \right)_1 \right] \quad (22b)$$

$$\mathbf{X}_{\dot{\alpha}} = -\frac{\bar{q}_1 Sc}{2mV_1^2} \left[\left(\frac{\partial C_A}{\partial \frac{\dot{\alpha}c}{2V}} \right)_1 - \frac{2V_1^2}{g_0 c} \cos \alpha_1 \left(\frac{\partial C_A}{\partial n} \right)_1 \right] + \frac{1}{mV_1} \left[\left(\frac{\partial F_{X,T}}{\partial \dot{\alpha}} \right)_1 - \frac{V_1}{g_0} \cos \alpha_1 \left(\frac{\partial F_{X,T}}{\partial n} \right)_1 \right] \quad (22c)$$

$$X_\theta = \frac{\bar{q}_1 S}{mV_1} \frac{g}{g_0} \sin \theta_1 \cos \phi \left(\frac{\partial C_A}{\partial n} \right)_1 - \frac{g \sin \theta_1 \cos \phi}{g_0 mV_1} \left(\frac{\partial F_{X,T}}{\partial n} \right)_1 \quad (22d)$$

$$X_q = -\frac{\bar{q}_1 S c}{2mV_1^2} \left[\left(\frac{\partial C_A}{\partial \frac{qc}{2V}} \right)_1 + \frac{2V_1^2}{g_0 c} \cos \alpha_1 \left(\frac{\partial C_A}{\partial n} \right)_1 \right] + \frac{1}{mV_1} \left[\left(\frac{\partial F_{X,T}}{\partial q} \right)_1 + \frac{V_1}{g_0} \cos \alpha_1 \left(\frac{\partial F_{X,T}}{\partial n} \right)_1 \right] \quad (22e)$$

$$X_{\dot{q}} = -\frac{\bar{q}_1 S}{mV_1} \left(\frac{\partial C_A}{\partial \dot{q}} \right)_1 + \frac{1}{mV_1} \left(\frac{\partial F_{X,T}}{\partial \dot{q}} \right)_1 \quad (22f)$$

$$X_{\hat{u}} = -\frac{\bar{q}_1 S}{mV_1} \left[\frac{V_1}{g_0} q_1 \cos \alpha_1 \left(\frac{\partial C_A}{\partial n} \right)_1 + M_1 \left(\frac{\partial C_A}{\partial M} \right)_1 + R_1 \left(\frac{\partial C_A}{\partial R} \right)_1 + 2\bar{q}_1 \left(\frac{\partial C_A}{\partial \bar{q}} \right)_1 + 2C_{A,1} \right] \\ + \frac{1}{mV_1} \left[\frac{V_1}{g_0} q_1 \cos \alpha_1 \left(\frac{\partial F_{X,T}}{\partial n} \right)_1 + M_1 \left(\frac{\partial F_{X,T}}{\partial M} \right)_1 + R_1 \left(\frac{\partial F_{X,T}}{\partial R} \right)_1 + 2\bar{q}_1 \left(\frac{\partial F_{X,T}}{\partial \bar{q}} \right)_1 \right] \quad (22g)$$

$$X_{\hat{u}}^* = \frac{\bar{q}_1 S}{mg_0} \sin \alpha_1 \left(\frac{\partial C_A}{\partial n} \right)_1 - \frac{1}{mg_0} \sin \alpha_1 \left(\frac{\partial F_{X,T}}{\partial n} \right)_1 \quad (22h)$$

$$X_T = -\frac{\bar{q}_1 S}{mV_1} \left(\frac{\partial C_A}{\partial T} \right)_1 + \frac{1}{mV_1} \left(\frac{\partial F_{X,T}}{\partial T} \right)_1 \quad (22i)$$

$$X_h = -\frac{\bar{q}_1 S}{mV_1} \left\{ -\frac{M_1}{a_1} \left(\frac{\partial a}{\partial h} \right)_1 \left(\frac{\partial C_A}{\partial M} \right)_1 + \left[\frac{R_1}{\rho_1} \left(\frac{\partial \rho}{\partial h} \right)_1 - \frac{R_1}{\mu_1} \left(\frac{\partial \mu}{\partial h} \right)_1 \right] \left(\frac{\partial C_A}{\partial R} \right)_1 + \frac{\bar{q}_1}{\rho_1} \left(\frac{\partial \rho}{\partial h} \right)_1 \left(\frac{\partial C_A}{\partial \bar{q}} \right)_1 \right. \\ \left. + \frac{1}{\rho_1} \left(\frac{\partial \rho}{\partial h} \right)_1 C_{A,1} \right\} + \frac{1}{mV_1} \left\{ -\frac{M_1}{a_1} \left(\frac{\partial a}{\partial h} \right)_1 \left(\frac{\partial F_{X,T}}{\partial M} \right)_1 + \left[\frac{R_1}{\rho_1} \left(\frac{\partial \rho}{\partial h} \right)_1 - \frac{R_1}{\mu_1} \left(\frac{\partial \mu}{\partial h} \right)_1 \right] \left(\frac{\partial F_{X,T}}{\partial R} \right)_1 \right. \\ \left. + \frac{\bar{q}_1}{\rho_1} \left(\frac{\partial \rho}{\partial h} \right)_1 \left(\frac{\partial F_{X,T}}{\partial \bar{q}} \right)_1 \right\} \quad (22j)$$

Equations (22) express the dimensional X derivatives in terms of the partial derivatives of C_A with respect to the physical variables. Equivalent expressions in terms of the complete coefficient form of the stability derivatives are

$$X_{\delta} = -\frac{\bar{q}_1 S}{mV_1} C_{A_{\delta}} + \frac{1}{mV_1} \left(\frac{\partial F_{X,T}}{\partial \delta} \right)_1 \quad (23a)$$

$$X_{\alpha} = -\frac{\bar{q}_1 S}{mV_1} C_{A_{\alpha}} + \frac{1}{mV_1} \left[\left(\frac{\partial F_{X,T}}{\partial \alpha} \right)_1 - \frac{V_1}{g_0} q_1 \sin \alpha_1 \left(\frac{\partial F_{X,T}}{\partial n} \right)_1 \right] \quad (23b)$$

$$X_{\dot{\alpha}} = -\frac{\bar{q}_1 S c}{2mV_1^2} C_{A_{\dot{\alpha}}} + \frac{1}{mV_1} \left[\left(\frac{\partial F_{X,T}}{\partial \dot{\alpha}} \right)_1 - \frac{V_1}{g_0} \cos \alpha_1 \left(\frac{\partial F_{X,T}}{\partial n} \right)_1 \right] \quad (23c)$$

$$X_{\theta} = -\frac{\bar{q}_1 S}{mV_1} C_{A_{\theta}} - \frac{g \sin \theta_1 \cos \phi}{g_0 mV_1} \left(\frac{\partial F_{X,T}}{\partial n} \right)_1 \quad (23d)$$

$$X_{q} = -\frac{\bar{q}_1 S c}{2mV_1^2} C_{A_q} + \frac{1}{mV_1} \left[\left(\frac{\partial F_{X,T}}{\partial q} \right)_1 + \frac{V_1}{g_0} \cos \alpha_1 \left(\frac{\partial F_{X,T}}{\partial n} \right)_1 \right] \quad (23e)$$

$$X_{\dot{q}} = -\frac{\bar{q}_1 S}{mV_1} C_{A_{\dot{q}}} + \frac{1}{mV_1} \left(\frac{\partial F_{X,T}}{\partial \dot{q}} \right)_1 \quad (23f)$$

$$X_{\hat{u}} = -\frac{\bar{q}_1 S}{mV_1} (C_{A_{\hat{u}}} + 2C_{A,1}) + \frac{1}{mV_1} \left[\frac{V_1}{g_0} q_1 \cos \alpha_1 \left(\frac{\partial F_{X,T}}{\partial n} \right)_1 + M_1 \left(\frac{\partial F_{X,T}}{\partial M} \right)_1 + R_1 \left(\frac{\partial F_{X,T}}{\partial R} \right)_1 + 2\bar{q}_1 \left(\frac{\partial F_{X,T}}{\partial \bar{q}} \right)_1 \right] \quad (23g)$$

$$X_{\hat{u}}^{\lambda} = -\frac{\bar{q}_1 S}{mV_1} C_{A_{\hat{u}}^{\lambda}} - \frac{1}{mg_0} \sin \alpha_1 \left(\frac{\partial F_{X,T}}{\partial n} \right)_1 \quad (23h)$$

$$X_T = -\frac{\bar{q}_1 S}{mV_1} C_{A_T} + \frac{1}{mV_1} \left(\frac{\partial F_{X,T}}{\partial T} \right)_1 \quad (23i)$$

$$X_h = -\frac{\bar{q}_1 S}{mV_1} \left[C_{A_h} + \frac{1}{\rho_1} \left(\frac{\partial \rho}{\partial h} \right)_1 C_{A,1} \right] + \frac{1}{mV_1} \left\{ -\frac{M_1}{a_1} \left(\frac{\partial a}{\partial h} \right)_1 \left(\frac{\partial F_{X,T}}{\partial M} \right)_1 + \left[\frac{R_1}{\rho_1} \left(\frac{\partial \rho}{\partial h} \right)_1 - \frac{R_1}{\mu_1} \left(\frac{\partial \mu}{\partial h} \right)_1 \right] \left(\frac{\partial F_{X,T}}{\partial R} \right)_1 + \frac{\bar{q}_1}{\rho_1} \left(\frac{\partial \rho}{\partial h} \right)_1 \left(\frac{\partial F_{X,T}}{\partial \bar{q}} \right)_1 \right\} \quad (23j)$$

The expressions for the Z stability derivatives can be written simply by replacing X with Z, C_A with C_N , and $F_{X,T}$ with $F_{Z,T}$ in equations (22) and (23). Similarly, expressions for the M stability derivatives are obtained by replacing X with M, C_A with $-cC_m$, $F_{X,T}$ with $M_{Y,T}$, and mV_1 with I_Y in equations (22) and (23).

The relationship of the stability derivatives developed herein to those discussed in references 2 and 3 is of interest. The derivatives with respect to physical variables as used in this paper are, in many cases, analogous to, and may be equal to, the derivatives termed "zero mass derivatives" in references 2 and 3. The stability derivatives of this paper (i.e., derivatives with respect to the motion variables) are analogous to those termed "equivalent elastic derivatives" in references 2 and 3. The values of the equivalent elastic derivatives as defined in references 2 and 3, however, will be different from those of the stability derivatives defined herein because the equivalent elastic derivatives were defined under the assumption of constant dynamic pressure. This assumption results not only in the omission of the dynamic-pressure contribution to the \hat{u} derivatives, but also in a completely different form for the normal-acceleration contribution to all derivatives. Note in particular that for an unaccelerated reference flight condition ($q_1 = 0$), equations (18) show that the derivatives with respect to angle of attack reflect no contributions from normal acceleration. In contrast, all the equivalent elastic derivatives of references 2 and 3 are influenced by normal-acceleration contributions termed "inertial relief."

Formulation of Equations of Motion

The equations of motion are formed by expressing the conditions for dynamic equilibrium in each degree of freedom (eqs. (1)) in terms of the motion variables. The stability derivatives defined in the preceding section represent the aerodynamic and thrust contributions in terms of the motion variables. The inertial contributions must now be expressed in terms of the same motion variables. For the airplane as a whole, the inertial reaction to gravity and translational accelerations in vector form is

$$\vec{F}_I = m \left(\vec{g} - \frac{d\vec{V}}{dt} \right) \quad (24)$$

where

$$\vec{g} = \vec{i}(-g \sin \theta) + \vec{j}(g \cos \theta \sin \phi) + \vec{k}(g \cos \theta \cos \phi)$$

$$\vec{V} = \vec{i}u + \vec{j}v + \vec{k}w$$

$$\frac{d\vec{V}}{dt} = \vec{i}\dot{u} + \vec{j}\dot{v} + \vec{k}\dot{w} + \vec{\omega} \times \vec{V}$$

and

$$\vec{\omega} = \vec{i}p + \vec{j}q + \vec{k}r$$

and \vec{i} , \vec{j} , and \vec{k} are unit vectors directed along the X, Y, and Z body axes, respectively.

Similarly, the inertial reaction in the airplane rotational degrees of freedom is

$$\vec{M}_I = -\frac{d\vec{H}}{dt} = -\vec{i}\dot{H}_X - \vec{j}\dot{H}_Y - \vec{k}\dot{H}_Z - \vec{\omega} \times \vec{H} \quad (25)$$

where the angular momentum \vec{H} can be written $\vec{H} = \overset{\bullet}{\mathbf{I}} \cdot \vec{\omega}$ and the components of the inertia dyadic $\overset{\bullet}{\mathbf{I}}$ in the body-axis system can be written in matrix form as

$$\overset{\bullet}{\mathbf{I}} = \begin{bmatrix} I_X & 0 & -I_{XZ} \\ 0 & I_Y & 0 \\ -I_{XZ} & 0 & I_Z \end{bmatrix}$$

if inertial symmetry about the X-Z plane is assumed.

After performing the indicated vector operations, the inertial components in the six airplane degrees of freedom are found to be

$$F_{X,I} = m(-g \sin \theta - \dot{u} - qw + rv) \quad (26a)$$

$$F_{Y,I} = m(g \cos \theta \sin \phi - \dot{v} - ru + pw) \quad (26b)$$

$$F_{Z,I} = m(g \cos \theta \cos \phi - \dot{w} - pv + qu) \quad (26c)$$

$$M_{X,I} = -I_X \dot{p} + I_{XZ} \dot{r} - (I_Z - I_Y)qr + I_{XZ}qp \quad (26d)$$

$$M_{Y,I} = -I_Y \dot{q} - (I_X - I_Z)pr - I_{XZ}(p^2 - r^2) \quad (26e)$$

$$M_{Z,I} = -I_Z \dot{r} + I_{XZ} \dot{p} - (I_Y - I_X)pq - I_{XZ}qr \quad (26f)$$

In order to relate the variables in equations (26) to the reference and perturbation values of the motion variables adopted in the preceding section, use will be made of the defining equations for angle of attack and sideslip,

$$\alpha = \tan^{-1} \frac{w}{u} \quad (27a)$$

$$\beta = \sin^{-1} \frac{v}{V} \quad (27b)$$

the expression for altitude rate,

$$\dot{h} = u \sin \theta - v \cos \theta \sin \phi - w \cos \theta \cos \phi \quad (28)$$

and the expressions for the Euler angle rates,

$$\dot{\theta} = q \cos \phi - r \sin \phi \quad (29a)$$

$$\dot{\phi} = p + (q \sin \phi + r \cos \phi) \tan \theta \quad (29b)$$

$$\dot{\psi} = (q \sin \phi + r \cos \phi) \sec \theta \quad (29c)$$

Note that equations (27) relate the linear velocity components to aerodynamic flow angles and equations (29) relate the angular velocity components to an earth-fixed reference. If a quiescent atmosphere and a nonrotating earth are assumed, the linear and angular velocities of equations (27) and (29) are identical to the velocities relative to inertial space appropriate for use in equations (24) and (25).

The acceleration sensed by a seismic translational accelerometer located at the airplane center of gravity is \vec{F}_I/m . The Z-component of this acceleration expressed in g units is defined herein as the normal acceleration n . Thus, from equation (26c)

$$n = \frac{g}{g_0} \cos \theta \cos \phi + \frac{1}{g_0} (-\dot{w} - pv + qu) \quad (30)$$

It should be noted that n is directed along the Z-axis and is, therefore, not identical with the load factor, which is usually defined as the component of inertial force normal to the flight path and the Y-axis, relative to the airplane weight,

$$\text{Load factor} = \frac{F_{Z,I} \cos \alpha - F_{X,I} \sin \alpha}{mg_0} \quad (31)$$

Equations (24) to (31) are applicable to large amplitude airplane motions in six degrees of freedom but are, in general, nonlinear. The linearized equations in the three longitudinal degrees of freedom usually have been derived by constraining the asymmetric motion variables (v, p, r, ϕ) and their time derivatives to zero and expressing the remaining variables as the sum of a steady reference value and a small time-dependent perturbation.

The equations are then linearized by neglecting squares and products of perturbations. On examining the impact of the above constraints on equations (29a) and (26a and c), it is concluded that the only reference flight conditions which are both symmetric and steady are those with zero pitching velocity, implying a straight flight path. If an altitude-dependent atmosphere is considered, the admissible reference flight conditions are further constrained to straight level flight.

It is apparent that analysis of flight at load factors significantly different from unity requires either violation of the small perturbation assumption or relaxation of either the symmetric constraint or the steady constraint on the reference flight condition. In order to retain small perturbations for elevated load factors, a symmetric, pseudosteady reference flight condition having constant pitching velocity has been assumed on occasion. This condition is visualized as a wings-level pullup with a vertically curved flight path. Reference values of θ , h , and \dot{h} can be defined only at one instant of time. Physical interpretation of the perturbations at other instants then becomes unclear under this assumption.

Alternatively, a steady, pseudosymmetric reference flight condition can be assumed. Steady flight is achieved by constraining the time derivatives of all variables to zero, which requires that the angular velocity vector $\vec{\omega}$ be directed along the gravity vector \vec{g} . This condition can be visualized as a constant-altitude banked turn, or if a uniform atmosphere is assumed, a climbing or diving spiral. Approximate symmetry is achieved by constraining only the sideslip angle to zero. The reference flight condition must then satisfy the conditions for static equilibrium in all degrees of freedom, and the linearized longitudinal equations of motion are formulated by allowing small perturbations in only the longitudinal degrees of freedom. The equations of motion developed herein will be formulated for this steady, pseudosymmetric class of reference conditions since the truly symmetric conditions are special cases of this class.

By applying equations (27) to the case of zero sideslip, the velocity components can be written as

$$u = V \cos \alpha$$

$$v = 0$$

$$w = V \sin \alpha$$

The longitudinal variables are stated in perturbation notation as

$$V = V_1(1 + \hat{u}) \quad (\text{See eq. (17).})$$

$$\alpha = \alpha_1 + \alpha_p$$

$$\theta = \theta_1 + \theta_p$$

$$q = q_1 + q_p$$

$$h = h_1 + \int_{t_1}^t \dot{h} dt$$

$$\dot{h} = \dot{h}_1 + \dot{h}_p$$

Then, for small perturbations

$$u = V_1 \cos \alpha_1 + \hat{u}V_1 \cos \alpha_1 - \alpha_p V_1 \sin \alpha_1$$

$$w = V_1 \sin \alpha_1 + \hat{u}V_1 \sin \alpha_1 + \alpha_p V_1 \cos \alpha_1$$

$$\dot{u} = \dot{\hat{u}}V_1 \cos \alpha_1 - \dot{\alpha}_p V_1 \sin \alpha_1$$

$$\dot{w} = \dot{\hat{u}}V_1 \sin \alpha_1 + \dot{\alpha}_p V_1 \cos \alpha_1$$

and, by substitution in equations (26), (28), and (30),

$$F_{X,I} = \underbrace{m(-g \sin \theta_1 - V_1 q_1 \sin \alpha_1)}_{\text{Reference value}} + \underbrace{mV_1(-\hat{u}q_1 \sin \alpha_1 - \dot{\hat{u}} \cos \alpha_1 - \alpha_p q_1 \cos \alpha_1 + \dot{\alpha} \sin \alpha_1 - q_p \sin \alpha_1 - \theta_p \frac{g}{V_1} \cos \theta_1)}_{\text{Perturbation}} \quad (32a)$$

$$F_{Y,I} = m(g \cos \theta_1 \sin \phi - V_1 r \cos \alpha_1 + V_1 p \sin \alpha_1) + mV_1 \left[\hat{u}(p \sin \alpha_1 - r \cos \alpha_1) + \alpha_p(p \cos \alpha_1 + r \sin \alpha_1) - \theta_p \frac{g}{V_1} \sin \theta_1 \sin \phi \right] \quad (32b)$$

$$F_{Z,I} = m(g \cos \theta_1 \cos \phi + V_1 q_1 \cos \alpha_1) + mV_1 \left(\hat{u}q_1 \cos \alpha_1 - \dot{\hat{u}} \sin \alpha_1 - \alpha_p q_1 \sin \alpha_1 - \dot{\alpha} \cos \alpha_1 + q_p \cos \alpha_1 - \theta_p \frac{g}{V_1} \sin \theta_1 \cos \phi \right) \quad (32c)$$

$$M_{X,I} = \overbrace{-(I_Z - I_Y)q_1 r + I_{XZ}pq_1}^{\text{Reference value}} + \overbrace{q_p [-(I_Z - I_Y)r + I_{XZ}p]}^{\text{Perturbation}} \quad (32d)$$

$$M_{Y,I} = -(I_X - I_Z)pr - I_{XZ}(p^2 - r^2) - \dot{q}I_Y \quad (32e)$$

$$M_{Z,I} = -(I_Y - I_X)pq_1 - I_{XZ}q_1 r + q_p [-(I_Y - I_X)p - I_{XZ}r] \quad (32f)$$

$$\begin{aligned} \dot{h} = V_1(\cos \alpha_1 \sin \theta_1 - \sin \alpha_1 \cos \theta_1 \cos \phi) &+ \hat{u}V_1(\cos \alpha_1 \sin \theta_1 - \sin \alpha_1 \cos \theta_1 \cos \phi) \\ &- \alpha_p V_1(\sin \alpha_1 \sin \theta_1 + \cos \alpha_1 \cos \theta_1 \cos \phi) \\ &+ \theta_p V_1(\cos \alpha_1 \cos \theta_1 + \sin \alpha_1 \sin \theta_1 \cos \phi) \end{aligned} \quad (33)$$

$$\begin{aligned} n = \frac{g}{g_0} \cos \theta_1 \cos \phi + \frac{V_1}{g_0} q_1 \cos \alpha_1 &+ \frac{V_1}{g_0} (\hat{u}q_1 \cos \alpha_1 - \dot{\hat{u}} \sin \alpha_1 - \alpha_p q_1 \sin \alpha_1 \\ &- \dot{\alpha} \cos \alpha_1 + q_p \cos \alpha_1) - \theta_p \frac{g}{g_0} \sin \theta_1 \cos \phi \end{aligned} \quad (34)$$

Unfortunately, equations (32b, d, and f) show that in turning flight, the lateral-directional components of the inertial reactions depend on the longitudinal motion perturbations. Clearly, the resulting lateral-directional perturbations could couple back into the longitudinal motions. In order to perform a longitudinal analysis without detailed knowledge of lateral-directional characteristics, the lateral-directional excitation will be neglected, with the knowledge that the error introduced diminishes to zero as the turn rate is reduced to zero.

For the steady, pseudosymmetric reference condition, assume that static equilibrium of rolling and yawing moments can be achieved at zero sideslip with no net lateral force arising from aerodynamic and thrust sources. Equation (32b) then becomes

$$\frac{g}{V_1} \cos \theta_1 \sin \phi - r \cos \alpha_1 + p \sin \alpha_1 = 0 \quad (35)$$

and from equations (29a and b)

$$q_1 \cos \phi - r \sin \phi = 0 \quad (36a)$$

$$p + (q_1 \sin \phi + r \cos \phi) \tan \theta_1 = 0 \quad (36b)$$

Static equilibrium in the longitudinal degrees of freedom is expressed by substitution of the reference portion of equations (32a, c, and e) into equations (2)

$$\mathbf{X}(\delta_1, \alpha_1, q_1, n_1, M_1, R_1, \bar{q}_1, T_1) = \frac{g}{V_1} \sin \theta_1 + q_1 \sin \alpha_1 \quad (37a)$$

$$\mathbf{Z}(\delta_1, \alpha_1, q_1, n_1, M_1, R_1, \bar{q}_1, T_1) = -\frac{g}{V_1} \cos \theta_1 \cos \phi - q_1 \cos \alpha_1 \quad (37b)$$

$$\mathbf{M}(\delta_1, \alpha_1, q_1, n_1, M_1, R_1, \bar{q}_1, T_1) = \frac{I_X - I_Z}{I_Y} p r + \frac{I_{XZ}}{I_Y} (p^2 - r^2) \quad (37c)$$

The system of eight equations made up of equations (35) to (37) and the reference portion of equations (33) and (34) is sufficient to define δ_1 , α_1 , q_1 , T_1 , θ_1 , ϕ , p , and r if values of V_1 , M_1 , R_1 , \bar{q}_1 , n_1 , and \dot{h}_1 are specified. It is interesting to note from equation (37c) that an inertial pitching moment exists in steady turning flight, which can influence the control-limited load factor of interest for fighter airplanes.

The system of linearized longitudinal perturbation equations can now be formed from equations (2) by expressing the aerodynamic and thrust contributions in terms of the dimensional stability derivatives, expressing the inertial contribution by equations (32a, c, and e), supplementing the system with the altitude equation (33), and subtracting the reference equations (37) and the reference part of equation (33). The resulting equations are

$$\begin{aligned} \dot{\hat{u}}(\dot{X}_{\hat{u}} - \cos \alpha_1) + \hat{u}(\dot{X}_{\hat{u}} - q_1 \sin \alpha_1) + \dot{\alpha}(\dot{X}_{\dot{\alpha}} + \sin \alpha_1) + \alpha_p(\dot{X}_{\alpha} - q_1 \cos \alpha_1) \\ + \dot{q}X_{\dot{q}} + q_p(\dot{X}_q - \sin \alpha_1) + \theta_p(\dot{X}_\theta - \frac{g}{V_1} \cos \theta_1) + h_p X_h + \delta_p X_\delta + T_p X_T = 0 \end{aligned} \quad (38a)$$

$$\begin{aligned} \dot{\hat{w}}(\dot{Z}_{\hat{w}} - \sin \alpha_1) + \hat{w}(\dot{Z}_{\hat{w}} + q_1 \cos \alpha_1) + \dot{\alpha}(\dot{Z}_{\dot{\alpha}} - \cos \alpha_1) + \alpha_p(\dot{Z}_{\alpha} - q_1 \sin \alpha_1) \\ + \dot{q}Z_{\dot{q}} + q_p(\dot{Z}_q + \cos \alpha_1) + \theta_p(\dot{Z}_\theta - \frac{g}{V_1} \sin \theta_1 \cos \phi) + h_p Z_h + \delta_p Z_\delta + T_p Z_T = 0 \end{aligned} \quad (38b)$$

$$\dot{\hat{M}}_u \dot{M}_{\hat{u}} + \hat{M}_u \dot{M}_{\hat{u}} + \dot{\alpha} M_{\dot{\alpha}} + \alpha_p M_{\alpha} + \dot{q}(M_{\dot{q}} - 1) + q_p M_q + \theta_p M_\theta + h_p M_h + \delta_p M_\delta + T_p M_T = 0 \quad (38c)$$

$$\begin{aligned} \hat{V}_1 (\cos \alpha_1 \sin \theta_1 - \sin \alpha_1 \cos \theta_1 \cos \phi) - \alpha_p V_1 (\sin \alpha_1 \sin \theta_1 + \cos \alpha_1 \cos \theta_1 \cos \phi) \\ + \theta_p V_1 (\cos \alpha_1 \cos \theta_1 + \sin \alpha_1 \sin \theta_1 \cos \phi) - \dot{h}_p = 0 \end{aligned} \quad (38d)$$

To obtain a solution, this set must be supplemented by equations for the two control systems, which will not be stated here, and by the perturbation equation obtained by subtracting equation (36a) from equation (29a), that is,

$$\dot{\theta}_p - q_p \cos \phi = 0 \quad (38e)$$

since $\dot{\theta}_1 = 0$.

For the special case of a steady, straight, symmetric reference flight condition, $\phi = p = q_1 = r = 0$ and the equations of motion are simplified accordingly. In particular, equation (38d) becomes

$$\hat{u}V_1 \sin(\theta_1 - \alpha_1) - \alpha_p V_1 \cos(\theta_1 - \alpha_1) + \theta_p V_1 \cos(\theta_1 - \alpha_1) - \dot{h}_p = 0 \quad (39)$$

and the reference equations are

$$\left. \begin{aligned} X_1 &= \frac{g}{V_1} \sin \theta_1 \\ Z_1 &= -\frac{g}{V_1} \cos \theta_1 \\ M_1 &= 0 \\ \dot{h}_1 &= V_1 \sin(\theta_1 - \alpha_1) \\ n_1 &= \frac{g}{g_0} \cos \theta_1 \end{aligned} \right\} \quad (40)$$

If the reference condition is further constrained to level flight, then $\theta_1 = \alpha_1$, and the resulting simplification of the equations of motion is obvious.

It should be noted that equations (38) can be considered to be a hybrid set of equations of motion in the sense that the motion variables are resolved on stability axes ($\hat{u}\vec{V}_1$ is directed along \vec{V}_1), whereas the X and Z forces are resolved on a body-fixed axis system whose orientation in the airplane plane of symmetry is arbitrary for rigid airplanes and is determined by structural consideration for elastic airplanes. The more conventional stability-axis system of equations of motion is obtained from equations (38) by simply setting $\alpha_1 = 0$. If the stability-axis system is to be used for elastic airplanes, it is recommended that the stability derivatives be determined first on a structurally appropriate body-axis system and then be transformed to the stability-axis system by the usual force transformation.

Calculation of Stability Derivatives

In this section, an influence-coefficient procedure for calculating the stability derivatives is outlined. This procedure has been implemented in a digital computer program which is presented and described in the appendix. In addition to the assumptions already made in defining the stability derivatives, the following assumptions are made in order to simplify the calculation procedure:

1. Aerodynamic loadings are derived from a linearized, inviscid, thin lifting-surface theory.
2. Singular aerodynamic loads arising from edge suction are neglected.
3. All unsteady aerodynamic effects are neglected.
4. All contributions of the propulsion system are neglected.

The effect of assumptions 1, 3, and 4 is to eliminate the variables R , $\dot{\alpha}$, and T from the list of physical variables in table I. Equations (6b) and (7b) are then represented by the matrix expression

$$\left\{ \frac{F_{Z,A}}{\bar{q}} \right\} = [A] \{ \alpha_l + \epsilon \} \quad (41)$$

where $[A]$ is an aerodynamic influence-coefficient matrix which can be obtained from any suitable lifting-surface theory for a given Mach number and paneling geometry. In the present development, aerodynamic symmetry is assumed, and each element of $[A]$ represents the aerodynamic normal force acting at a load point $(x_f, y_f, 0)$ due to a unit change in mean-camber-surface slope at a symmetric pair of control points $(x_a, \pm y_a, 0)$ for unit dynamic pressure.

The structural operator \mathcal{S} in equation (10) can also be represented by an influence-coefficient matrix such that

$$\{ \epsilon_F \} = [S] \left\{ \bar{q} \left\{ \frac{F_{Z,A}}{\bar{q}} \right\} + \{ F_{Z,I} \} \right\} \quad (42)$$

where each element of $[S]$ is the elastic change in mean-camber-surface slope at an aerodynamic control point $(x_a, y_a, 0)$ due to a unit force applied at a symmetric pair of load points $(x_f, \pm y_f, 0)$. Combining equations (8a), (9), (11), (41), and (42) and solving for the aerodynamic-force set give

$$\left\{ \frac{F_{Z,A}}{\bar{q}} \right\} = \left[\underline{1} - \bar{q} \underline{A} \underline{S} \right]^{-1} \underline{A} \left\{ \epsilon_{jig} \right\} + \alpha \{1\} + \delta \{ \epsilon_{\delta} \} - \frac{qc}{2V} \left\{ \frac{2x_a}{c} \right\} + \underline{S} \left\{ n g_o \underline{m} \{1\} + (\dot{q} - pr) \underline{m} \{x_f\} \right\} \quad (43)$$

The coefficients C_N and C_m can now be written

$$C_N = -\frac{2}{S} \{1\}^T \left\{ \frac{F_{Z,A}}{\bar{q}} \right\} \quad (44a)$$

$$C_m = -\frac{2}{Sc} \{x_f\}^T \left\{ \frac{F_{Z,A}}{\bar{q}} \right\} \quad (44b)$$

Under the second assumption stated at the beginning of this section, aerodynamic edge suction is neglected, and the aerodynamic force on each panel then acts normal to the mean camber surface at that panel. If the mean-camber-surface slope is small everywhere, the axial-force coefficient is approximately

$$C_A = -\frac{2}{S} \{ \epsilon_f \}^T \left\{ \frac{F_{Z,A}}{\bar{q}} \right\} \quad (44c)$$

where $\{ \epsilon_f \}$ is the set of mean-camber-surface slopes at the panel load points

$$\{ \epsilon_f \} = \{ \epsilon_{jig,f} \} + \delta \{ \epsilon_{\delta,f} \} + \underline{S}_f \left\{ \bar{q} \left\{ \frac{F_{Z,A}}{\bar{q}} \right\} + \{ F_{Z,I} \} \right\} \quad (45)$$

It should be observed, however, that the neglect of edge suction implies a rather gross oversimplification of the true aerodynamic loads, particularly in subsonic flight, and the resulting axial-force coefficient must be considered incomplete. Despite this shortcoming, the axial stability derivatives will be formulated herein to provide a basis for future refinement and to allow an examination of their possible significance to the stability of elastic airplanes.

The stability derivatives are calculated by substituting the partial derivatives of equations (44) with respect to each of the physical variables α , δ , $qc/2V_1$, n , \dot{q} , M , and \bar{q} into the coefficient form of equations (18). By denoting any physical variable by p ,

$$\frac{\partial \mathbf{C}_N}{\partial p} = -\frac{2}{S} \langle \mathbf{1} \rangle^T \left\{ \frac{\partial \mathbf{F}_{Z,A}/\bar{q}}{\partial p} \right\}_1 \quad (46a)$$

$$\frac{\partial \mathbf{C}_m}{\partial p} = -\frac{2}{S c} \langle \mathbf{x}_f \rangle^T \left\{ \frac{\partial \mathbf{F}_{Z,A}/\bar{q}}{\partial p} \right\}_1 \quad (46b)$$

$$\frac{\partial \mathbf{C}_A}{\partial p} = -\frac{2}{S} \langle \epsilon_f \rangle_1^T \left\{ \frac{\partial \mathbf{F}_{Z,A}/\bar{q}}{\partial p} \right\}_1 - \frac{2}{S} \left\{ \frac{\partial \epsilon_f}{\partial p} \right\}_1^T \left\{ \frac{\mathbf{F}_{Z,A}}{\bar{q}} \right\}_1 \quad (46c)$$

The right-hand side of equation (43) can be interpreted as the product of an aeroelastic correction matrix, the aerodynamic influence-coefficient matrix, and a vector of pseudorigid aerodynamic boundary conditions which includes structural distortion from only the inertial loads. To simplify the notation, the aeroelastic correction matrix can be defined as

$$\mathbf{[B]} = \left[\mathbf{[1]} - \bar{q} \mathbf{[A]} \mathbf{[S]} \right]^{-1} \quad (47)$$

and the vector of boundary conditions as

$$\langle \sigma \rangle = \langle \epsilon_{jig} \rangle + \alpha \langle \mathbf{1} \rangle + \delta \langle \epsilon_\delta \rangle - \frac{qc}{2V_1} \left\{ \frac{2x_a}{c} \right\} + \mathbf{[S]} \left\{ n_{g_0} \mathbf{[m]} \langle \mathbf{1} \rangle + (\dot{q} - pr) \mathbf{[m]} \langle \mathbf{x}_f \rangle \right\} \quad (48)$$

At the reference flight condition,

$$\langle \sigma \rangle_1 = \langle \epsilon_{jig} \rangle + \alpha_1 \langle \mathbf{1} \rangle + \delta_1 \langle \epsilon_\delta \rangle - \frac{q_1 c}{2V_1} \left\{ \frac{2x_a}{c} \right\} + \mathbf{[S]} \left\{ n_1 g_0 \mathbf{[m]} \langle \mathbf{1} \rangle - pr \mathbf{[m]} \langle \mathbf{x}_f \rangle \right\} \quad (49)$$

$$\left\{ \frac{\mathbf{F}_{Z,A}}{\bar{q}} \right\}_1 = \mathbf{[B]}_1 \mathbf{[A]}_1 \langle \sigma \rangle_1 \quad (50)$$

and

$$\langle \epsilon_f \rangle_1 = \langle \epsilon_{jig,f} \rangle + \delta_1 \langle \epsilon_{\delta,f} \rangle + \mathbf{[S]}_1 \left\{ \bar{q}_1 \mathbf{[B]}_1 \mathbf{[A]}_1 \langle \sigma \rangle_1 + n_1 g_0 \mathbf{[m]} \langle \mathbf{1} \rangle - pr \mathbf{[m]} \langle \mathbf{x}_f \rangle \right\} \quad (51)$$

The partial derivatives appearing on the right-hand side of equations (46) can be evaluated in a straightforward manner with respect to the first five physical variables α , δ , $qc/2V_1$, n , and \dot{q} . A finite-difference technique has been chosen to evaluate the derivatives with respect to M and \bar{q} . For increments in M and \bar{q} which are small relative to the reference-condition values, the following matrices are defined:

$$[B_{\bar{q}}] = \frac{[\bar{1}] - (\bar{q}_1 + \Delta\bar{q})[A]_1[S]}{2\Delta\bar{q}}^{-1} - \frac{[\bar{1}] - (\bar{q}_1 - \Delta\bar{q})[A]_1[S]}{2\Delta\bar{q}}^{-1}$$

$$[B_{MA_M}] = \frac{[\bar{1}] - \bar{q}_1[A_{M,1+\Delta M}][S]}{2\Delta M}^{-1}[A_{M,1+\Delta M}] - \frac{[\bar{1}] - \bar{q}_1[A_{M,1-\Delta M}][S]}{2\Delta M}^{-1}[A_{M,1-\Delta M}]$$

The matrices of the partial derivatives of $F_{Z,A}/\bar{q}$ and ϵ_f with respect to each physical variable are expressed in table III. These values along with the reference-condition values of equations (49) to (51) are used in equations (46) to find the derivatives of C_A , C_N , and C_m which are in turn substituted into the coefficient form of equations (18) to find the stability derivatives.

TABLE III. - THE PARTIAL-DERIVATIVE MATRICES $\left\{ \frac{\partial F_{Z,A}/\bar{q}}{\partial p} \right\}$ AND $\left\{ \frac{\partial \epsilon_f}{\partial p} \right\}$

Physical variable, p	$\left\{ \frac{\partial F_{Z,A}/\bar{q}}{\partial p} \right\}$	$\left\{ \frac{\partial \epsilon_f}{\partial p} \right\}$
α	$[B]_1[A]_1\{1\}$	$\bar{q}_1[S_f][B]_1[A]_1\{1\}$
δ	$[B]_1[A]_1\{\epsilon_\delta\}$	$\bar{q}_1[S_f][B]_1[A]_1\{\epsilon_\delta\} + \{\epsilon_{\delta,f}\}$
$\frac{qc}{2V_1}$	$[B]_1[A]_1\left\{ \frac{2x_a}{c} \right\}$	$\bar{q}_1[S_f][B]_1[A]_1\left\{ \frac{2x_a}{c} \right\}$
n	$g_o[B]_1[A]_1[S][m]\{1\}$	$g_o[S_f][\bar{1}] + \bar{q}_1[B]_1[A]_1[S][m]\{1\}$
\dot{q}	$[B]_1[A]_1[S][m]\{x_f\}$	$[S_f][\bar{1}] + \bar{q}_1[B]_1[A]_1[S][m]\{x_f\}$
M	$[B_{MA_M}]\{\sigma\}_1$	$\bar{q}_1[S_f][B_{MA_M}]\{\sigma\}_1$
\bar{q}	$[B_{\bar{q}}][A]_1\{\sigma\}_1$	$[S_f][\bar{q}_1[B_{\bar{q}}] + [B]_1][A]_1\{\sigma\}_1$

Evaluation of equations (49) to (51) requires knowledge of the mean-camber-surface slopes of the jig shape $\{\epsilon_{jig}\}$ and $\{\epsilon_{jig,f}\}$ as well as the reference-condition values of α_1 , δ_1 , q_1 , n_1 , p , and r . Assume that the airplane configuration has been fully defined at a single, straight, level design flight condition and that the design air-load distribution is known. By applying equations (9), (42), and (45), the jig shape slopes are found to be

$$\{\epsilon_{jig}\} = \{\epsilon_{des}\} - \delta_{des}\{\epsilon_{\delta}\} - [S] \left\{ \bar{q}_{des} \left\{ \frac{F_{Z,A}}{\bar{q}} \right\}_{des} + n_{des} g_0 [m_{des}] \{1\} \right\} \quad (52a)$$

$$\{\epsilon_{jig,f}\} = \{\epsilon_{des,f}\} - \delta_{des}\{\epsilon_{\delta,f}\} - [S_f] \left\{ \bar{q}_{des} \left\{ \frac{F_{Z,A}}{\bar{q}} \right\}_{des} + n_{des} g_0 [m_{des}] \{1\} \right\} \quad (52b)$$

The values of the physical variables at any desired reference flight condition can be found by applying equations (33) to (37). Some simplification results, however, from the present assumptions under which the effects of thrust and nonlinear aerodynamics are neglected. If the thrust is assumed just sufficient to balance the X forces, equation (37a) can be neglected. Equations (37b and c) can be restated as

$$\begin{aligned} C_{N,jig} + \alpha_1 \frac{\partial C_N}{\partial \alpha} + \delta_1 \frac{\partial C_N}{\partial \delta} + \frac{q_1 c}{2V_1} \frac{\partial C_N}{\partial \left(\frac{qc}{2V_1} \right)} + n_1 \frac{\partial C_N}{\partial n} - pr \frac{\partial C_N}{\partial \dot{q}} \\ = \frac{mV_1}{\bar{q}_1 S} \left(\frac{g}{V_1} \cos \theta_1 \cos \phi + q_1 \cos \alpha_1 \right) \end{aligned} \quad (53a)$$

$$\begin{aligned} C_{m,jig} + \alpha_1 \frac{\partial C_m}{\partial \alpha} + \delta_1 \frac{\partial C_m}{\partial \delta} + \frac{q_1 c}{2V_1} \frac{\partial C_m}{\partial \left(\frac{qc}{2V_1} \right)} + n_1 \frac{\partial C_m}{\partial n} - pr \frac{\partial C_m}{\partial \dot{q}} \\ = \frac{1}{\bar{q} S c} \left[(I_Z - I_X) pr - I_{XZ} (p^2 - r^2) \right] \end{aligned} \quad (53b)$$

where

$$C_{N,jig} = -\frac{2}{S} \{1\}^T [B]_1 [A]_1 \{\epsilon_{jig}\}$$

and

$$C_{m,jig} = -\frac{2}{Sc} \langle x_f \rangle^T [B]_1 [A]_1 \langle \epsilon_{jig} \rangle$$

The derivatives with respect to \dot{q} are used to express the pr contributions since the inertial-force distribution for unit \dot{q} is shown by equation (11) to be equal to that for a unit value of -pr. For specified values of M_1 and \bar{q}_1 , the derivatives appearing in equations (53) can be calculated by using equations (46) and table III. The reference flight condition can then be fully defined by solution of equations (33) to (36) and (53).

Effect of Structural Fixity Point Location

The influence-coefficient procedure for calculating stability derivatives of an elastic airplane, as outlined in the preceding section, makes use of a structural influence-coefficient matrix $[S]$, each element of which is the elastic change in mean-camber-surface slope at an aerodynamic control point due to a pair of unit forces applied at a symmetric pair of load points. Evaluation of this matrix requires that the structure be assumed clamped at a structural fixity point. Any nonequilibrium distribution of loads applied to the structure must then be reacted by a force and moment imposed at the fixity point, and the deformed shape, calculated by using the matrix $[S]$, will include implicitly the effects of these reactions. The deformed shape depends, therefore, on the fixity point location. Since the load distribution arising from a unit perturbation of any single physical variable is, in general, not in equilibrium, the values of the stability derivatives calculated by the procedure outlined will depend on fixity point location.

When a complete and consistent set of stability derivatives is used in the equations of motion derived from the conditions for dynamic equilibrium, the reactions at the fixity point vanish and the deformed shape at any instant is, in a coordinate-free sense, independent of fixity point location. Some of the motion variables, however, for example, α , θ , and their time derivatives, are not coordinate-free but are defined relative to the reference axis system. Moreover the elastic surface slope changes defined by the matrix $[S]$ are also expressed relative to the reference axis system and must be zero at the fixity point. Thus, the orientation of the reference axis system must be considered invariant with respect to a material element located at the fixity point, as indicated in figure 1.

It is apparent, then, that after application of the equations of motion, any quantities that are independent of reference axis system orientation in the airplane, such as characteristic roots, the variables \hat{u} , δ , h , and the magnitudes of resultant force, moment, or acceleration vectors, are also independent of the fixity point location. Those quantities dependent on reference axis system orientation, such as the variables α , θ , q ,

and components of force or acceleration vectors, are also dependent on the location of the fixity point assumed in the definition of the matrix $[\bar{S}]$.

ILLUSTRATIVE ANALYSIS

The Example Airplane

To illustrate the calculation and use of the stability derivatives defined in this paper, a longitudinal quasi-steady aeroelastic analysis of a high-performance supersonic transport airplane configuration has been performed. Although the analysis was performed in U.S. Customary Units, the results are presented in the International System of units (SI). The configuration selected was that used in reference 5 to illustrate a number of aerodynamic design integration features. This configuration was also the subject of a preliminary design study by The Boeing Company during which airplane weight and balance information and elastic properties of the structure were developed. The author gratefully acknowledges the cooperation of The Boeing Company in supplying a symmetric structural slope influence-coefficient matrix and weight distribution data for use in the present analysis. It should be emphasized that these data resulted from a preliminary design study and are not necessarily applicable to an airplane design meeting all the requirements of a commercial supersonic transport airplane. In particular, the structural elastic characteristics do not reflect any additional stiffening which might be necessary to achieve adequate controllability and flutter margin.

For the present study, the aerodynamic effects of the vertical tails and engine nacelles were neglected and a new mean camber surface was designed to minimize the drag due to lift and to trim the airplane with zero control-surface deflection at $M = 2.7$, $C_N = 0.07914$, and a center-of-gravity location at $0.417c$. The configuration planform and the paneling geometry used for subsonic and supersonic analyses are illustrated in figure 2. Corresponding aerodynamic influence-coefficient matrices were calculated by using the vortex-lattice method of reference 6 for the subsonic analysis ($M_1 = 0.8$) and a procedure based on the method of reference 7 for the supersonic analysis ($M_1 = 2.7$). The load points and aerodynamic control points were located at the quarter-chord and three-quarter-chord points, respectively, of the panel midspan chords for the subsonic case and at the panel centroids and 0.95 panel chord points, respectively, for the supersonic case.

The structural influence-coefficient matrix supplied by The Boeing Company was transformed to the appropriate forms for the subsonic and supersonic panel arrangements by using a second-order, bidirectional interpolation procedure applied successively to the slope-point and load-point transformations. The fixity point of the structural influence-coefficient matrix used in the present analysis was located at $0.33c$.

The weight distribution supplied by The Boeing Company was transformed by distributing each original weight element among the three closest load points of the new panel layout in such a way that the moments about the X- and Y-axes were unchanged. The distribution of structure, contents, and payload weight, totaling 1.56 MN (351 560 lb), was considered invariant. Fuel capacity constraints, based on the fuel weight distribution supplied by The Boeing Company, were assigned to each panel. Within these constraints, fuel weight distributions yielding the following combinations of airplane weight, center-of-gravity location, and pitching moment of inertia were developed:

Weight		$\left(\frac{x}{c}\right)_{c.g.}$	$I_Y \times 10^{-6}$	
MN	lb		kg-m ²	slug-ft ²
2.67	600 000	0.41	61.61	45.44
2.67	600 000	.47	62.43	46.05
1.87	420 000	.41	56.33	41.55
1.87	420 000	.47	57.43	42.36

The weight distribution for the design condition, $W = 2.10$ MN (472 500 lb) and center of gravity at 0.417c, was also developed.

The chordwise distributions of mean-camber-surface slope for the design shape ϵ_{des} and the jig shape ϵ_{jig} at several spanwise stations are shown in figure 3. These slopes are referred to a reference axis system oriented in such a manner that the angle of attack at the design condition is 2.8° . This orientation was chosen so that the average slope of the design mean camber surface was approximately zero.

The longitudinal characteristics of the example airplane have been analyzed for a series of reference flight conditions including center-of-gravity locations of 0.41c and 0.47c, the two airplane weights noted previously, and either five values of dynamic pressure ranging from 7.2 kN/m^2 (150 lb/ft^2) to 47.9 kN/m^2 (1000 lb/ft^2) for $M = 0.8$ or four values of dynamic pressure ranging from 14.4 kN/m^2 (300 lb/ft^2) to 47.9 kN/m^2 (1000 lb/ft^2) for $M = 2.7$. All reference flight conditions corresponded to straight level flight. For comparison, the rigid airplane having the design mean camber surface was also analyzed.

Longitudinal control and trim were achieved by equal deflection of the inboard and outboard trailing-edge control surfaces outlined in figure 2. Because the control surface edges were not coincident with panel boundaries, control deflections were represented by assigning to each panel a value of ϵ_δ equal to the ratio of the control surface area lying within that panel to the total panel area. For each panel, the values of $\epsilon_{\delta,f}$ and ϵ_δ were assumed to be identical.

Aerodynamic Derivatives

The computer program described in the appendix was used to calculate the longitudinal stability derivatives together with parameters describing the reference flight conditions. The values of angle of attack, control deflection, and normal- and axial-force coefficients calculated for the reference flight conditions are plotted in figure 4 for the rigid and elastic airplanes at the two center-of-gravity locations. The axial-force coefficient includes an increment of 0.00550 to represent skin friction and form drag at $M = 0.8$ or an increment of 0.00533 to represent skin friction and wave drag due to volume at $M = 2.7$. The aeroelastic effects on trim angle of attack, control deflection, and axial-force coefficient are apparent from figure 4.

The partial derivatives of C_A , C_N , and C_m with respect to the physical variables are shown in figures 5, 6, and 7. Because unsteady aerodynamic effects were neglected, no partial derivatives with respect to $\dot{\alpha}$ were calculated. When the stability derivatives are formed by using equations (18), however, stability derivatives with respect to $\dot{\alpha}$ will exist for the elastic airplane because of the contribution of the partial derivatives with respect to n . For the rigid airplane, all derivatives with respect to n , \dot{q} , and \bar{q} are zero. All C_A derivatives and the derivatives of C_N and C_m with respect to Mach number depend on the reference values of α and δ and consequently vary with dynamic pressure. Partial derivatives of C_N and C_m with respect to the remaining physical variables are independent of the reference flight condition for the rigid airplane.

The effects of aeroelasticity on the partial derivatives are apparent from figures 5, 6, and 7. Note in particular the large destabilizing aeroelastic effect on $\partial C_m / \partial \alpha$.

The Characteristic Stability Roots

The longitudinal stability derivatives were calculated by applying equations (18) to the partial derivatives of figures 5, 6, and 7. The three-degree-of-freedom linearized equations of motion (eqs. (38)) were then solved for the characteristic roots and the transfer functions \hat{u}/δ_p and n_p/δ_p . The perturbation part of equation (34) was included in the system of equations to define n_p . The altitude-dependent parameters required for the solution are shown in figure 8 and are based on the 1962 U.S. Standard Atmosphere (ref. 8). Solutions corresponding to a locally uniform atmosphere were also obtained by setting the derivatives X_h , Z_h , and M_h equal to zero.

The real and imaginary parts of the characteristic roots are presented as functions of dynamic pressure for the rigid airplane in figure 9 and for the elastic airplane in figure 10. Real roots are shown as faired lines without symbols. The calculated real and imaginary parts of complex roots are indicated by symbols, with the same symbol shape used for the real and imaginary parts of any particular conjugate pair of complex roots.

Calculations were made at only four or five values of dynamic pressure, and therefore, the lines faired between calculated points should be considered as only illustrative. In particular, the locations of branch points, that is, points of transition between a pair of real roots and a pair of complex roots, are only approximate.

The system of equations yields five characteristic roots including one root arising from the differentiation of h in the altitude equation (38d). For the cases representing a locally uniform atmosphere, the altitude equation is uncoupled from the remaining equations and one root is always zero. With a standard atmosphere, the altitude root was usually too small to be apparent in figures 9 and 10 except for the aft c.g. cases at $M = 0.8$ (figs. 9(b) and 10(b)) where the altitude root can be seen at low dynamic pressure. The remaining roots in most cases can be clearly identified as a short-period pair and a phugoid pair although these root pairs were not always oscillatory. When the remaining roots are all complex, they can be recognized clearly as a phugoid pair and a short-period pair, with the phugoid pair having the smaller magnitude (smaller undamped natural frequency). Identification of real roots is not as straightforward, but in most cases, the faired lines in figures 9 and 10 can be used to relate real roots to either the phugoid or the short-period mode at other values of dynamic pressure.

The assumption of a locally uniform atmosphere had a destabilizing effect on the phugoid roots, usually manifested as a reduction in phugoid frequency, but had little effect on the short-period mode, particularly when this mode was oscillatory. A comparison of figures 9 and 10 shows that the effect of aeroelasticity on the short-period root pair was to reduce both frequency and damping with the frequency reduction being more pronounced. As a result, the short-period mode of the elastic airplane in many cases became over-critically damped and therefore yielded two aperiodic (real) roots. This tendency was most apparent with heavy weight, aft c.g., high dynamic pressure, and subsonic speed. In all cases, however, the short-period root pair remained stable as indicated by the negative real parts.

The phugoid roots of the rigid airplane (fig. 9) were always small in magnitude and corresponded to either a lightly damped low-frequency oscillation or a mild aperiodic divergence. In contrast, the elastic airplane (fig. 10) exhibited, in many cases, phugoid roots which were much larger in magnitude and were strongly divergent in either an oscillatory or aperiodic manner. Again this tendency was most apparent with heavy weight, aft c.g., high dynamic pressure, and subsonic speed and appeared to be particularly sensitive to changes in weight or possibly weight distribution.

In an attempt to identify the reasons for the aperiodic short-period roots and the strong phugoid divergence, the equations of motion were simplified to two second-order sets yielding decoupled approximations to the short-period and phugoid modes. For a locally uniform atmosphere and a wings-level reference flight condition, equation (38d)

can be omitted and equation (38e) becomes $\dot{\theta}_p = q_p$. After resolving the force equations onto stability axes and applying the Laplace transformation, equations (38a, b, and c) can be written in matrix form as

$$\begin{bmatrix} s(1 - X_{\hat{u},s}) - X_{\hat{u},s} & -sX_{\dot{\alpha},s} - X_{\alpha,s} & -s^2X_{\dot{q},s} - sX_{q,s} - X_{\theta,s} + \frac{g}{V_1} \\ -sZ_{\hat{u},s} - Z_{\hat{u},s} & s(1 - Z_{\dot{\alpha},s}) - Z_{\alpha,s} & -s^2Z_{\dot{q},s} - s(1 + Z_{q,s}) - Z_{\theta,s} \\ -sM_{\hat{u}} - M_{\hat{u}} & -sM_{\dot{\alpha}} - M_{\alpha} & s^2(1 - M_{\dot{q}}) - sM_q - M_{\theta} \end{bmatrix} \begin{Bmatrix} \hat{u} \\ \alpha_p \\ \theta_p \end{Bmatrix} = \begin{Bmatrix} X_{\delta,s} \\ Z_{\delta,s} \\ M_{\delta} \end{Bmatrix} \delta_p \quad (54)$$

A decoupled approximation to the short-period mode is obtained by constraining \hat{u} to zero and assuming $Z_{\theta,s}$ and M_{θ} to be negligible

$$\begin{bmatrix} s(1 - Z_{\dot{\alpha},s}) - Z_{\alpha,s} & -sZ_{\dot{q},s} - (1 + Z_{q,s}) \\ -sM_{\dot{\alpha}} - M_{\alpha} & s(1 - M_{\dot{q}}) - M_q \end{bmatrix} \begin{Bmatrix} \alpha_p \\ q_p \end{Bmatrix} = \begin{Bmatrix} Z_{\delta,s} \\ M_{\delta} \end{Bmatrix} \delta_p \quad (55)$$

The decoupled short-period roots are then the roots of

$$s^2 + 2\zeta_{sp}\omega_{sp}s + \omega_{sp}^2 = 0$$

where

$$\omega_{sp}^2 = \frac{Z_{\alpha,s}M_q - M_{\alpha}(1 + Z_{q,s})}{(1 - Z_{\dot{\alpha},s})(1 - M_{\dot{q}}) - Z_{\dot{q},s}M_{\dot{\alpha}}} \quad (56a)$$

$$2\zeta_{sp}\omega_{sp} = -\frac{(1 - Z_{\dot{\alpha},s})M_q - (1 - M_{\dot{q}})Z_{\alpha,s} - Z_{\dot{q},s}M_{\alpha} - M_{\dot{\alpha}}(1 + Z_{q,s})}{(1 - Z_{\dot{\alpha},s})(1 - M_{\dot{q}}) - Z_{\dot{q},s}M_{\dot{\alpha}}} \quad (56b)$$

A decoupled approximation to the phugoid mode is obtained by retaining only the zero-order terms in the moment equation and assuming $X_{\dot{q},s}$ and $Z_{\dot{q},s}$ to be negligible

$$\begin{bmatrix} s(1 - X_{\hat{u},s}) - X_{\hat{u},s} & -sX_{\dot{\alpha},s} - X_{\alpha,s} & -sX_{q,s} - X_{\theta,s} + \frac{g}{V_1} \\ -sZ_{\hat{u},s} - Z_{\hat{u},s} & s(1 - Z_{\dot{\alpha},s}) - Z_{\alpha,s} & -s(1 + Z_{q,s}) - Z_{\theta,s} \\ -M_{\hat{u}} & -M_{\alpha} & -M_{\theta} \end{bmatrix} \begin{Bmatrix} \hat{u} \\ \alpha_p \\ \theta_p \end{Bmatrix} = \begin{Bmatrix} X_{\delta,s} \\ Z_{\delta,s} \\ M_{\delta} \end{Bmatrix} \delta_p \quad (57)$$

The decoupled phugoid roots are the roots of

$$s^2 + 2\xi_p\omega_p s + \omega_p^2 = 0$$

where ω_p^2 and $2\xi_p\omega_p$ are found by expanding the determinant of the matrix in equation (57).

Figure 11 presents a comparison of the decoupled root parameters from equations (55) and (57) with those from the coupled system (eq. (54)) for the elastic airplane with forward center-of-gravity location at $M = 0.8$. The coupled and decoupled short-period parameters are in good agreement except for those cases in which the short-period mode was aperiodic. The decoupled phugoid approximation, however, was generally poor and, in particular, failed to yield the large phugoid magnitude shown by the coupled solution for the higher dynamic pressures with heavy weight. Observe, however, that the total damping $2\xi_{sp}\omega_{sp} + 2\xi_p\omega_p$ was well represented by the decoupled solutions at high dynamic pressure. This fact implies that the coupled system provides a mechanism for transfer of damping from the phugoid into the short-period mode. Examination of other simplifications of equation (54) has led to the conclusion that the root-coupling mechanism is provided primarily through the derivatives M_q and $M_{\dot{\alpha}}$ and becomes important when the numerator of equation (56a) $Z_{\alpha,s}M_q - M_{\alpha}(1 + Z_{q,s})$ is small.

It should be noted that for the elastic airplane, the inertial contributions to the derivatives M_q , Z_q , $M_{\dot{\alpha}}$, and $Z_{\dot{\alpha}}$ arising from normal-acceleration effects (eqs. (18)) were much larger than the aerodynamic contributions and were responsible for large negative values of M_q and Z_q and large positive values of $M_{\dot{\alpha}}$ and $Z_{\dot{\alpha}}$. As a result, the value of ω_{sp}^2 remained positive (stable) for the lightweight cases and near zero for the heavyweight cases of figure 11 in spite of the large unstable values of M_{α} . The effect of weight on ω_{sp}^2 resulted primarily from the larger magnitude of Z_{α} arising from the reduced mass of the lightweight condition.

Static-Stability Considerations

Static longitudinal stability can be interpreted as the tendency for either speed or normal acceleration to be restored to its equilibrium value following a disturbance. The

two types of static stability to be discussed, therefore, will be termed speed stability and maneuvering stability. The concepts of static margin and maneuver margin have been used as direct quantitative measures of the two types of static stability. These stability margins are visualized as the distance from the c.g. to either the neutral point or the maneuver point where these points are the c.g. locations for which either the speed stability or the maneuver stability is zero. The stability margins can be quantified, therefore, as values of the total derivative dC_m/dC_N evaluated under constraints appropriate to a disturbance in either speed or normal acceleration. Approximate expressions for the stability margins in terms of the stability derivatives exist in the literature, but their applicability to elastic airplanes should be examined.

Other measures of static stability express the observable consequences of the interaction of static stability with other airplane properties. For example, the undamped natural frequencies of the phugoid and short-period modes reflect the interaction of the speed stability and maneuvering stability, respectively, with the inertial properties of the airplane. Similarly, the static control parameters δ_p/\hat{u} and δ_p/n_p are measures of speed stability and maneuvering stability, respectively, relative to control effectiveness. In the present analysis, the static control parameters are determined from transfer functions obtained from solution of the equations of motion and, along with the stability margins, will be utilized in describing the static stability.

The asymptote form of the frequency response amplitude of the \hat{u}/δ_p and n_p/δ_p transfer functions is illustrated in figure 12 for the elastic airplane in the heavy condition with c.g. at $0.41c$ and $M = 0.8$ for five values of \bar{q} . This form of plot, commonly termed Bode plot or corner plot, is made up of straight-line segments connecting points at the pole and zero frequencies of the respective transfer functions. For the cases shown, the values of \log_{10} of the phugoid frequency range from about -1.25 at the lowest dynamic pressure to about -0.5 at the highest dynamic pressure. Note that in the \hat{u}/δ_p responses, a plateau exists at frequencies just below the phugoid frequency in which the amplitude \hat{u}/δ_p is independent of frequency. For the uniform-atmosphere cases, this amplitude level is equal to the zero-frequency asymptote and can be used to obtain a static value of the static speed control parameter δ_p/\hat{u} . The value of δ_p/\hat{u} thus obtained corresponds to a constant-altitude constraint because even though the final altitude following a step control input is different, in general, from the initial altitude, the altitude change has no effect under the assumption of a uniform atmosphere. The sign of δ_p/\hat{u} is determined from the phase angle of the asymptote form of the frequency response (which is either 0° or 180°) in this same frequency range.

For the standard-atmosphere cases, the zero-frequency asymptote of \hat{u}/δ_p has little significance because of the long time required for the aircraft motions to approach the final conditions. The value of δ_p/\hat{u} corresponding to frequencies just below the

phugoid frequency, on the other hand, is believed to represent a meaningful measure of the tendency within a time range measured in minutes for the speed to return to its trim value under conditions of no control action, that is, no altitude constraint. Thus, a distinction is drawn between two speed stability indices, both expressed as values of δ_p/\hat{u} . One, determined from the standard-atmosphere solutions, is a measure of the unconstrained speed restoring tendency, and the other, determined from the uniform-atmosphere solutions, is a measure of the control required to change speed at constant altitude.

The static maneuvering control parameter δ_p/n_p is traditionally determined from solution of a two-degree-of-freedom (decoupled short period) set of equations of motion. The n_p/δ_p frequency response curves identified as "constant speed" in figure 12 were obtained from solutions of equation (55) combined with an appropriate form of the normal-acceleration equation. The asymptote form of the frequency response of n_p/δ_p obtained from the standard-atmosphere and uniform-atmosphere solutions of the complete three-degree-of-freedom equations of motion are also shown for comparison. For the lower three values of dynamic pressure, the levels of n_p/δ_p in the frequency range between the phugoid and short-period frequencies from the standard- and uniform-atmosphere solutions are identical with the zero-frequency asymptote of the constant-speed solutions. Note that at these three values of \bar{q} , the short-period mode is oscillatory and its frequency is well separated from that of the phugoid mode. For the two higher values of \bar{q} , the short-period root pair has branched into two real roots, and the frequency range of the n_p/δ_p plateau between the phugoid roots and the smaller root of the short-period pair is greatly diminished or nonexistent. The plateau level of n_p/δ_p from the three-degree-of-freedom solution is no longer identical to the zero-frequency asymptote of the two-degree-of-freedom solution. While the static maneuvering control parameter δ_p/n_p obtained from the three-degree-of-freedom solution is probably more representative of the actual case than that from the constant-speed solution, this distinction may be of only academic interest when the large dynamic instability of the phugoid mode for these high-dynamic-pressure cases (fig. 10) is recalled.

The values of δ_p/\hat{u} and δ_p/n_p obtained from the appropriate three-degree-of-freedom transfer functions by the procedure just described are presented in figure 13 for the rigid airplane and in figure 14 for the elastic airplane. In a few cases, the pole-zero configurations of the transfer functions were such that the appropriate plateaus in the frequency response curves did not exist, and these points are omitted from figures 13 and 14. The assumption of a locally uniform atmosphere had little effect on the maneuver control parameter δ_p/n_p but showed a destabilizing effect on the speed control parameter δ_p/\hat{u} , particularly at supersonic speed. This result implies that the unconstrained speed-restoring tendency, indicated by the standard-atmosphere results, is significantly more stable than would be inferred from measurements of the control gradient with speed at constant altitude, as indicated by the uniform-atmosphere results.

The static speed control parameter and maneuvering control parameter for the rigid airplane reflect the expected reduction in static stability with rearward center-of-gravity movement and increase in control sensitivity with increasing \bar{q} . Comparison of figures 13 and 14 reveals several manifestations of aeroelasticity. At low dynamic pressure, an aeroelastic reduction in static stability is indicated by reduced magnitudes of both δ_p/\hat{u} and δ_p/n_p . The subsequent increase in the magnitude of δ_p/n_p at high dynamic pressures is related to the aeroelastic loss in the control effectiveness derivative $C_{m\delta}$. The aeroelastic loss in $C_{m\delta}$ is not sufficient, however, to explain the large increase in δ_p/\hat{u} at high dynamic pressures shown in figure 14, particularly when the large destabilizing aeroelastic effect on the partial derivative $\partial C_m/\partial \alpha$ shown in figure 7 is recalled.

Further insight into the nature of aeroelastic effects on static stability may be gained by an examination of approximate forms relating static margin and maneuver margin to the stability derivatives. If the atmosphere is assumed to be locally uniform, the reference flight condition to be straight and level with α_1 small, and the perturbed flight condition to be steady trimmed flight along a curved path, then

$$C_N = C_{N,1} + \alpha_p C_{N\alpha} + \hat{u} C_{N\hat{u}} + q_p \frac{c}{2V_1} C_{Nq} + \delta_p C_{N\delta}$$

$$C_m = 0 = \alpha_p C_{m\alpha} + \hat{u} C_{m\hat{u}} + q_p \frac{c}{2V_1} C_{mq} + \delta_p C_{m\delta}$$

Also,

$$C_N = \frac{nW}{\bar{q}S} \cong \frac{W}{\bar{q}_1 S} (n_1 + n_p) (1 - 2\hat{u})$$

$$n_p = \frac{V_1}{g_0} q_p$$

Thus, by substitution

$$\alpha_p C_{N\alpha} + \hat{u} (2C_{N,1} + C_{N\hat{u}}) + n_p \left(\frac{g_0 c}{2V_1} C_{Nq} - \frac{W}{\bar{q}_1 S} \right) + \delta_p C_{N\delta} = 0 \quad (58a)$$

$$C_m = \alpha_p C_{m\alpha} + \hat{u} C_{m\hat{u}} + n_p \frac{g_0 c}{2V_1} C_{mq} + \delta_p C_{m\delta} = 0 \quad (58b)$$

The stability margins can be expressed as values of the total derivative dC_m/dC_N for the untrimmed perturbed state ($C_m \neq 0$) obtained by constraining δ_p to zero. The

form of an additional constraint is used to distinguish between static margin and maneuver margin. For level flight at varying speed, the constraint $n_p = 0$ is imposed and

$$\text{Static margin} = \left(\frac{dC_m}{dC_N} \right)_{n_p = \delta_p = 0} = \frac{C_{m\alpha}}{C_{N\alpha}} \left(1 + \frac{C_{N\hat{u}}}{2C_{N,1}} \right) - \frac{C_{m\hat{u}}}{2C_{N,1}} \quad (59a)$$

Similarly, for maneuvering flight at constant speed, \hat{u} is constrained to zero and

$$\text{Maneuver margin} = \left(\frac{dC_m}{dC_N} \right)_{\hat{u} = \delta_p = 0} = \frac{C_{m\alpha}}{C_{N\alpha}} \left(1 - \frac{g_0 \rho S c}{4W} C_{Nq} \right) + \frac{g_0 \rho S c}{4W} C_{mq} \quad (59b)$$

Alternatively, by constraining either n_p or \hat{u} to zero, equations (58) can be solved directly for the static control parameters

$$\frac{\delta_p}{\hat{u}} = 2C_{N,1} \frac{\text{Static margin}}{C_{m\delta} - C_{N\delta} \frac{C_{m\alpha}}{C_{N\alpha}}} \quad (60a)$$

$$\frac{\delta_p}{n_p} = - \frac{W}{\bar{q}_1 S} \frac{\text{Maneuver margin}}{C_{m\delta} - C_{N\delta} \frac{C_{m\alpha}}{C_{N\alpha}}} \quad (60b)$$

The approximations provided by equations (60) are plotted in figures 13 and 14 and, in nearly all cases, agree very well with the results from the transfer function solutions for the uniform-atmosphere cases. Thus, the mechanism responsible for the extreme values of δ_p/\hat{u} observed for the elastic airplane at the highest dynamic pressure must be embodied in equations (59) and (60). Equations (60) imply that the aeroelastic reduction in $C_{m\delta}$ should affect both δ_p/\hat{u} and δ_p/n_p in a similar fashion. It might be noted in passing that the combined control effectiveness parameter $C_{m\delta} - C_{N\delta} \frac{C_{m\alpha}}{C_{N\alpha}}$ was found to be independent of center-of-gravity position even for the elastic airplane.

The difference between the trends of δ_p/\hat{u} and δ_p/n_p with dynamic pressure arises from the difference between the static margin and maneuver margin. These stability margins evaluated from equations (59) are shown for the rigid airplane in figure 15 and for the elastic airplane in figure 16. Values of $C_{m\alpha}/C_{N\alpha}$, which is indicative of the distance from the center of gravity to the aerodynamic center, are also shown to demonstrate the contribution of $C_{N\hat{u}}$ and $C_{m\hat{u}}$ to the static margin and the contribution of

C_{Nq} and C_{mq} to the maneuver margin. Considering first the rigid airplane (fig. 15), the maneuver margin is shown to be more negative (stable) than $C_{m\alpha}/C_{N\alpha}$, particularly at the subsonic speed. The generally stabilizing contribution of C_{mq} to the maneuver margin is thoroughly documented in the literature. The contributions of the \hat{u} derivatives to the static margin are not as well documented but are shown by figure 15 to be significant for the cases considered. For the rigid airplane, the \hat{u} derivatives arise only from the effects of Mach number perturbation. Their contribution to the static margin is generally stabilizing at $M = 2.7$ but destabilizing at $M = 0.8$. For the subsonic cases with the rearward c.g. location, the static margin is shown to be positive (unstable) in spite of the value of $C_{m\alpha}/C_{N\alpha}$ of -0.03 . This result is compatible with the existence of a divergent root of the phugoid pair shown for the uniform-atmosphere cases in figure 9(b). Figure 15 also shows that the change in static margin with a change in c.g. location is significantly different from the change in $\left(\frac{x}{c}\right)_{c.g.}$. This result arises primarily from the effect of $C_{N\hat{u}}$. The contribution of C_{Nq} to the maneuver margin was found to be much less significant.

For the elastic airplane (fig. 16), the values of $C_{m\alpha}/C_{N\alpha}$ became highly positive at high dynamic pressure. The \hat{u} derivatives now include the aeroelastic effects arising from dynamic-pressure perturbations (eqs. (18)) which were found to predominate over the Mach number effects. Similarly, the q derivatives include the aeroelastic effects from n_p which were much larger than the direct aerodynamic effects of pitching velocity. The resulting contributions of $C_{m\hat{u}}$ to static margin and of C_{mq} to maneuver margin were always stabilizing. Moreover, the effects of $C_{N\hat{u}}$ and C_{Nq} were significant and always acted to reduce the contribution of $C_{m\alpha}/C_{N\alpha}$ to the stability margins. In particular, for the highest dynamic pressure at $M = 0.8$, the values of $C_{N\hat{u}}/2C_{N,1}$ were of the order of -1 ; the contribution of $C_{m\alpha}/C_{N\alpha}$ in equation (59a) was therefore of little significance and the static margin became extremely stable, leading to the large values of δ_p/\hat{u} previously noted.

Figure 16 also shows that as dynamic pressure was increased, the stability margins became less sensitive to c.g. location, and the trend of static margin with c.g. location actually reversed at high dynamic pressures for $M = 0.8$. Furthermore, calculations made at intermediate c.g. locations showed that the variations of both static margin and maneuver margin with c.g. location became nonlinear in such a manner as to cast doubt on the existence of a neutral point or maneuver point.

Added confidence in the validity of equations (59) is gained by correlating the results shown in figure 16 with the characteristic roots for the uniform-atmosphere cases of figure 10. Note that a divergent real root is shown in figure 10 for each case for which either the static margin or maneuver margin is unstable as shown in figure 16. Furthermore, the appearance of an aperiodic short-period mode at intermediate values of dynamic

pressure for the lightweight, rearward c.g., subsonic condition (fig. 10(b)) appears to be related to the minimum in the stable values of maneuver margin shown in figure 16(a) at intermediate values of dynamic pressure for the corresponding condition. This latter correlation is suggested by the similarity between the form of equation (59b) for maneuver margin and that of equation (56a) for ω_{sp}^2 .

Effect of Dynamic-Pressure Derivatives

One of the departures from past practice embodied in the present development is the inclusion of the aeroelastic effects of dynamic-pressure perturbations in the stability derivatives with respect to \hat{u} used in the three-degree-of-freedom dynamic analysis. To illustrate the significance of this feature, stability analyses were made for a single (forward) c.g. location with the dynamic-pressure contribution to the derivatives $X_{\hat{u}}$, $Z_{\hat{u}}$, and $M_{\hat{u}}$ omitted. The aeroelastically corrected Mach number contributions were included, however. The resulting characteristic stability roots are compared in figure 17 with those from the more complete analyses under the assumption of a locally uniform atmosphere. The omission of the \bar{q} contribution had little effect on the short-period roots except for those cases in which coupling between the short-period and phugoid roots resulted in a coupled oscillatory mode. The omission had a strong destabilizing effect on the phugoid mode, however, particularly for the subsonic conditions, and resulted in an aperiodic divergence for all but the lowest dynamic pressures. The resulting effect on the static control parameters is shown in figure 18 by the curves paired with solid lines. As would be expected from the characteristic roots, omission of the \bar{q} contribution had little effect on the maneuvering control parameter δ_p/n_p but resulted in strongly unstable values of the speed control parameter δ_p/\hat{u} .

Alternative Formulations for Normal-Acceleration Contribution

In the present formulation, the effects of aeroelastic distortion due to normal acceleration are embodied implicitly in the stability derivatives as indicated by the terms in equations (18) involving partial derivatives with respect to n . One alternative formulation which has been used in some segments of the industry results from omitting these terms from the stability derivatives defined by equations (18) and retaining derivatives with respect to n as explicit coupling terms in the three force and moment equations of motion. The set of equations of motion must then include an additional equation such as equation (34) to define the role of these coupling terms in the dynamic solution. The resulting solution is identical to that from the present formulation, but approximate expressions for static stability and control parameters would appear more complicated than those presented herein.

Another alternative formulation is that denoted in reference 2 as "Formulation I" and in reference 3 as the "Direct Formulation." In these formulations, the normal-acceleration contributions are broken down into inertial derivatives with respect to variables representing linear acceleration \dot{w} , centrifugal acceleration q , and gravity orientation θ . These inertial derivatives appear in the equations of motion along with aerodynamic derivatives representative of the "zero mass" elastic airplane. The dynamic solution of these equations is equivalent in all important respects to that from the present formulation with the reservation that the contribution of dynamic-pressure perturbations to the forward-speed derivatives is not included in the dynamic formulations of references 2 and 3. Although the inertial derivatives appear in combination with aerodynamic derivatives in the equations of motion, it is not recognized in references 2 and 3 that these combined derivatives can be considered as stability derivatives generally applicable to static stability, control, and performance analysis, as well as dynamic analysis.

The final formulation to be discussed is that denoted in reference 2 as "Formulation II" and in reference 3 as the "Indirect Formulation." It is stated in those references that this formulation "represents what has been the standard method of accounting for inertial effects, or as it is frequently called, inertial relief." The derivation of this formulation makes use of the expression

$$n = 1 + n_p = 1 + \frac{C_{L,p}}{C_{L,1}} \quad (61)$$

Note that this expression implies that n is the load factor rather than the component of acceleration normal to a structural reference plane. Note also that this expression is valid only for constant dynamic pressure.

To describe the concept of the indirect formulation in the notation of the present paper,

$$C_L = C_{L,1} + \sum_{k=1}^K p_{p,k} \frac{\partial C_L}{\partial p_k} \quad (62a)$$

$$C_m = C_{m,1} + \sum_{k=1}^K p_{p,k} \frac{\partial C_m}{\partial p_k} \quad (62b)$$

$$C_D = C_{D,1} + \sum_{k=1}^K p_{p,k} \frac{\partial C_D}{\partial p_k} \quad (62c)$$

where p_k is a set of K physical variables having n as a member. The indirect formulation makes use of equation (61) to show that the following expressions are equivalent to equations (62):

$$C_L = C_{L,1} + \sum_{k=1}^{K-1} p_{p,k} \left(\frac{\frac{\partial C_L}{\partial p_k}}{1 - \frac{1}{C_{L,1}} \frac{\partial C_L}{\partial n}} \right) \quad (63a)$$

$$C_m = C_{m,1} + \sum_{k=1}^{K-1} p_{p,k} \left(\frac{\frac{\partial C_m}{\partial p_k} + \frac{\frac{\partial C_m}{\partial n} \frac{\partial C_L}{\partial p_k}}{C_{L,1} - \frac{\partial C_L}{\partial n}}}{C_{L,1} - \frac{\partial C_L}{\partial n}} \right) \quad (63b)$$

$$C_D = C_{D,1} + \sum_{k=1}^{K-1} p_{p,k} \left(\frac{\frac{\partial C_D}{\partial p_k} + \frac{\frac{\partial C_D}{\partial n} \frac{\partial C_L}{\partial p_k}}{C_{L,1} - \frac{\partial C_L}{\partial n}}}{C_{L,1} - \frac{\partial C_L}{\partial n}} \right) \quad (63c)$$

where n is not included in the set of $K - 1$ physical variables p_k . The expressions in parentheses in equations (63) can then be transformed into stability derivatives with respect to the motion variables by a procedure analogous to that used in the present formulation.

The indirect formulation was applied to the forward c.g., uniform-atmosphere cases of the present analysis. The resulting characteristic roots are compared with those from the present formulation in figure 19, and the static control parameters obtained from the transfer function solutions are shown in figure 18. Although the contributions of dynamic-pressure perturbation were not included in the indirect formulation of references 2 and 3, it is clear from equations (63) that \bar{q} could be either included in or excluded from the set of physical variables. Both conditions are represented by the results given in figures 18 and 19. The effects of omitting the \bar{q} contribution in the indirect formulation are similar to the effects already discussed relative to the present formulation.

The indirect formulation predicts a significantly greater speed stability than the present formulation as evidenced by larger values of both the speed control parameter $\delta p / \hat{u}$ and the phugoid frequency. This discrepancy of speed-related characteristics

should be anticipated from the invalidity of equation (61) under conditions of varying dynamic pressure. A more subtle inadequacy of the indirect formulation is revealed by observing that although the maneuver control parameter δ_p/n_p is accurately predicted, the magnitude of the short-period roots is consistently underpredicted. This discrepancy is apparently related to the inappropriate application of inertial relief, under the indirect formulation, to all derivatives including those describing control effectiveness.

CONCLUDING REMARKS

A set of longitudinal stability derivatives has been defined, and the corresponding equations of motion formulated, applicable to the analysis of longitudinal static and dynamic stability, control, and performance of elastic airplanes. This development is subject to the assumptions of small perturbations from a steady reference flight condition, structural deflection constrained to a direction normal to a structural reference plane, and the quasi-steady aeroelastic assumption of structural deflections proportional to applied loads. The development described herein avoids any constraint on the forward-speed degree of freedom, and the resulting stability derivatives exhibit two important departures from past practice: (1) The aeroelastic contributions of dynamic-pressure perturbations are included, and (2) the aeroelastic contributions of normal acceleration appear primarily in the derivatives with respect to pitching velocity and angle-of-attack rate and, for an unaccelerated reference flight condition, do not influence the derivatives with respect to angle of attack.

Approximate expressions for the static and maneuvering stability margin and control parameters in terms of the stability derivatives defined herein have been shown by means of illustrative calculations to correlate well with the characteristic stability roots and response to control inputs calculated by solution of the dynamic equations of motion. Some results of illustrative analyses of an elastic airplane cast doubt on the general existence of a neutral point or maneuver point where these points are defined as center-of-gravity locations corresponding to zero static margin or maneuver margin, respectively. Some of the results for an elastic airplane at high dynamic pressure indicate that for stable values of both the static margin and maneuver margin, as the maneuver margin becomes small, coupling between the short-period and the phugoid modes can result in a strongly unstable phugoid oscillation at a significantly increased frequency. Further increases in phugoid frequency result from consideration of the variation of atmospheric properties with altitude.

The present formulation of the longitudinal stability and control problem for elastic airplanes is shown to be more complete than several alternative formulations, and one

commonly used alternative is shown to yield significantly inaccurate predictions of not only the speed stability and phugoid characteristics, but also the short-period frequency and damping.

Langley Research Center,
National Aeronautics and Space Administration,
Hampton, Va., January 21, 1972.

APPENDIX

A FORTRAN PROGRAM FOR CALCULATING LONGITUDINAL STABILITY DERIVATIVES OF ELASTIC OR RIGID AIRPLANES

The FORTRAN program described herein calculates the longitudinal stability derivatives of an elastic airplane using the procedure outlined in the section of this paper entitled "Calculation of Stability Derivatives." The aerodynamic and structural influence-coefficient matrices and the airplane jig shape are not calculated in the program but must be supplied as inputs. The program is written in CDC FORTRAN IV, version 2.3 to run on Control Data 6000 series computers with the SCOPE 3.0 operating system and library tape. The statements in the program most likely to require change to run on other operating systems are those calling the library subroutine MATRIX, which is used in this program only for matrix multiplication and inversion. The program is dimensioned to accommodate up to 120 panels on one side of the aircraft plane of symmetry and requires a field length of approximately 140 000g words. Input and output data are in U.S. Customary Units.

Input Data

The force sign convention used in the program is such that positive forces act in the negative Z-direction. The elements of both the aerodynamic and the structural matrices, therefore, have signs opposite to those of the $[A]$ and $[S]$ matrices as defined in the body of this paper. Units of the matrix elements are feet² for the $[A]$ matrix and 1/pound for the $[S]$ matrix.

Tape inputs. - TAPE 1 must contain the elements of three aerodynamic influence-coefficient matrices: The first corresponds to the nominal Mach number AM , the second to a slightly higher Mach number $AM + DM$, and the third to a slightly lower Mach number $AM - DM$. A value of DM of about 2 to 4 percent of AM is suggested. Each matrix has dimensions $M \times M$, where M is the number of panels on one side of the aircraft plane of symmetry. The matrix elements are arranged in the following order: $A(1,1)$, $A(1,2)$, . . . , $A(1,M)$, $A(2,1)$, . . . , $A(2,M)$, . . . , $A(M,M)$, where the first index is the aerodynamic control point (slope point) index and the second is the load point index. No end-of-file code is to be used between successive matrices.

TAPE 2 must contain the elements of two structural slope influence-coefficient matrices: The first relates slopes at slope points to unit loads at load points, and the second relates slopes at load points to unit loads at load points. Each matrix has dimensions $M \times M$, and the matrix elements are arranged in order: $S(1,1)$, $S(1,2)$, . . . , $S(2,M)$, . . . , $S(M,M)$, where the first index is the slope point index and the second is the load point index. No end-of-file code is to be used between the two matrices.

APPENDIX - Continued

Card inputs. - The program is organized to execute multiple cases by use of nested DO loops. The outer loop provides for various center-of-gravity locations, and successive inner loops provide for various airplane weights at each center of gravity, various dynamic pressures at each weight, and various load factors at each dynamic pressure. Level 1 input cards apply to all cases and are read once. Level 2 cards must be supplied for each center of gravity, level 3 for each weight and center of gravity, and level 4 for each dynamic pressure, weight, and center of gravity.

Level 1

Card 1, Format(3I1,2I3,5F10.0)

IFLEX Set 1 for elastic case, requires TAPE 1 and TAPE 2. Set 0 for rigid case, requires TAPE 1 only.

LIST Set 1 for output listing of elastic air loads and flexible slope increments due to jig shape, alpha, delta, and normal acceleration and total slopes for reference flight condition. Set 0 to delete above listings from output.

LFT Set 1 for banked-turn reference flight condition. Set 0 for wings-level reference flight condition.

M number of panels on one side of aircraft plane of symmetry

NC number of center-of-gravity locations

AM Mach number of reference flight condition

DM Mach number increment used in preparing TAPE 1

SREF reference wing area, feet²

CBAR reference chord, feet

CAF increment in axial-force coefficient (skin friction, wave drag due to volume, etc.) to be added to that calculated from pressures normal to mean camber surface.

Each of the following arrays is required in format (8F10.0), I ranges from 1 to M:

APPENDIX – Continued

TSR(I,1)	mean-camber-surface slope at control point I due to jig shape, $\{\epsilon_j\}$, radians
TSR(I,3)	increment in mean-camber-surface slope at control point I due to unit δ , $\{\epsilon_{\delta}\}$, radians
TLRJ(I)	mean-camber-surface slope at load point I due to jig shape, $\{\epsilon_{j,f}\}$, radians
TLRD(I)	increment in mean-camber-surface slope at load point I due to unit δ , $\{\epsilon_{\delta,f}\}$, radians
XSO(I)	x-coordinate of slope point I from nominal origin, X positive forward, feet
XLO(I)	x-coordinate of load point I, feet

Level 2

Card 1, Format(I3,F10.0)

NW	number of airplane weights
XCG	x-coordinate of center of gravity from nominal origin, X positive forward, feet

Level 3

Card 1, Format(I3,4F10.0)

NQ	number of dynamic pressures
W	airplane weight, pounds
YI	moment of inertia in pitch, I_y , slug-feet ²
Y1	$(I_z - I_x)/I_y$ (A value of 1.0 is appropriate if the actual value is unknown.)
Y2	I_{xz}/I_y (A value of 0. is appropriate if the actual value is unknown.)

The following array is required only if IFLEX has been set to 1, format (6F12.0), I ranges from 1 to M:

FI(I)	weight assigned to panel I, assumed to be located at load point I, pounds
-------	---

APPENDIX – Continued

Level 4

Card 1, Format(I3,6F10.0)

NN	number of load-factor values
Q	dynamic pressure in reference flight condition, pounds/foot ²
V	true airplane velocity in reference flight condition, feet/second
G	gravity acceleration in reference flight condition, feet/second ²
RHO	air density in reference flight condition, ρ_1 , slugs/foot ³
RHOH	$\left(\frac{\partial \rho}{\partial h}\right) / \rho_1$, 1/foot
AH	$\left(\frac{\partial a}{\partial h}\right) / a_1$, 1/foot

Card(s) 2, Format(8F10.0)

FL(I)	load factor in reference flight condition, I ranges from 1 to NN (Note that FL = G/32.174 for a straight, level reference condition.)
-------	---

Output Data

Program output is listed in two parts. The first part is identified by the values of Mach number, center-of-gravity location, weight, and dynamic pressure read in as input. This part presents a tabulation over all panel load points of the aerodynamic normal force divided by dynamic pressure and the flexible increment in mean-camber-surface slope produced by the jig shape and by unit values of angle of attack, control deflection, and normal acceleration.

The second part is repeated for each input value of load factor and presents data in five groups identified as trim values, derivative contributions, stability derivatives, static parameters, and total trim condition slopes. The trim values define the reference flight condition and include $C_{A,1}$, $C_{N,1}$, $C_{m,1}$, α_1 , δ_1 , θ_1 , ϕ , n_1 , and $q_1 c / 2V_1$ along with the number of iterations used to solve the nonlinear reference equations. The derivative contributions include the increments in C_N and C_m due to jig shape and the partial derivatives of C_A , C_N , and C_m with respect to α , δ , $qc/2V$, n , \dot{q} , M , and \bar{q} . The stability derivatives are presented in both coefficient form (C_A , C_N , and C_m) and dimensional form (X , Z , and M) as derivatives of these quantities with respect to \hat{u} , $\hat{\dot{u}}$,

APPENDIX – Continued

α , $\dot{\alpha}$, θ , q (or $qc/2V$ in the case of the coefficient derivatives), \dot{q} , δ , and h . Unsteady aerodynamic effects are not considered in the program, and therefore the values of the derivatives with respect to \dot{u} , $\dot{\alpha}$, and \dot{q} reflect only the aeroelastic effects arising from inertial loading. The static parameters include the stability derivative ratio $C_{m\alpha}/C_{N\alpha}$ and the values of static margin, maneuver margin, δ_p/\hat{u} , and δ_p/n_p calculated from equations (59) and (60) of this paper. The mean-camber-surface slopes in the reference flight condition are tabulated over all panel slope points and load points.

The units of all output quantities not defined as input data are as defined in the main text of this paper except that normal force per unit dynamic pressure is in feet² and altitude is in feet.

Sample Cases

Listings of input data cards and program output for two sample cases are given on the following pages. Both cases correspond to the airplane used for the illustrative analysis of this paper flying at its supersonic design condition. Sample case 1 is for the rigid airplane, and sample case 2 is for the flexible airplane. The nominal origin of x-coordinates is at 0.33c. The airplane is represented by 110 panels numbered consecutively from leading edge to trailing edge in rows progressing from root to tip. The supersonic paneling arrangement includes 11 chordwise rows with 10 panels per row. Data tabulated over all panels are listed in the order of panel numbers.

Program compilation and execution required 7 seconds of central processor time for sample case 1 and 48 seconds for sample case 2.

APPENDIX - Continued

106.718	84.264	61.810	39.356	16.901	-5.553	-28.007	-50.461	} x _a
-72.915	-65.372	55.089	44.755	30.422	16.089	1.756	-12.578	
-26.511	-41.244	-55.577	-69.914	40.796	28.387	15.977	3.568	
-8.841	-21.250	-33.660	-46.069	-58.478	-70.888	22.414	11.835	
1.256	-5.323	-19.901	-30.480	-41.059	-51.638	-62.217	-72.796	
3.947	-4.892	-13.730	-22.569	-31.407	-40.246	-49.084	-57.922	
-66.761	-75.599	-14.613	-21.809	-29.004	-36.200	-43.395	-50.591	
-37.786	-64.982	-72.177	-79.373	-33.227	-28.835	-44.443	-50.052	
-55.660	-61.269	-66.877	-72.486	-78.094	-83.703	-51.854	-55.890	
-55.526	-63.962	-67.998	-72.035	-76.071	-80.107	-84.143	-86.179	
-66.429	-65.252	-72.075	-74.898	-77.722	-80.545	-83.368	-86.191	
-39.014	-51.837	-76.963	-78.944	-80.526	-82.907	-84.889	-86.871	
-88.852	-90.834	-92.816	-94.757	-87.514	-88.672	-89.831	-90.989	
-92.148	-93.306	-94.465	-95.623	-96.782	-97.940			
121.227	98.029	74.820	51.612	28.403	5.195	-18.014	-41.223	
-54.431	-87.640	65.759	51.403	37.047	22.651	8.335	-6.021	
-20.378	-34.724	-45.090	-83.448	46.620	34.188	21.755	9.322	
-3.110	-15.543	-27.975	-40.408	-52.841	-65.273	27.446	16.842	
6.238	-4.366	-14.971	-25.575	-36.179	-46.783	-57.388	-67.992	
8.220	-6.635	-5.500	-18.366	-27.231	-36.096	-44.961	-52.826	
-62.691	-71.557	-11.017	-18.242	-25.468	-32.693	-39.918	-47.143	
-54.368	-61.554	-68.819	-76.044	-30.251	-35.896	-41.541	-47.187	
-52.832	-58.477	-64.122	-65.767	-75.413	-81.058	-49.410	-53.497	
-57.584	-61.671	-65.759	-69.846	-73.933	-78.020	-82.107	-86.195	
-64.884	-67.728	-70.573	-73.418	-76.262	-79.107	-81.952	-84.796	
-87.641	-90.486	-75.690	-77.701	-75.711	-81.722	-83.732	-85.743	
-87.753	-89.764	-91.775	-93.785	-86.350	-87.557	-88.763	-89.970	
-91.176	-92.383	-93.599	-94.796	-96.002	-97.209			
1-9.823								
1472F0C.	4256C916.	1.	0.				Level 2	
1556.615	2613.82	31.973	.CCCC17465	-.CCCC475 C.			Level 3	
.993753							Level 4	

APPENDIX - Continued

PROGRAM OUTPUT - SAMPLE CASE 1

AEROELASTIC DERIVATIVES, M= 2.700, XCG= -9.823, W= 472500, QBAR= 596.62

ELASTIC AIRLOADS PER Q DUE TC JIG SHAPE							
4.405167	5.086942	6.407287	5.590033	4.137748	1.658043	-1.973766	-4.281655
-8.101925	-5.825629	2.066525	3.560051	3.310008	2.858762	2.303882	1.333546
.371886	-.545671	-1.497147	-2.352072	-.653648	3.177942	2.440543	2.408191
2.124071	1.518737	1.015405	.307909	-.344136	-.949054	-2.276323	1.950561
1.846014	2.000352	1.950671	1.554878	1.197829	.774787	.332770	-.040082
-3.577497	.861491	1.613613	1.468820	1.537863	1.432235	1.180391	.962500
.749346	.489162	-4.567554	.003242	1.076597	1.013636	1.113711	1.216811
1.157658	.988819	.800750	.650775	-5.144581	-1.041628	.626273	.865549
.794494	.7C7317	.726670	.774167	.737781	.600802	-5.457209	-1.526993
-.306045	.263062	.378186	.378769	.320750	.242784	.295200	.434817
-3.965022	-2.247014	-1.251506	-.588971	-.150487	.135972	.244314	.231376
.162971	.085693	-1.451682	-2.063045	-1.750670	-1.370496	-1.039768	-.781034
-.522849	-.289209	-.119487	-.023573	.055301	-.623199	-.926234	-1.128723
-1.165501	-1.117301	-1.034143	-.942978	-.849150	-.752640		

ELASTIC AIRLOADS PER Q DUE TC ALPHA							
149.818868	99.252230	99.386244	116.837692	126.397336	134.199253	137.049141	134.909163
104.610133	52.649335	170.638300	92.936603	78.378010	75.325785	74.677153	75.125170
75.136618	74.665779	72.390064	66.481118	180.308611	100.213469	81.761404	74.373917
71.263026	70.013380	68.565508	68.104686	66.901651	64.536145	183.797293	102.669730
82.799433	72.631784	67.249463	65.149742	63.293960	61.576594	60.865743	59.815470
182.627076	102.495503	81.837039	70.107545	63.472436	59.577503	58.183180	56.485101
54.687695	53.506766	177.915649	100.487495	77.388528	66.896804	59.962141	55.245622
52.180692	50.892719	49.937338	48.327395	169.214616	95.769864	71.727225	61.029331
55.441732	51.305983	47.478609	44.581055	43.062685	43.184773	155.538858	88.224507
65.643622	52.061183	45.853602	45.481612	44.911300	43.635639	41.604817	39.146471
109.312972	78.634141	60.797135	49.212877	41.186243	34.759944	32.125564	31.094826
30.735940	30.495578	58.849529	64.530916	57.373415	49.801898	43.254497	38.002822
33.034518	28.656907	25.071517	22.740085	26.594636	28.584089	30.718088	32.887397
33.654015	32.852887	31.404300	29.787274	28.086723	26.314033		

ELASTIC AIRLOADS PER Q DUE TO DELTA							
0.000000	0.000000	0.000000	0.000000	0.000000	0.000000	0.000000	.410456
3.796512	5.776272	0.000000	0.000000	0.000000	0.000000	0.000000	0.000000
0.000000	.036935	.703706	8.182117	0.000000	0.000000	0.000000	0.000000
0.000000	0.000000	0.000000	.008863	5.904510	53.047485	0.000000	0.000000
0.000000	0.000000	0.000000	0.000000	0.000000	.001893	32.852237	50.013243
0.000000	0.000000	0.000000	0.000000	0.000000	0.000000	0.000000	.000347
4.269627	18.657504	0.000000	0.000000	0.000000	0.000000	0.000000	0.000000
0.000000	.000053	31.418286	48.231617	0.000000	0.000000	0.000000	0.000000
0.000000	0.000000	0.000000	.000005	49.519799	52.151664	0.000000	0.000000
0.000000	0.000000	0.000000	0.000000	0.000000	12.447534	30.458912	30.913052
0.000000	0.000000	0.000000	0.000000	0.000000	0.000000	0.000000	0.000000
.596008	2.451511	0.000000	0.000000	0.000000	0.000000	0.000000	0.000000
0.000000	0.000000	0.000000	0.000000	0.000000	0.000000	0.000000	0.000000
0.000000	0.000000	0.000000	0.000000	0.000000	0.000000	0.000000	0.000000

APPENDIX - Continued

LOAD FACTOR = .99375

TRIM VALUES (2 ITERATIONS)
 CA = .004759 ALPHA = .048506 PHI = 0.000000
 CN = .079145 DELTA = .000002 AN, G = .992584
 CM = 0.000000 THETA = .048506 QC/ZV = .000000

DERIVATIVE CONTRIBUTIONS								
JIG SHAPE	ALPHA	DELTA	QC/ZV	AN, G	QDOT	MACH	DYN PRESS	
CA	-.0301833	.0031426	.0038041	0.0000000	0.0000000	.0006716	0.00000000	
CN	.003698	1.555408	.088980	.672663	0.000000	0.000000	-0.018491	0.0000000
CM	.009699	-.199950	-.049690	-.539630	0.000000	0.000000	.003161	0.0000000

STABILITY DERIVATIVES									
	U	UDDT	ALPHA	ALPHA DDT	THETA	Q	QDOT	DELTA	ALTITUDE
CA	.0018134	-0.0000000	-.0301833	-0.0000000	-0.0000000	.0038041	0.0000000	.0031426	0.
CN	-.049926	-0.000000	1.555408	-0.000000	-0.000000	.672663	0.000000	.088980	0.
CM	.008535	-0.000000	-.199950	-0.000000	-0.000000	-.539630	0.000000	-.049690	0.
X	-.001749	-0.000000	.004660	0.000000	-0.000000	-.000013	-0.000000	-.000485	3.48992E-08
Z	-.016729	-0.000000	-.240115	0.000000	-0.000000	-.002242	-0.000000	-.013736	5.80350E-07
M	.134113	0.000000	-3.141995	0.000000	0.000000	-.183071	0.000000	-.780820	0.

STATIC PARAMETERS
 CM ALPHA/CN ALPHA = -.128552
 STATIC MARGIN = -.141924
 MANEUVER MARGIN = -.130062
 DELTA/U = -.587300
 DELTA/AN, G = -.271118

TOTAL TRIM CONDITION SLOPES AT SLOPE POINTS								
-.0020858	.0217330	.0649896	.0721554	.0677656	.0584697	.0391723	.0218184	
-.0198222	-.0640468	-.0173182	.0054653	.0166327	.0223163	.0250962	.0253127	
.0236214	.0206850	.0164318	.0115639	-.0407757	-.0091252	-.0024986	.0047684	
.0093366	.0117246	.0128243	.0128901	.0118662	.0102982	-.0523926	-.0241893	
-.0143258	-.0061958	-.0008557	.0028021	.0053965	.0064772	.0073867	.0080739	
-.0646976	-.0367379	-.0204279	-.0144045	-.0089829	-.0049710	-.0015805	.0008318	
.0026083	.0040618	-.0768725	-.0474848	-.0314948	-.0236675	-.0175863	-.0126706	
-.0091525	-.0057909	-.0031590	-.0009919	-.0851170	-.0639445	-.0418934	-.0302575	
-.0242494	-.0208992	-.0176371	-.0140687	-.0112742	-.0093190	-.0979577	-.0725046	
-.0571262	-.0479388	-.0421487	-.0357561	-.0312538	-.0292484	-.0266985	-.0228268	
-.0668034	-.0616627	-.0569024	-.0507564	-.0464143	-.0432134	-.0397698	-.0373008	
-.0355413	-.0340052	-.0292534	-.0403315	-.0423783	-.0430595	-.0435389	-.0438973	
-.0442617	-.0445019	-.0446310	-.0446310	.0063823	-.0255481	-.0370163	-.0436609	
-.0436609	-.0436609	-.0436609	-.0436609	-.0436609	-.0436609			

TOTAL TRIM CONDITION SLOPES AT LOAD POINTS								
-.0436609	.1331082	.0554699	.0755199	.0738231	.0657633	.0510243	.0254630	
.0046529	-.0542514	-.0404669	-.0031124	.0133642	.0208076	.0247195	.0260645	
.0248230	.0224995	.0186951	.0137779	-.0615084	-.0174436	-.0048858	.0023824	
.0079625	.0111000	.0127531	.0132559	.0126468	.0110417	-.0688493	-.0334654	
-.0183140	-.0089998	-.0021476	.0012953	.0050137	.0060814	.0071688	.0078379	
-.0866568	-.0458547	-.0260490	-.0171017	-.0105445	-.0065365	-.0026051	.0000706	
.0020907	.0035243	-.0961399	-.0585720	-.0374848	-.0260449	-.0201491	-.0140063	
-.0105827	-.0069518	-.0039599	-.0018000	-.0883117	-.0722898	-.0505014	-.0335301	
-.0255958	-.0219175	-.0189672	-.0153701	-.0118612	-.0099250	-.0844228	-.0872726	
-.0613408	-.0487982	-.0435496	-.0370947	-.0308534	-.0283111	-.0269140	-.0230371	
-.0637906	-.0650822	-.0602126	-.0542942	-.0480599	-.0454076	-.0415073	-.0383499	
-.0363429	-.0343914	-.0176354	-.0369715	-.0420562	-.0428395	-.0434637	-.0437361	
-.0441703	-.0444051	-.0445780	-.0446094	.0253262	-.0117544	-.0343573	-.0437926	
-.0436609	-.0436609	-.0436609	-.0436609	-.0436609	-.0436609			

APPENDIX -- Continued

106.718	84.264	61.810	39.356	16.901	-5.553	-28.007	-50.461	} x_a	} Level 1		
-72.915	-95.372	59.089	44.755	30.422	16.089	1.756	-12.578				
-26.911	-41.244	-55.577	-69.514	40.796	28.387	15.977	3.568				
-8.841	-21.250	-33.660	-46.069	-58.478	-70.888	22.414	11.835				
1.256	-9.223	-19.901	-30.480	-41.059	-51.638	-62.217	-72.796				
3.547	-4.892	-13.730	-22.569	-31.407	-40.246	-49.084	-57.922				
-66.761	-75.599	-14.613	-21.809	-29.004	-36.200	-43.395	-50.591				
-57.786	-64.982	-72.177	-79.373	-33.227	-38.835	-44.443	-50.052				
-55.660	-61.269	-66.877	-72.486	-78.094	-83.703	-51.854	-55.890				
-59.926	-63.962	-67.998	-72.035	-76.071	-80.107	-84.143	-88.179				
-66.429	-69.252	-72.075	-74.898	-77.722	-80.545	-83.368	-86.191				
-89.014	-91.827	-76.953	-78.944	-80.926	-82.907	-84.889	-86.871				
-88.852	-90.834	-92.816	-94.757	-87.514	-88.672	-89.831	-90.989				
-92.148	-93.306	-94.465	-95.623	-96.782	-97.940						
121.237	98.029	74.820	51.612	28.403	5.195	-18.014	-41.223				
-64.421	-67.640	65.759	51.403	37.047	22.691	8.335	-6.021				
-20.378	-34.734	-49.090	-63.448	46.620	34.188	21.755	9.322				
-3.110	-15.543	-27.975	-40.408	-52.841	-65.273	27.446	16.842				
6.238	-4.366	-14.971	-25.575	-36.179	-46.783	-57.388	-67.992				
8.230	-6.635	-9.500	-18.366	-27.231	-36.096	-44.961	-53.826				
-62.691	-71.557	-11.017	-13.242	-25.468	-32.693	-39.918	-47.143				
-54.368	-61.594	-68.819	-76.144	-30.251	-35.896	-41.541	-47.187				
-52.822	-58.477	-64.122	-69.767	-75.413	-81.058	-49.410	-53.497				
-37.584	-61.671	-65.759	-69.846	-73.933	-78.020	-82.107	-86.195				
-64.884	-67.728	-70.573	-73.418	-76.262	-79.107	-81.952	-84.796				
-37.641	-90.486	-75.690	-77.701	-79.711	-81.722	-83.732	-85.743				
-87.753	-89.764	-91.775	-93.785	-86.350	-87.557	-88.763	-89.970				
-91.176	-92.383	-93.589	-94.796	-96.002	-97.209						
1-9.823										} Level 2	
1472500.	42560916. 1.	C.									
12392.932	5082.200	9545.400	8512.878	7968.411	8564.713					} W	} Level 3
10408.682	11051.640	5265.812	7899.260	-566.222	5861.568						
273.140	7257.929	4890.585	9056.290	1568.800	1867.500						
5627.078	3729.010	382.190	61.068	2540.879	-518.031						
11191.308	1621.030	1301.480	1285.460	1553.850	8894.700						
603.320	2833.442	8190.606	C.000	2915.319	2215.237						
2208.050	2011.224	942.290	-23.882	664.260	1825.644						
1558.755	4428.328	2486.367	2418.258	2099.000	1652.776						
16456.017	704.510	246.882	850.899	871.566	1036.160						
1772.157	1183.848	986.766	979.438	1086.094	280.930						
993.273	1196.724	197.690	902.372	1126.448	852.943						
1454.355	-72.070	385.106	236.080	779.323	664.872						
717.529	0.000	772.506	771.619	810.895	361.850						
485.540	375.130	72.122	67.310	67.575	293.290						
156.540	361.920	229.960	496.010	117.050	148.060						
202.010	0.000	112.950	145.890	-11.100	47.608						
27.619	58.599	2.417	68.255	127.410	42.469						
C.000	42.469	42.469	C.000	64.388	0.000						
64.388	0.000										
1596.615	2613.82	31.973	.00017463	-.0000475 0.				} Level 4			
.993753											

APPENDIX - Continued

PROGRAM OUTPUT - SAMPLE CASE 2

AEROELASTIC DERIVATIVES, M= 2.700, XCG= -9.823, W= 472500, QBAR= 596.62

ELASTIC AIRLOADS PER Q DUE TO JIG SHAPE								
5.810704	5.793022	6.845511	5.747565	3.9E5016	.918621	-2.722166	-5.006404	
-8.567500	-5.897203	3.406742	4.049156	3.4E1013	2.809673	2.043070	.927896	
.007622	-.832394	-1.798315	-2.459552	.423105	3.613570	2.557279	2.324106	
1.897848	1.281391	.625758	.345853	-.391292	-.912634	-1.523217	2.295400	
1.959128	1.577447	1.878833	1.560583	1.240003	1.062064	.561957	.198910	
-3.131752	1.115842	1.837161	1.641616	1.710963	1.665462	1.469050	1.379527	
1.223425	1.027146	-4.106022	.329446	1.418165	1.337896	1.461160	1.625356	
1.671620	1.688508	1.684915	1.422207	-4.430626	-.539993	1.087457	1.333185	
1.357799	1.295655	1.423311	1.565572	1.5E7636	1.412448	-4.307457	-.781343	
.332300	.864164	1.052227	1.052091	1.0E2808	.982056	1.030886	1.159961	
-2.719483	-1.313296	-.440357	.131023	.521116	.801604	1.052415	1.246255	
1.148631	.898492	-.279069	-.954255	-.745794	-.464117	-.201243	-.001218	
.265585	.586256	.740627	.795548	.990463	.295702	-.014005	-.211753	
-.259594	-.229951	-.229331	-.183912	-.123204	-.056915			
ELASTIC AIRLOADS PER Q DUE TO ALPHA								
181.747855	117.051975	112.840587	127.273047	127.33C816	102.387782	92.614373	81.607987	
53.749616	23.664056	204.221516	106.640154	85.393469	75.638748	67.436587	53.893921	
48.112704	44.413387	34.523597	29.612750	211.412819	112.278084	86.477548	71.116363	
59.323128	46.249564	41.394186	28.882309	24.5246C9	24.953513	208.707701	111.283724	
83.712699	64.515888	51.245323	41.223431	34.472135	19.153164	17.554378	20.617842	
198.649289	106.666429	76.167912	55.525492	43.213370	33.141160	27.311789	18.638318	
15.575241	15.795472	177.608525	94.736399	65.6E2674	48.966157	37.180852	28.768145	
22.431963	15.688969	10.856547	11.909068	149.974245	79.907197	54.957269	41.110378	
30.662899	24.940629	19.251603	14.520721	11.273539	11.697674	116.586145	63.242091	
43.957051	31.674819	23.106955	22.045206	19.8C4528	18.287747	16.364708	14.017691	
69.523591	49.144325	35.974603	27.326434	21.220555	15.059433	10.061113	5.605167	
5.505273	7.8967C1	25.954001	32.743521	29.0E1866	24.630426	20.419141	16.976281	
12.660722	7.583080	4.587620	3.011404	3.E22053	5.793406	7.929713	9.911498	
11.006C76	1C.8E5143	11.142255	10.682785	5.935126	9.048998			
ELASTIC AIRLOADS PER Q DUE TO DELTA								
-.036512	-.02C877	-.015470	-.000235	.022378	-1.405023	-3.205775	-4.672643	
-2.995317	1.232063	-.041325	-.001117	.059493	-.021189	-.204019	-1.111716	
-2.062385	-2.961556	-4.583256	2.124872	.05C6355	.068301	.035234	-.220115	
-.643060	-1.3764C5	-2.512645	-5.943394	-2.382481	45.543862	.073895	.004073	
-.145799	-.610768	-1.232489	-2.139722	-3.4C0072	-7.696791	23.261931	41.913720	
-.024656	-.263321	-.601959	-1.199788	-2.014875	-3.534259	-4.908C71	-7.585171	
-3.671926	10.658253	-.6300C3	-.788765	-1.31C599	-2.188441	-3.411694	-4.663785	
-5.443196	-5.773664	21.49C756	40.186445	-2.472974	-1.959883	-2.237820	-3.119007	
-4.557911	-5.335321	-4.450549	-5.745179	41.282109	44.599598	-5.380092	-3.689807	
-3.3148E4	-1.398184	-4.257249	-4.577133	-4.967545	7.598386	25.752840	26.242722	
-6.250481	-4.536476	-3.566472	-3.057982	-2.615758	-2.610402	-2.470375	-2.312453	
-1.841749	-.194833	-4.313958	-4.205368	-2.543032	-2.920926	-2.416751	-2.023752	
-1.632819	-1.211648	-1.105218	-1.132324	-1.637002	-1.772055	-1.837880	-1.861547	
-1.815626	-1.687032	-1.609774	-1.482138	-1.335146	-1.206799			
ELASTIC AIRLOADS PER C DUE TO AN, G								
-2.973795	-1.58C326	-1.099015	-.7598C6	.1C7229	2.296836	2.920626	3.3276C8	
2.947689	1.486455	-2.989642	-1.162037	-.515246	.033682	.615704	1.444497	
1.684988	1.765338	2.149542	1.907288	-2.603851	-1.028039	-.348273	-.243226	
.810289	1.301237	1.5168C4	1.8776C5	2.116383	1.896195	-1.975876	-.768129	
-.158782	.395574	.853672	1.1624E3	1.3E5254	1.7E4550	1.886074	1.675090	
-1.232475	-.431047	.051963	.519137	.8159C0	1.057363	1.218719	1.431338	
1.416585	1.303411	-.449881	-.047302	.229487	.550347	.764423	.884001	
.938373	1.019C15	1.024510	1.006941	.247051	.271121	.356211	.503910	
.645970	.694601	.6810E7	.675702	.692556	.725895	.749428	.472464	
.419244	.393323	.435E54	.470539	.453432	.497904	.4962C1	.501350	
.655369	.504723	.395586	.347474	.302145	.295311	.267939	.227860	
.244542	.289372	.429761	.441503	.379793	.320990	.274796	.245237	
.204232	.151471	.13805E	.1423C3	.174226	.187926	.1985C9	.202841	
.157818	.184113	.182560	.1718E7	.158509	.145498			

APPENDIX - Continued

FLEXIBLE SLOPE INCREMENTS AT LOAD POINTS DUE TO JIG SHAPE

.0093265	.0091802	.0062758	.0068154	.0041498	.0015830	-.0004448	-.0004662
.0006476	.0007980	.0073509	.0064657	.0053294	.0039300	.0018475	.0002913
-.0005372	-.0007779	-.0007730	-.0003592	-.0052643	.0043764	.0003199	.0021558
.0005720	.0002365	-.0004512	-.0030058	-.0049405	-.0053916	.0029295	.0022681
.0014482	.0004625	-.0007366	-.0015592	-.0021212	-.0056999	-.00085141	-.0090988
.0003423	.0001810	-.0003467	-.0012194	-.0023196	-.0040738	-.0057783	-.0090779
-.0109831	-.0113168	-.0016547	-.0020683	-.0027845	-.0039609	-.0054903	-.0007422
-.0097738	-.0117936	-.0159548	-.0172270	-.0054048	-.0059996	-.0070136	-.0083952
-.0104494	-.0129421	-.0145660	-.0162609	-.0157281	-.0200938	-.0110115	-.0117441
-.0131881	-.0149815	-.0176375	-.0186922	-.0202817	-.0211958	-.0211937	-.0210694
-.0190899	-.0198061	-.0212909	-.0224324	-.0234134	-.0243034	-.0253232	-.0282140
-.0290716	-.0281724	-.0237654	-.0241633	-.0252019	-.0255808	-.0258463	-.0263332
-.0269567	-.0292188	-.0298155	-.0293416	-.0263197	-.0266395	-.0269513	-.0269314
-.0263350	-.0264693	-.0265132	-.0256829	-.0258345	-.0261660		

FLEXIBLE SLOPE INCREMENTS AT LOAD POINTS DUE TO ALPHA

.2718150	.2653555	.2395407	.2004067	.1269749	.0412762	-.1042503	-.1480572
-.1612471	-.1637413	.2184813	.1925376	.1595792	.1195562	-.0493260	-.0323341
-.1028083	-.1515475	-.1806034	-.2044741	.1823259	.1437793	.1042767	.0630070
-.0123659	-.0846672	-.1305557	-.2383490	-.3224186	-.3452587	.1257243	.0817493
.0316665	-.0218588	-.0548301	-.1661607	-.2091656	-.3364940	-.4250158	-.4429938
.0511167	.00077199	-.0576662	-.1397261	-.2073474	-.2938092	-.3562284	-.4431237
-.4854933	-.4917673	-.1076155	-.1651017	-.2438254	-.3176108	-.3689685	-.4309577
-.4956519	-.5599290	-.6386993	-.6645427	-.3111987	-.3683608	-.4418872	-.4935266
-.5475559	-.6000526	-.6366479	-.6923714	-.7456908	-.7546954	-.5492655	-.5885788
-.6395889	-.6537276	-.7586683	-.7716118	-.7595206	-.8124320	-.8086727	-.8043788
-.7659422	-.7808528	-.8272612	-.8658580	-.8997523	-.9282906	-.9703982	-.1.1254435
-1.1704522	-1.1213711	-.9742791	-.9781178	-1.0145050	-1.0472356	-1.0876102	-1.1276822
-1.1736419	-1.3057618	-1.3458948	-1.2218345	-1.1878695	-1.2101109	-1.2365246	-1.2868478
-1.3320485	-1.3877344	-1.4177012	-1.3918812	-1.4161577	-1.4417986		

FLEXIBLE SLOPE INCREMENTS AT LOAD POINTS DUE TO DELTA

-.0002942	-.0002654	-.0003076	-.0002935	-.0002632	-.0012147	-.0110868	-.0173026
-.0192187	-.0198353	-.0002903	-.0002683	-.0001929	-.0000675	-.0000577	-.0044752
-.0106517	-.0178087	-.0242425	-.0258412	.0002191	.0010895	.0011256	.0002690
-.0034019	-.0074713	-.0114313	-.0372757	-.0697415	-.0814037	.0005580	.0007344
-.0007055	-.0034182	-.0089286	-.0169098	-.0241130	-.0586673	-.0955201	-.1065206
.0010480	-.0014968	-.0056345	-.0112731	-.0183115	-.0356909	-.0524458	-.0829878
-.0998058	-.1024402	-.0047338	-.0089856	-.0162095	-.0277846	-.0420577	-.0629740
-.0838032	-.0804850	-.1336482	-.1496426	-.0284944	-.0341563	-.0456250	-.0595292
-.0773259	-.0583646	-.1121435	-.1078841	-.1632385	-.1675837	-.0690619	-.0761233
-.0904911	-.1027895	-.1220787	-.1299337	-.1416876	-.1505454	-.1565484	-.1566422
-.1225453	-.1247763	-.1254691	-.1266107	-.1248482	-.1217907	-.1184183	-.1056200
-.1019926	-.1063898	-.1234189	-.1210463	-.1169590	-.1109565	-.1048641	-.0980896
-.0903709	-.0760489	-.0711093	-.0731299	-.0864065	-.0852106	-.0806223	-.0742764
-.0685278	-.0615235	-.0566827	-.0572186	-.0530778	-.0496569		

FLEXIBLE SLOPE INCREMENTS AT LOAD POINTS DUE TO AN, G

-.0268041	-.0259856	-.0225443	-.0180043	-.0107137	-.0035940	.0056305	.0084406
.0108165	.0113741	-.0193221	-.0168675	-.0137837	-.0100688	-.0042747	.0012337
.0005197	.0082619	.0103155	.0126788	-.0138108	-.0113385	-.0083431	-.0048901
.0003562	.0043495	.0070338	.0110650	.0154848	.0170706	-.0079015	-.0056559
-.0029126	.0002944	.0043538	.0074153	.0093750	.0137153	.0175523	.0186144
-.0016081	.0002251	.0027609	.0058058	.0081682	.0112828	.0132437	.0159840
.0172588	.0171381	.0048172	.0063574	.0086204	.0108256	.0124939	.0142663
.0153492	.0161858	.0161123	.0159463	.0104969	.0115695	.0130912	.0142618
.0151451	.0157920	.0160051	.0157588	.0154953	.0154811	.0149438	.0152722
.0154900	.0157221	.0158358	.0155771	.0153745	.0151743	.0151385	.0151884
.0154060	.0154449	.0152302	.0149953	.0146808	.0143669	.0139186	.0115150
.0181888	.0115696	.0140530	.0138967	.0135250	.0130663	.0125265	.0120453
.0114763	.0094645	.0088746	.0092519	.0110281	.0109195	.0106546	.0100214
.0092955	.0084688	.0080728	.0085677	.0082501	.0078779		

APPENDIX - Continued

LEAD FACTOR = .59375

TRIM VALUES (2 ITERATIONS)
 CA = .004759 ALPHA = .048458 PHI = 0.000000
 CN = .079145 DELTA = -.001151 AN, G = .992585
 CM = 0.000000 THETA = .048458 QC/2V = .000000

DERIVATIVE CONTRIBUTIONS

JIG SHAPE	ALPHA	DELTA	QC/2V	AN, G	QDOT	PACH	DYN PRESS
CA	-.0396468	.0012515	-.0099517	.0001567	-.0012869	.0008278	-.0000000
CN	.014051	1.119244	.020705	.154543	.010917	-.031269	-.0000255
CM	.005452	.042187	-.018252	-.372356	-.007624	-.000896	.0000174

STABILITY DERIVATIVES

	U	LDCT	ALPHA	ALPHA DOT	THETA	Q	QDOT	DELTA	ALTITUDE
CA	.0016779	-.0006172	-.0396468	-.5890383	-.0000076	.5790866	-.0012869	.0012515	1.32361E-08
CN	-.060885	-.042955	1.119244	-41.030608	-.000526	41.225150	-.022467	.020705	7.23373E-07
CM	.018285	.030027	.043187	28.655362	.000367	-29.027718	.001052	-.018252	-4.91711E-07
X	-.001728	.000095	.006120	.001563	.000001	-.001930	.000199	-.000193	3.28540E-08
Z	-.015037	.006637	-.172782	.136749	.000081	-.137397	.005012	-.003196	4.68681E-07
M	.287332	.471844	.678637	9.721432	.005772	-9.847756	.016531	-.286803	-7.72668E-06

STATIC PARAMETERS
 CM ALPHA/CN ALPHA = .038586
 STATIC MARGIN = -.051774
 MANEUVER MARGIN = -.063460
 DELTA/U = .762541
 DELTA/AN, G = -.265611

TOTAL TRIM COEFFICIENT SLOPES AT SLOPE POINTS

-.0020586	.0217548	.0653027	.0721608	.0677658	.0584700	.0391715	.0218080
-.0198535	-.0640678	-.0173102	.0054710	.0166357	.0223172	.0250997	.0253133
.0236225	.0206882	.0164255	.0115561	-.0407771	-.0051254	-.0025005	.0047652
.0093337	.0117247	.0128286	.0129417	.0118786	.0098395	-.0524002	-.0241931
-.0143279	-.0061938	-.0008480	.0028211	.0054285	.0065721	.0070841	.0073536
-.0647082	-.0367440	-.0204247	-.0143891	-.0089509	-.0049122	-.0014923	.0009690
.0027601	.0042169	-.0786635	-.0474647	-.0314577	-.0236140	-.0175042	-.0125537
-.0090044	-.0056184	-.0034212	-.0016896	-.0850557	-.0638657	-.0417912	-.0301311
-.0240834	-.0207000	-.0174310	-.0138160	-.0119256	-.0101637	-.0978100	-.0723314
-.0569273	-.0477079	-.0418801	-.0354738	-.0209467	-.0292457	-.0272503	-.0233828
-.0565331	-.0613836	-.0566100	-.0504553	-.0461084	-.0429040	-.0394450	-.0369537
-.0351936	-.0336651	-.0289370	-.0400142	-.0420570	-.0427407	-.0432207	-.0435807
-.0435389	-.0441645	-.0442936	-.0442990	.0066955	-.0252318	-.0367012	-.0433458
-.0433476	-.0433460	-.0433572	-.0423594	-.0433567	-.0433567		

TOTAL TRIM COEFFICIENT SLOPES AT LEAD POINTS

-.0436302	.1331363	.0554864	.0755257	.0738253	.0657601	.0510246	.0254600
.0046302	-.0542782	-.0404578	-.0031056	.0133686	.0208093	.0247193	.0260647
.0248239	.0225010	.0186945	.0137691	-.0615112	-.0174440	-.0048862	.0023758
.0079593	.0110990	.0127458	.0132864	.0126506	.0105862	-.0688567	-.0334707
-.0183161	-.0090000	-.0021438	.0013085	.0050326	.0061520	.0068567	.0071206
-.0866681	-.0458635	-.0260509	-.0170926	-.0105223	-.0064905	-.0025338	.0001894
.0022373	.0036779	-.0561360	-.0585583	-.0374574	-.0259988	-.0200820	-.0139061
-.0104473	-.0068051	-.0042518	-.0024812	-.0882575	-.0722216	-.0504121	-.0334187
-.0254524	-.0217348	-.0187572	-.0151476	-.0125261	-.0107558	-.0842833	-.0871175
-.0611572	-.0485862	-.0432948	-.0368230	-.0305567	-.0283125	-.0274670	-.0235512
-.0635242	-.0648090	-.0599264	-.0539571	-.0477563	-.0450994	-.0411916	-.0380085
-.0359937	-.0340455	-.0173197	-.0366564	-.0417364	-.0425208	-.0431453	-.0434177
-.0438509	-.0440652	-.0442386	-.0442742	.0256357	-.0114377	-.0340408	-.0434761
-.0433465	-.0433451	-.0433468	-.0433562	-.0433570	-.0433564		

APPENDIX – Continued

Program Listing

The source program listing is presented on the following pages. The listing for subroutine MATRIX is not given, but its function can be performed by any standard routines for matrix multiplication and inversion. In the listing presented, any CALL MATRIX statement having a first argument of 20 calls for multiplication of the matrix starting at the address named in the fifth argument into the matrix starting at the address named in the seventh argument, the results to be stored starting at the address named in the ninth argument. Any CALL MATRIX statement having a first argument of 10 calls for inversion of the matrix starting at the address named in the fifth argument, the inverted matrix to be stored starting at the same address, and the determinant to be stored at the address named in the seventh argument. The determinant is not used in the present program. The remaining arguments transmit instructions and dimensions required by subroutine MATRIX.

APPENDIX - Continued

	READ (5,55) (TLRD(I),I=1,M)	AED 590
	REWIND 1	AED 600
	READ (1) ((A(I,J),J=1,M),I=1,M)	AED 610
	IR=1	AED 620
	DO 2 I=1,M	AED 630
2	TSR(I,2)=1.	AED 640
C		AED 650
C	COMPUTE RIGID LOADS DUE TO JIG SHAPE, ALPHA AND DELTA	AED 660
C		AED 670
	DO 3 K=1,3	AED 680
	CALL MATRIX (20,M,M,1,A,120,TSR(1,K),120,FRA(1,K),120)	AED 690
3	CONTINUE	AED 700
	READ (5,55) (XSO(I),I=1,M)	AED 710
	READ (5,55) (XLO(I),I=1,M)	AED 720
	SRC2=SREF/2.	AED 730
	DO 53 IC=1,NC	AED 740
C		AED 750
C	COMPUTE RIGID LOADS DUE TO QC/2V	AED 760
C		AED 770
	READ (5,56) NW,XCG	AED 780
	DO 4 I=1,M	AED 790
	XS(I)=XSO(I)-XCG	AED 800
	XL(I)=XLO(I)-XCG	AED 810
4	TSR(I,4)=-XS(I)*2./CBAR	AED 820
	IF (IR.EQ.1) GO TO 5	AED 830
	REWIND 1	AED 840
	READ (1) ((A(I,J),J=1,M),I=1,M)	AED 850
	IR=1	AED 860
5	CALL MATRIX (20,M,M,1,A,120,TSR(1,4),120,FRA(1,4),120)	AED 870
	DO 52 IW=1,NW	AED 880
	READ (5,56) NQ,W,YI,Y1,Y2	AED 890
C		AED 900
C	ESTABLISH INERTIAL LOADS DUE TO LOAD FACTOR AND QDOT	AED 910
C		AED 920
	IF (IFLEX.EQ.0) GO TO 7	AED 930
	READ (5,57) (FI(I,1),I=1,M)	AED 940
	DO 6 I=1,M	AED 950
	FI(I,1)=-FI(I,1)	AED 960
6	FI(I,2)=FI(I,1)*XL(I)/32.174	AED 970
7	DO 51 IQ=1,NQ	AED 980
	READ (5,56) NN,Q,V,G,RHC,RHOH,AH	AED 990
	READ (5,55) (FL(I),I=1,NN)	AED1000
	WRITE (6,58) AM,XCG,W,Q	AED1010
C		AED1020
C	READ BASIC A AND S MATRICES	AED1030
C		AED1040
	IF (IR.EQ.1) GO TO 8	AED1050
	REWIND 1	AED1060
	READ (1) ((A(I,J),J=1,M),I=1,M)	AED1070
8	IF (IFLEX.EQ.0) GO TO 13	AED1080
	REWIND 2	AED1090
	READ (2) ((S(I,J),J=1,M),I=1,M)	AED1100
C		AED1110
C	FIND AIR LOADS DUE TO INERTIAL DISTORTION	AED1120
C		AED1130
	DO 9 KI=1,2	AED1140
	K=KI+4	AED1150
	CALL MATRIX (20,M,M,1,S,120,FI(1,KI),120,TSR(1,K),120)	AED1160
9	CALL MATRIX (20,M,M,1,A,120,TSR(1,K),120,FRA(1,K),120)	AED1170
C		AED1180
C	COMPUTE BASIC AEROELASTIC CORRECTION MATRIX	AED1190

APPENDIX - Continued

C	CALL MATRIX (20,M,M,M,A,120,S,120,A,120)	AED1200
	DO 10 J=1,M	AED1210
	DO 10 I=1,M	AED1220
	A(I,J)=-Q*A(I,J)	AED1230
	IF (I.EQ.J) A(I,J)=A(I,J)+1.	AED1240
10	CONTINUE	AED1250
	CALL MATRIX (10,M,M,2,A,120,DETERM)	AED1260
C		AED1270
C	APPLY AEROELASTIC CORRECTION TO FIRST SIX SETS OF AIR LOADS	AED1280
C		AED1290
	DO 11 K=1,6	AED1300
11	CALL MATRIX (20,M,M,1,A,120,FRA(1,K),120,FEA(1,K),120)	AED1310
C		AED1320
C	SUM AIR AND INERTIAL LOADS FOR INERTIAL LOAD SOURCES	AED1330
C		AED1340
	DO 12 KI=1,2	AED1350
	K=KI+4	AED1360
	DO 12 I=1,M	AED1370
12	FIA(I,KI)=FEA(I,K)+FI(I,KI)/Q	AED1380
	K1=6	AED1390
	GO TO 16	AED1400
13	DO 15 I=1,M	AED1410
	DO 14 K=5,6	AED1420
	TSR(I,K)=0.	AED1430
14	FRA(I,K)=0.	AED1440
	DO 15 K=1,6	AED1450
15	FEA(I,K)=FRA(I,K)	AED1460
	CN(5)=0.	AED1470
	CN(6)=0.	AED1480
	CM(5)=0.	AED1490
	CM(6)=0.	AED1500
	K1=4	AED1510
16	DO 18 K=1,K1	AED1520
C		AED1530
C	COMPUTE CN AND CM DUE TO FIRST SIX LOAD SOURCES	AED1540
C		AED1550
	CN(K)=0.	AED1560
	CM(K)=0.	AED1570
	DO 17 I=1,M	AED1580
	CN(K)=CN(K)+FEA(I,K)	AED1590
17	CM(K)=CM(K)+FEA(I,K)*XL(I)	AED1600
	CN(K)=CN(K)/SRO2	AED1610
18	CM(K)=CM(K)/(SRO2*CBAR)	AED1620
	IR=0	AED1630
	IF (LIST.EQ.0) GO TO 19	AED1640
	WRITE (6,59) (FEA(I,1),I=1,M)	AED1650
	WRITE (6,60) (FEA(I,2),I=1,M)	AED1660
	WRITE (6,61) (FEA(I,3),I=1,M)	AED1670
	IF (IFLEX.NE.0) WRITE (6,62) (FEA(I,5),I=1,M)	AED1680
19	DO 50 IN=1,NN	AED1690
C		AED1700
C	COMPUTE TRIM CONDITIONS	AED1710
C		AED1720
	CALL TRIM (CN,CM,W,FL(IN),LFT,Q,SREF,CBAR,V,G,YI,Y1,Y2,AT,DT,ANT,CAED1740	
	INT,CMT,QT,PR,PHI,T,ITER)	AED1750
	IF (ITER.GE.100) GO TO 49	AED1760
C		AED1770
C	COMPUTE TRIM SETS OF RIGID SLOPES, RIGID AIR LOADS AND ELASTIC	AED1780
C	AIR LOADS	AED1790
C		AED1800

APPENDIX - Continued

```

DO 20 I=1,M AED1810
TSR(I,7)=TSR(I,1)+AT+DT*TSR(I,3)+QT*TSR(I,4)+ANT*TSR(I,5)-PR*TSR( AED1820
1,6) AED1830
FRA(I,7)=FRA(I,1)+AT*FRA(I,2)+DT*FRA(I,3)+QT*FRA(I,4)+ANT*FRA(I,5) AED1840
1-PR*FRA(I,6) AED1850
20 FEA(I,9)=FEA(I,1)+AT*FEA(I,2)+DT*FEA(I,3)+QT*FEA(I,4)+ANT*FEA(I,5) AED1860
1-PR*FEA(I,6) AED1870
IF (IFLEX.EQ.0) GO TO 25 AED1880
DO 21 I=1,M AED1890
21 FIA(I,3)=FEA(I,9)+(ANT*FI(I,1)-PR*FI(I,2))/Q AED1900
C AED1910
C CORRECT TRIM RIGID AIRLOADS FOR AEROELASTICITY AT HIGHER Q AED1920
C AED1930
QP=1.05*Q AED1940
REWIND 1 AED1950
READ (1) ((A(I,J),J=1,M),I=1,M) AED1960
CALL MATRIX (20,M,M,M,A,120,S,120,A,120) AED1970
DO 22 J=1,M AED1980
DO 22 I=1,M AED1990
A(I,J)=-QP*A(I,J) AED2000
IF (I.EQ.J) A(I,J)=A(I,J)+1. AED2010
22 CONTINUE AED2020
CALL MATRIX (10,M,M,2,A,120,DETERM) AED2030
CALL MATRIX (20,M,M,1,A,120,FRA(1,7),120,FEA(1,8),120) AED2040
C AED2050
C CORRECT TRIM RIGID AIRLOADS FOR AEROELASTICITY AT LOWER Q AED2060
C AED2070
QP=.95*Q AED2080
REWIND 1 AED2090
READ (1) ((A(I,J),J=1,M),I=1,M) AED2100
CALL MATRIX (20,M,M,M,A,120,S,120,A,120) AED2110
DO 23 J=1,M AED2120
DO 23 I=1,M AED2130
A(I,J)=-QP*A(I,J) AED2140
IF (I.EQ.J) A(I,J)=A(I,J)+1. AED2150
23 CONTINUE AED2160
CALL MATRIX (10,M,M,2,A,120,DETERM) AED2170
CALL MATRIX (20,M,M,1,A,120,FRA(1,7),120,FEA(1,7),120) AED2180
C AED2190
C COMPUTE ELASTIC AIRLOADS DUE TO Q AED2200
C AED2210
DO 24 I=1,M AED2220
24 FEA(I,8)=(FEA(I,8)-FEA(I,7))/(.1*Q) AED2230
GO TO 27 AED2240
25 DO 26 I=1,M AED2250
26 FEA(I,8)=0. AED2260
C AED2270
C USING TRIM RIGID SLOPES, COMPUTE RIGID AND ELASTIC AIR LOADS AED2280
C AT HIGHER MACH AED2290
C AED2300
27 READ (1) ((A(I,J),J=1,M),I=1,M) AED2310
CALL MATRIX (20,M,M,1,A,120,TSR(1,7),120,FEA(1,7),120) AED2320
IF (IFLEX.EQ.0) GO TO 29 AED2330
CALL MATRIX (20,M,M,M,A,120,S,120,A,120) AED2340
DO 28 J=1,M AED2350
DO 28 I=1,M AED2360
A(I,J)=-Q*A(I,J) AED2370
IF (I.EQ.J) A(I,J)=A(I,J)+1. AED2380
28 CONTINUE AED2390
CALL MATRIX (10,M,M,2,A,120,DETERM) AED2400
CALL MATRIX (20,M,M,1,A,120,FEA(1,7),120,FEA(1,7),120) AED2410

```

APPENDIX - Continued

C		AED2420
C	USING TRIM RIGID SLOPES, COMPUTE RIGID AND ELASTIC AIR LOADS	AED2430
C	AT LOWER MACH	AED2440
C		AED2450
29	READ (1) ((A(I,J),J=1,M),I=1,M)	AED2460
	CALL MATRIX (20,M,M,1,A,120,TSR(1,7),120,TLE(1,1),120)	AED2470
	IF (IFLEX.EQ.0) GO TO 31	AED2480
	CALL MATRIX (20,M,M,M,A,120,S,120,A,120)	AED2490
	DO 30 J=1,M	AED2500
	DO 30 I=1,M	AED2510
	A(I,J)=-Q*A(I,J)	AED2520
	IF (I.EQ.J) A(I,J)=A(I,J)+1.	AED2530
30	CONTINUE	AED2540
	CALL MATRIX (10,M,M,2,A,120,DETERM)	AED2550
	CALL MATRIX (20,M,M,1,A,120,TLE(1,1),120,TLE(1,1),120)	AED2560
C		AED2570
C	COMPUTE ELASTIC AIRLOADS DUE TO MACH	AED2580
C		AED2590
31	DO 32 I=1,M	AED2600
32	FEA(I,7)=(FEA(I,7)-TLE(I,1))/(2.*DM)	AED2610
C		AED2620
C	FIND CN AND CM DUE TO Q AND MACH	AED2630
C		AED2640
	DO 34 K=7,8	AED2650
	CN(K)=0.	AED2660
	CM(K)=0.	AED2670
	DO 33 I=1,M	AED2680
	CN(K)=CN(K)+FEA(I,K)	AED2690
33	CM(K)=CM(K)+FEA(I,K)*XL(I)	AED2700
	CN(K)=CN(K)/SRO2	AED2710
34	CM(K)=CM(K)/(SRO2*CBAR)	AED2720
	IF (IFLEX.EQ.0) GO TO 36	AED2730
C		AED2740
C	COMPUTE TRIM CONDITION SLOPES AT SLOPE POINTS	AED2750
C		AED2760
	CALL MATRIX (20,M,M,1,S,120,FIA(1,3),120,TLE(1,9),120)	AED2770
	DO 35 I=1,M	AED2780
35	TSR(I,7)=TLE(I,9)*Q+TSR(I,1)+DT*TSR(I,3)	AED2790
	GO TO 39	AED2800
36	DO 37 I=1,M	AED2810
37	TSR(I,7)=TSR(I,1)+DT*TSR(I,3)	AED2820
	DO 38 K=1,9	AED2830
	DO 38 I=1,M	AED2840
38	TLE(I,K)=0.	AED2850
	GO TO 43	AED2860
C		AED2870
C	COMPUTE SLOPES AT LOAD POINTS FOR ALL LOAD SOURCES	AED2880
C		AED2890
39	READ (2) ((S(I,J),J=1,M),I=1,M)	AED2900
	DO 40 K=1,8	AED2910
	IF (K.EQ.5.OR.K.EQ.6) GO TO 43	AED2920
	CALL MATRIX (20,M,M,1,S,120,FEA(1,K),120,TLE(1,K),120)	AED2930
40	CONTINUE	AED2940
	DO 41 K=5,7	AED2950
	K1=K-4	AED2960
	L=K	AED2970
	IF (K.EQ.7) L=9	AED2980
41	CALL MATRIX (20,M,M,1,S,120,FIA(1,K1),120,TLE(1,L),120)	AED2990
	CALL MATRIX (20,M,M,1,S,120,FEA(1,9),120,FIA(1,3),120)	AED3000
	DO 42 K=1,9	AED3010
	DO 42 I=1,M	AED3020

APPENDIX - Continued

	TLE(I,K)=TLE(I,K)*Q	AED3030
	IF (K.NE.8) GO TO 42	AED3040
	TLE(I,8)=TLE(I,8)+FIA(I,3)	AED3050
42	CONTINUE	AED3060
	IF (IFLEX.EQ.0.OR.LIST.EQ.0) GO TO 43	AED3070
	IF (IN.NE.1) GO TO 43	AED3080
	WRITE (6,63) (TLE(I,1),I=1,M)	AED3090
	WRITE (6,64) (TLE(I,2),I=1,M)	AED3100
	WRITE (6,65) (TLE(I,3),I=1,M)	AED3110
	WRITE (6,66) (TLE(I,5),I=1,M)	AED3120
C		AED3130
C	COMPUTE AXIAL FORCE COEFFICIENT AND DERIVATIVES	AED3140
C		AED3150
43	CAT=0.	AED3160
	DO 44 I=1,M	AED3170
	TLE(I,3)=TLE(I,3)+TLRD(I)	AED3180
	TLE(I,9)=TLE(I,9)+TLRJ(I)+DT*TLRD(I)	AED3190
44	CAT=CAT+(TLE(I,9)*FEA(I,9))/SRQ2	AED3200
	DO 46 K=2,8	AED3210
	CA(K)=0.	AED3220
	DO 45 I=1,M	AED3230
45	CA(K)=CA(K)+(TLE(I,9)*FEA(I,K)+TLE(I,K)*FEA(I,9))/SRQ2	AED3240
46	CONTINUE	AED3250
	CAT=CAT+CAF	AED3260
	WRITE (6,67) FL(IN)	AED3270
	WRITE (6,68) ITER,CAT,AT,PHI,CNT,DT,ANT,CMT,T,QT	AED3280
	WRITE (6,69) (CA(K),K=2,8),CN,CM	AED3290
C		AED3300
C	COMPUTE COMBINED STABILITY DERIVATIVES	AED3310
C		AED3320
	FN=2.*V*V/(32.174*CBAR)	AED3330
	VOG=V/32.174	AED3340
	CSA=CCS(AT)	AED3350
	SNA=SIN(AT)	AED3360
	ST=SIN(T)	AED3370
	CP=COS(PHI)	AED3380
	SCA(1)=FN*QT*CSA*CA(5)+AM*CA(7)+2.*Q*CA(8)	AED3390
	SCN(1)=FN*QT*CSA*CN(5)+AM*CN(7)+2.*Q*CN(8)	AED3400
	SCM(1)=FN*QT*CSA*CM(5)+AM*CM(7)+2.*Q*CM(8)	AED3410
	SCA(2)=-VOG*SNA*CA(5)	AED3420
	SCN(2)=-VOG*SNA*CN(5)	AED3430
	SCM(2)=-VOG*SNA*CM(5)	AED3440
	SCA(3)=CA(2)-FN*QT*SNA*CA(5)	AED3450
	SCN(3)=CN(2)-FN*QT*SNA*CN(5)	AED3460
	SCM(3)=CM(2)-FN*QT*SNA*CM(5)	AED3470
	SCA(4)=-FN*CSA*CA(5)	AED3480
	SCN(4)=-FN*CSA*CN(5)	AED3490
	SCM(4)=-FN*CSA*CM(5)	AED3500
	SCA(5)=-ST*CP*CA(5)*G/32.174	AED3510
	SCN(5)=-ST*CP*CN(5)*G/32.174	AED3520
	SCM(5)=-ST*CP*CM(5)*G/32.174	AED3530
	SCA(6)=CA(4)+FN*CSA*CA(5)	AED3540
	SCN(6)=CN(4)+FN*CSA*CN(5)	AED3550
	SCM(6)=CM(4)+FN*CSA*CM(5)	AED3560
	SCA(7)=CA(6)	AED3570
	SCN(7)=CN(6)	AED3580
	SCM(7)=CM(6)	AED3590
	SCA(8)=CA(3)	AED3600
	SCN(8)=CN(3)	AED3610
	SCM(8)=CM(3)	AED3620
	SCA(9)=Q*RHOH*CA(8)-AM*AH*CA(7)	AED3630

APPENDIX - Continued

```

SCN(9)=Q*RHOH*CN(8)-AM*AH*CN(7)
SCM(9)=Q*RHOH*CM(8)-AM*AH*CM(7)
QM=32.174*Q*SREF/(W*V)
QI=Q*SREF*CBAR/YI
SX(1)=-QM*(SCA(1)+2.*CAT)
SZ(1)=-QM*(SCN(1)+2.*CNT)
SM(1)=QI*(SCM(1)+2.*CMT)
DO 47 K=2,8
SX(K)=-QM*SCA(K)
SZ(K)=-QM*SCN(K)
SM(K)=QI*SCM(K)
47 DO 48 K=4,6,2
SX(K)=SX(K)*CBAR/(2.*V)
SZ(K)=SZ(K)*CBAR/(2.*V)
48 SM(K)=SM(K)*CBAR/(2.*V)
SX(9)=-CM*(SCA(9)+RHOH*CAT)
SZ(9)=-CM*(SCN(9)+RHOH*CNT)
SM(9)=QI*(SCM(9)+RHOH*CMT)
WRITE (6,70) SCA,SCN,SCM,SX,SZ,SM
C
C COMPUTE STATIC PARAMETERS
C
CMCN=SCM(3)/SCN(3)
CMNU=CMCN*(1.+SCN(1)/(2.*CNT))-SCM(1)/(2.*CNT)
B=32.174*RHO*SREF*CBAR/(4.*W)
CMNN=CMCN*(1.-B*SCN(6))+B*SCM(6)
DU=2.*CNT*CMNU/(SCM(8)-CMCN*SCN(8))
DA=-W*CMNN/(Q*SREF*(SCM(8)-CMCN*SCN(8)))
WRITE (6,71) CMCN,CMNU,CMNN,DU,DA
IF (LIST.EQ.C) GO TO 50
WRITE (6,72) (TSR(I,7),I=1,M)
WRITE (6,73) (TLE(I,9),I=1,M)
GO TO 50
49 WRITE (6,74) CN,CM
50 CONTINUE
51 CONTINUE
52 CONTINUE
53 CONTINUE
STOP
C
54 FORMAT (3I1,2I3,5F10.0)
55 FORMAT (8F10.0)
56 FORMAT (I3,6F10.0)
57 FORMAT (6F12.0)
58 FORMAT (1H1,5X,27H AERDELASTIC DERIVATIVES, M=,F6.3,6H, XCG=,F8.3,4
1H, W=,F9.0,7H, QBAR=,F8.2)
59 FORMAT (//10X,39HELASTIC AIRLOADS PER Q DUE TO JIG SHAPE/(1X,8F12.
16))
60 FORMAT (//10X,35HELASTIC AIRLOADS PER Q DUE TO ALPHA/(1X,8F12.6))
61 FORMAT (//10X,35HELASTIC AIRLOADS PER Q DUE TO DELTA/(1X,8F12.6))
62 FORMAT (//10X,35HELASTIC AIRLOADS PER Q DUE TO AN, G/(1X,8F12.6))
63 FORMAT (//10X,57HFLEXIBLE SLOPE INCREMENTS AT LOAD POINTS DUE TO
1IG SHAPE/(1X,8F12.7))
64 FORMAT (//10X,53HFLEXIBLE SLOPE INCREMENTS AT LOAD POINTS DUE TO
1LPHA/(1X,8F12.7))
65 FORMAT (//10X,53HFLEXIBLE SLOPE INCREMENTS AT LOAD POINTS DUE TO
1ELTA/(1X,8F12.7))
66 FORMAT (//10X,53HFLEXIBLE SLOPE INCREMENTS AT LOAD POINTS DUE TO
1N, G/(1X,8F12.7))
67 FORMAT (//5X,13HLOAD FACTOR =,F9.5)
68 FORMAT (//10X,14HTRIM VALUES (,I3,12H ITERATIONS)/3X,4HCA =,F10.6,

```

AED3640
AED3650
AED3660
AED3670
AED3680
AED3690
AED3700
AED3710
AED3720
AED3730
AED3740
AED3750
AED3760
AED3770
AED3780
AED3790
AED3800
AED3810
AED3820
AED3830
AED3840
AED3850
AED3860
AED3870
AED3880
AED3890
AED3900
AED3910
AED3920
AED3930
AED3940
AED3950
AED3960
AED3970
AED3980
AED3990
AED4000
AED4010
AED4020
AED4030
AED4040
AED4050
AED4060
AED4070
AED4080
AED4090
AED4100
AED4110
AED4120
AED4130
AED4140
AED4150
AED4160
AED4170
AED4180
AED4190
AED4200
AED4210
AED4220
AED4230
AED4240

APPENDIX - Continued

```

13X,7HALPHA =,F10.6,3X,7HPHI   =,F10.6/3X,4HCN =,F10.6,3X,7HDELTA =AED4250
2,F10.6,3X,7HAN, G =,F10.6/3X,4HCM =,F10.6,3X,7HTHETA =,F10.6,3X,7HAED4260
3QC/2V =,F10.6) AED4270
69  FORMAT (/10X,24HDERIVATIVE CONTRIBUTIONS/8X,9HJIG SHAPE,5X,5HALPHAAED4280
1,7X,5HDELTA,7X,5HQC/2V,7X,5HAN, G,8X,4HQDOT,8X,4HMACH,5X,9HDYN PREAED4290
2SS/3F CA,F26.7,5F12.7,F13.8/4H CN ,7F12.6,F13.7/4H CM ,7F12.6,F13.AED4300
37) AED4310
70  FORMAT (/10X,21HSTABILITY DERIVATIVES/12X,1HU,10X,4HUDDOT,7X,5HALPHAED4320
1A,5X,9HALPHA DOT,5X,5HTHETA,9X,1HQ,10X,4HQDOT,7X,5HDELTA,6X,8HALTIAED4330
2TUDE/5H CA ,8F12.7,E12.5/4H CN ,8F12.6,E13.5/4H CM ,8F12.6,E13.5/AED4340
34H X ,8F12.6,E13.5/4H Z ,8F12.6,E13.5/4H M ,8F12.6,E13.5) AED4350
71  FORMAT (/10X,17HSTATIC PARAMETERS/2CH CM ALPHA/CN ALPHA =,F10.6/14AED4360
1H STATIC MARGIN,5X,1H=,F10.6/20H MANEUVER MARGIN   =,F10.6/8H DELTAED4370
2A/L,11X,1H=,F10.6/12H DELTA/AN, G,7X,1H=,F10.6) AED4380
72  FORMAT (/10X,43HTOTAL TRIM CONDITION SLOPES AT SLOPE POINTS/(1X,8AED4390
1F12.7)) AED4400
73  FORMAT (/10X,42HTOTAL TRIM CONDITION SLOPES AT LOAD POINTS/(1X,8FAED4410
112.7)) AED4420
74  FORMAT (/5X,14HUNABLE TO TRIM/3X,3HCN=,8F12.6/3X,3HCM=,8F12.6) AED4430
END AED4440-

```

APPENDIX - Continued

```

SUBROUTINE TRIM (CN,CM,W,FL,LFT,Q,S,C,V,G,YI,Y1,Y2,AL,DEL,AN,CNT,CTRM  10
IMT,QF,PR,PHI,T,I1) TRM  20
DIMENSICN CN(8), CM(8) TRM  30
WQQS=W/(Q*S) TRM  40
GOGO=G/32.174 TRM  50
A=CM(2)/CM(3)-CN(2)/CN(3) TRM  60
B=(WQQS-CN(5))/CN(3)+CM(5)/CM(3) TRM  70
IF (LFT.GE.1.AND.FL.GT.GOGO) GO TO 3 TRM  80
QF=(32.174*FL-G)*C/(2.*V*V) TRM  90
D=(CN(1)+QF*CN(4))/CN(3)-(CM(1)+QF*CM(4))/CM(3) TRM 100
AL1=(D-FL*B)/A TRM 110
DO 1 I=1,100 TRM 120
I1=I TRM 130
AN=FL*COS(AL1) TRM 140
AL=(D-AN*B)/A TRM 150
IF (ABS(AL-AL1).LE..0000005) GO TO 2 TRM 160
AL1=AL TRM 170
1 CONTINUE TRM 180
2 AN=FL*CGS(AL) TRM 190
DEL=(-CM(1)-AL*CM(2)-QF*CM(4)-AN*CM(5))/CM(3) TRM 200
CNT=WQQS*AN TRM 210
CMT=0. TRM 220
PR=0. TRM 230
PHI=0. TRM 240
T=AL TRM 250
RETURN TRM 260
3 FW=WQQS*GOGO TRM 270
FI=YI/(Q*S*C) TRM 280
F1=FI*Y1 TRM 290
F2=FI*Y2 TRM 300
AL1=0. TRM 310
TT=0. TRM 320
CT=1. TRM 330
ST=0. TRM 340
CA=1. TRM 350
SA=0. TRM 360
I=0 TRM 370
CP=GOGO/FL TRM 380
4 QV=FL/GCGO-CT*CP*CA-ST*SA TRM 390
Q1=QV*G/V. TRM 400
QF=Q1*C/(2.*V) TRM 410
QP=QV*CA/(2.*CT) TRM 420
CP=SQRT(1.-QV*TT*SA/CT+QP*QP)-QP TRM 430
IF (CP-1.) 6,5,5 TRM 440
5 R=C. TRM 450
P=C. TRM 460
SP=0. TRM 470
GO TO 7 TRM 480
6 SP=SQRT(1.-CP*CP) TRM 490
P=-Q1*TT/SP TRM 500
R=Q1*CP/SP TRM 510
7 AN=GOGO*(CT*CP+QV*CA) TRM 520
PR=P*R TRM 530
CMT=F2*(P*P-R*R)-F1*PR TRM 540
IF (I.L1.0) GO TO 9 TRM 550
D=(CMT-CM(1)-QF*CM(4)+PR*CM(6))/CM(3)+(CN(1)+QF*CN(4)-PR*CN(6))/CN TRM 560
I(3) TRM 570
AL=(D-AN*B)/A TRM 580
CA=COS(AL) TRM 590
SA=SIN(AL) TRM 600

```

APPENDIX - Concluded

	TT=SA*CP/CA	TRM 610
	T=ATAN2(SA*CP,CA)	TRM 620
	CT=COS(T)	TRM 630
	ST=SIN(T)	TRM 640
	IF (ABS(AL-AL1).LE..0000005) GO TO 8	TRM 650
	IF (I.GE.100) GO TO 8	TRM 660
	I=I+1	TRM 670
	II=I	TRM 680
	AL1=AL	TRM 690
	GO TO 4	TRM 700
8	I=-1	TRM 710
	GO TO 4	TRM 720
9	CNT=WCQS*AN	TRM 730
	DEL=(CMT-CM(1)-AL*CM(2)-QF*CM(4)-AN*CM(5)+PR*CM(6))/CM(3)	TRM 740
	PHI=ATAN2(SP,CP)	TRM 750
	RETURN	TRM 760
	END	TRM 770-

REFERENCES

1. Wykes, John H.; and Lawrence, Robert E.: Aerothermoelasticity: Its Impact on Stability and Control of Winged Aerospace Vehicles. *J. Aircraft*, vol. 2, no. 6, Nov.-Dec. 1965, pp. 517-526.
2. Aerodynamics & Structures Res. Organizations: An Analysis of Methods for Predicting the Stability Characteristics of an Elastic Airplane. D6-20659-1 (Contract NAS 2-3662), Boeing Co., Nov. 1968. (Available as NASA CR-73277.)
3. Roskam, J.: Comments, Interpretation and Application of a Method for Predicting Aerodynamic Characteristics of Large Flexible Airplanes. Aeroelastic Effects From a Flight Mechanics Standpoint, AGARD CP No. 46, Apr. 1969, pp. 13-1 - 13-18.
4. Etkin, Bernard: Dynamics of Flight. John Wiley & Sons, Inc., c.1959, p. 108.
5. Baals, Donald D.; Robins, A. Warner; and Harris, Roy V., Jr.: Aerodynamic Design Integration of Supersonic Aircraft. *J. Aircraft*, vol. 7, no. 5, Sept.-Oct. 1970, pp. 385-394.
6. Margason, Richard J.; and Lamar, John E.: Vortex-Lattice FORTRAN Program for Estimating Subsonic Aerodynamic Characteristics of Complex Planforms. NASA TN D-6142, 1971.
7. Woodward, Frank A.: Analysis and Design of Wing-Body Combinations at Subsonic and Supersonic Speeds. *J. Aircraft*, vol. 5, no. 6, Nov.-Dec. 1968, pp. 528-534.
8. Anon.: U.S. Standard Atmosphere, 1962. NASA, U.S. Air Force, and U.S. Weather Bur., 1962.

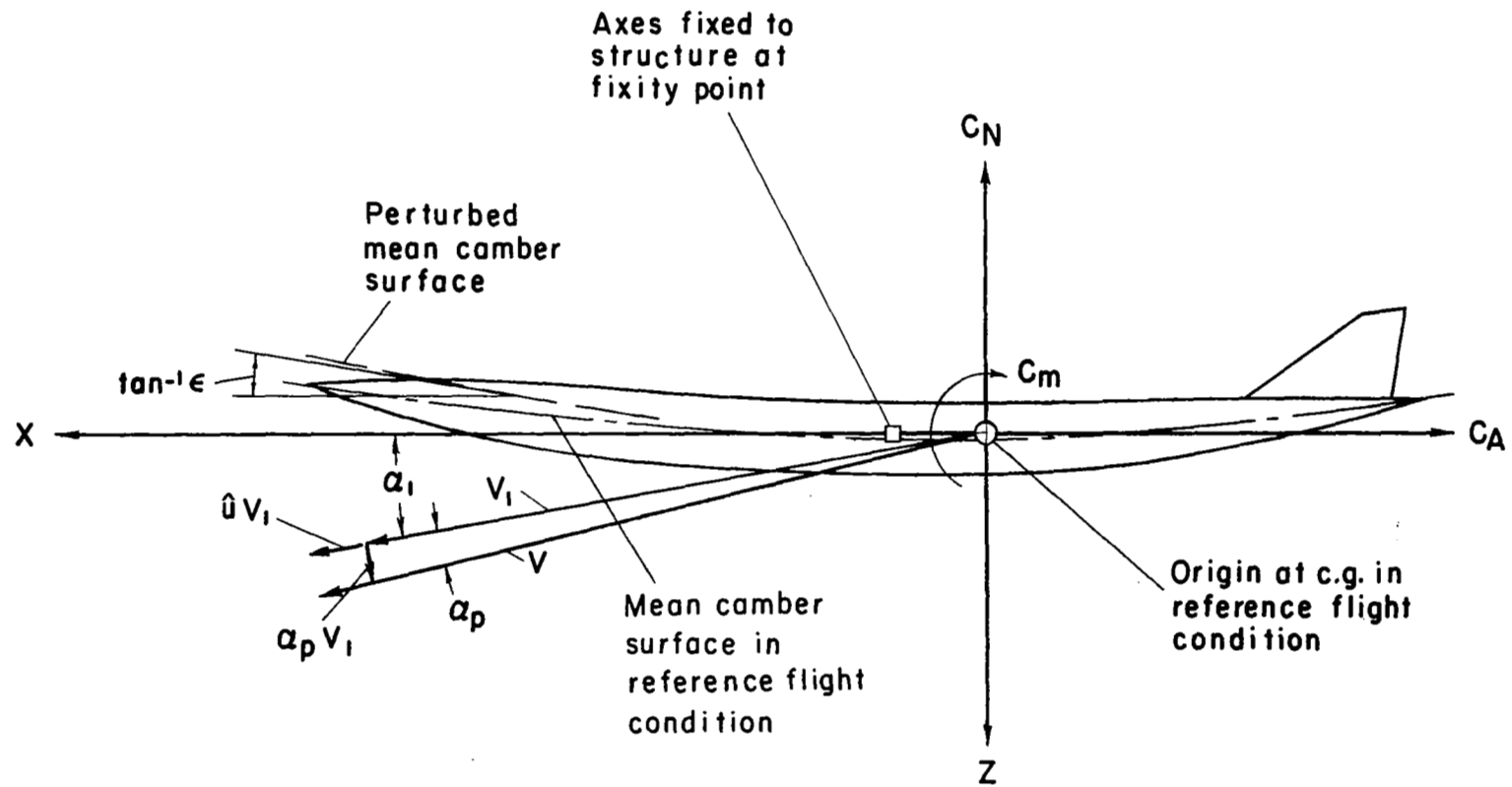


Figure 1.- Illustration of reference axis system and several fundamental parameters.

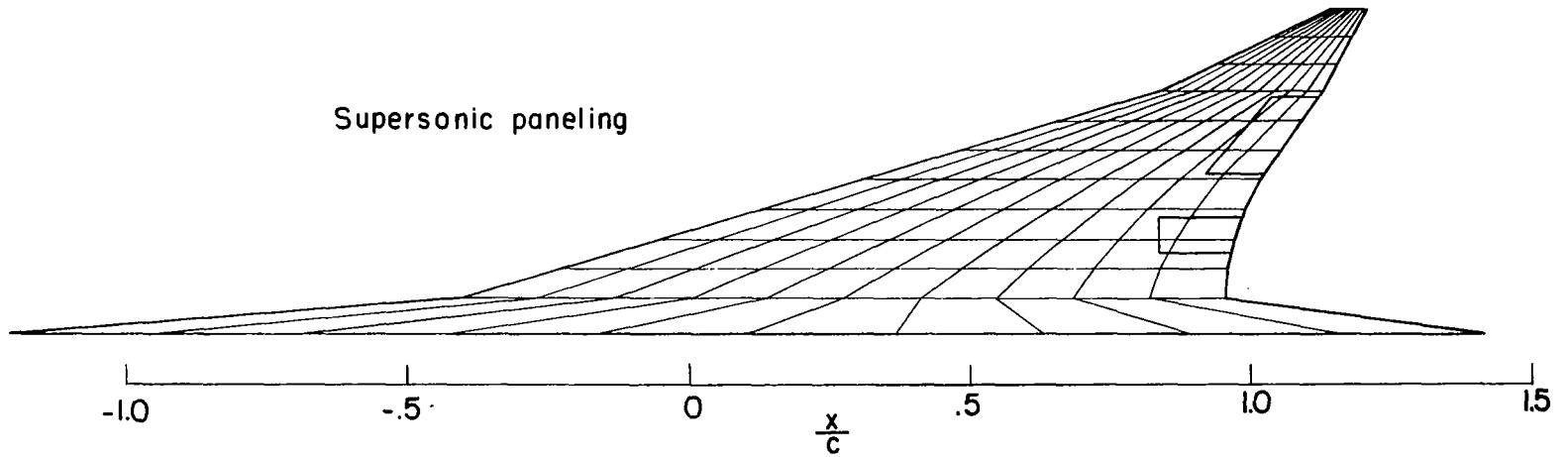
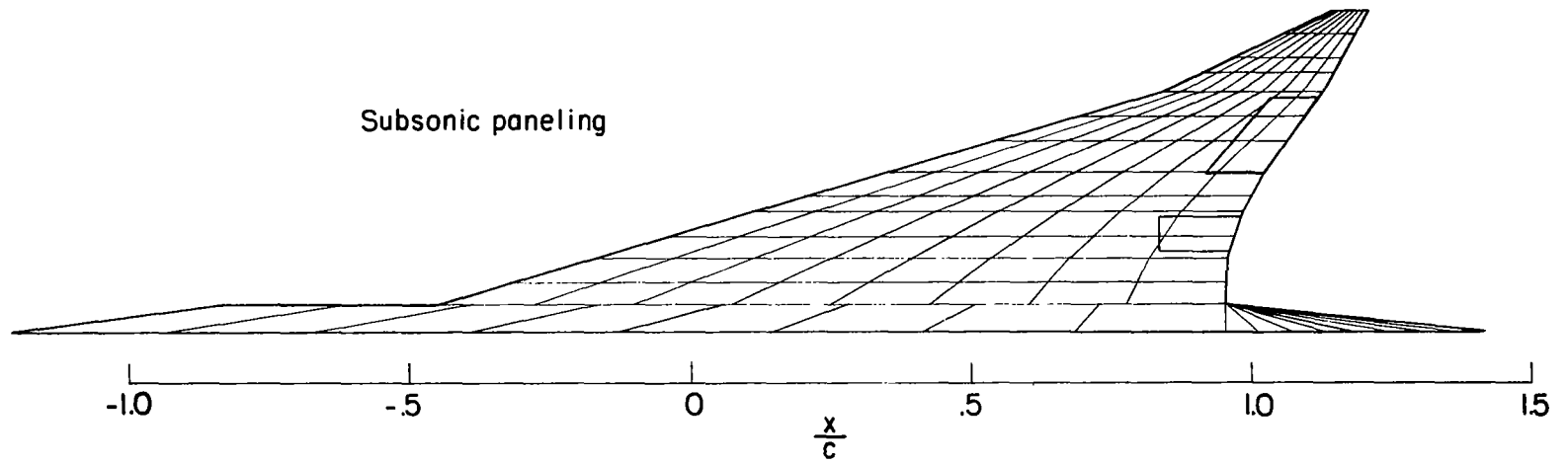


Figure 2.- Panel arrangements used to represent example airplane.

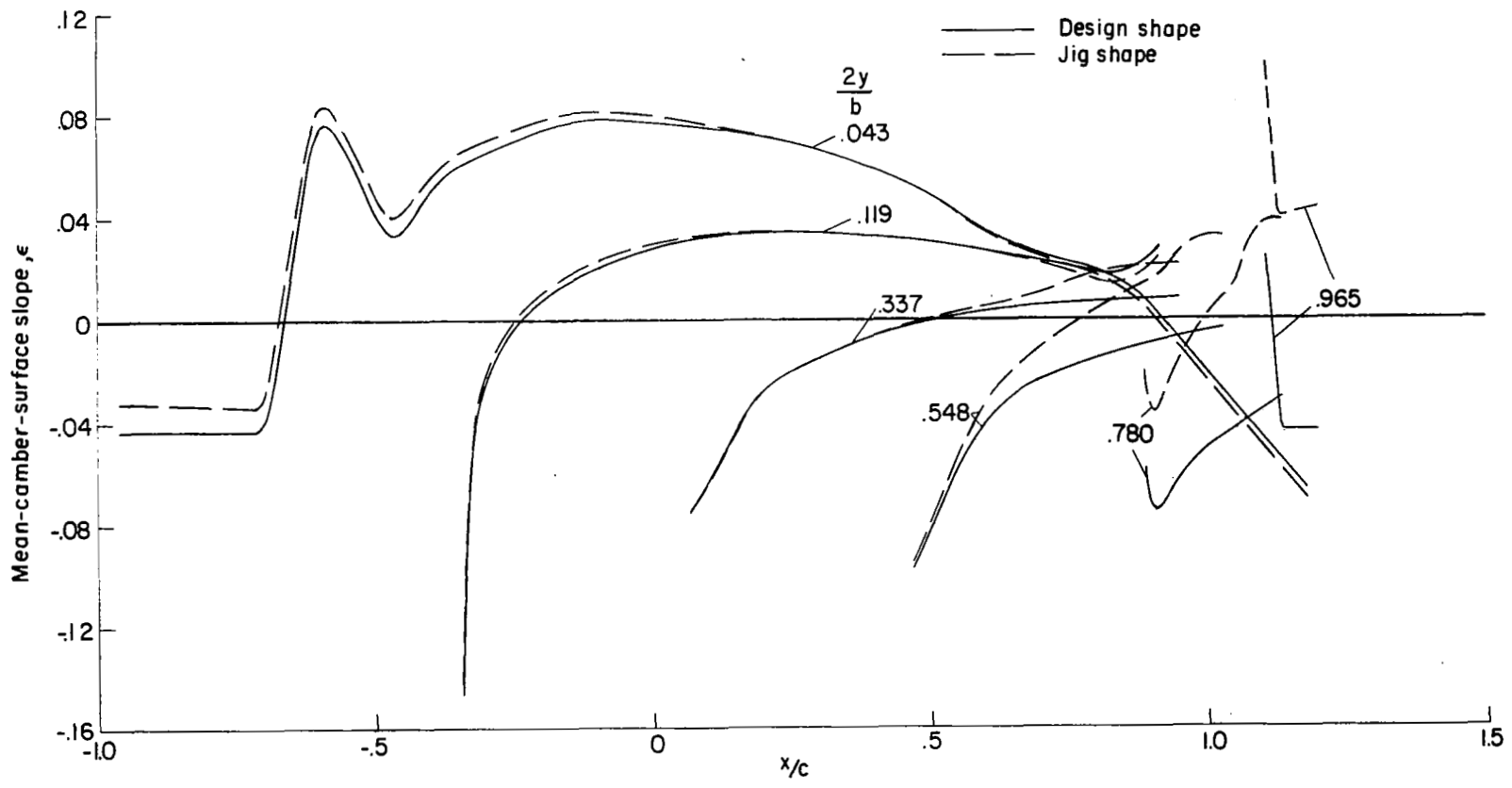
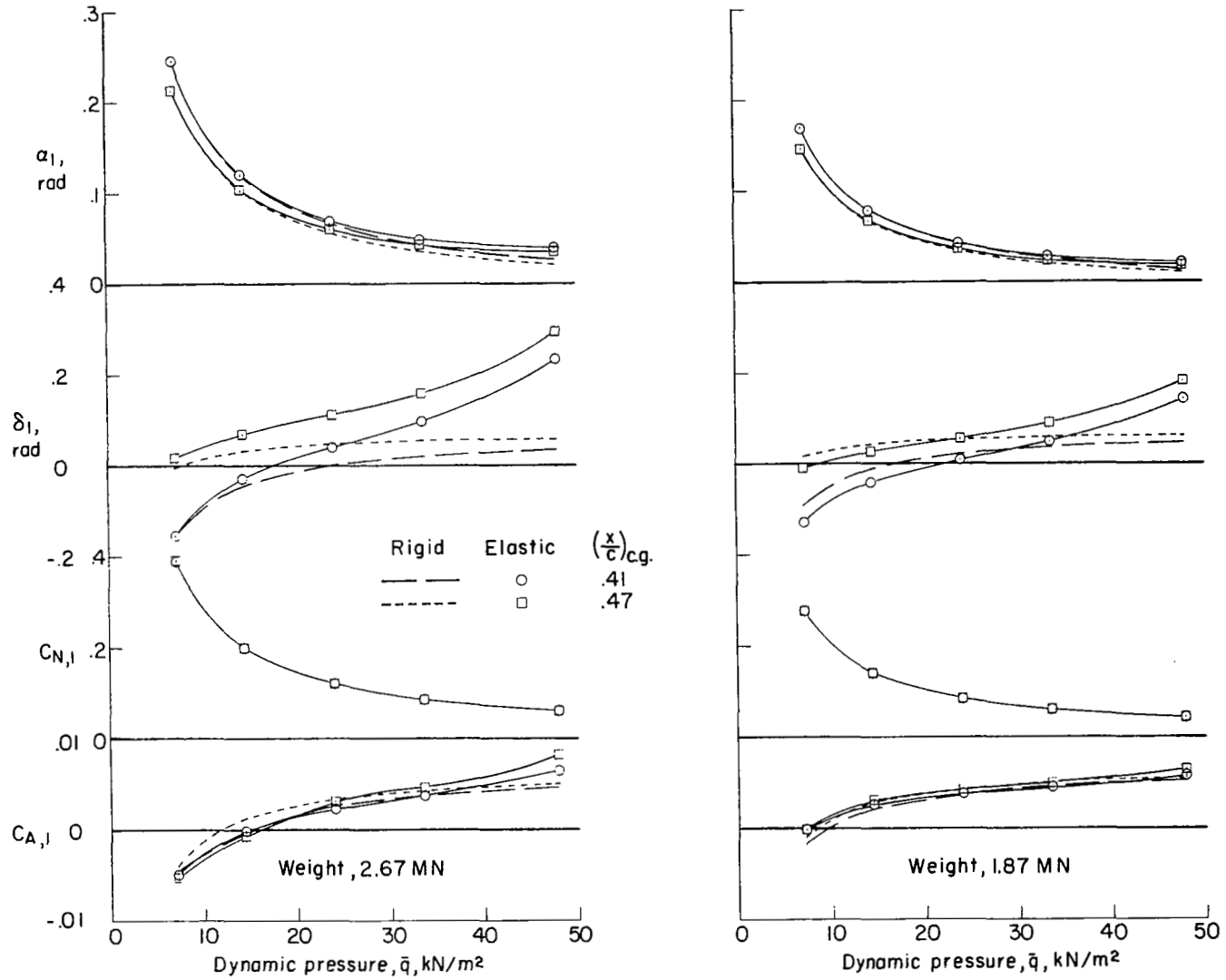
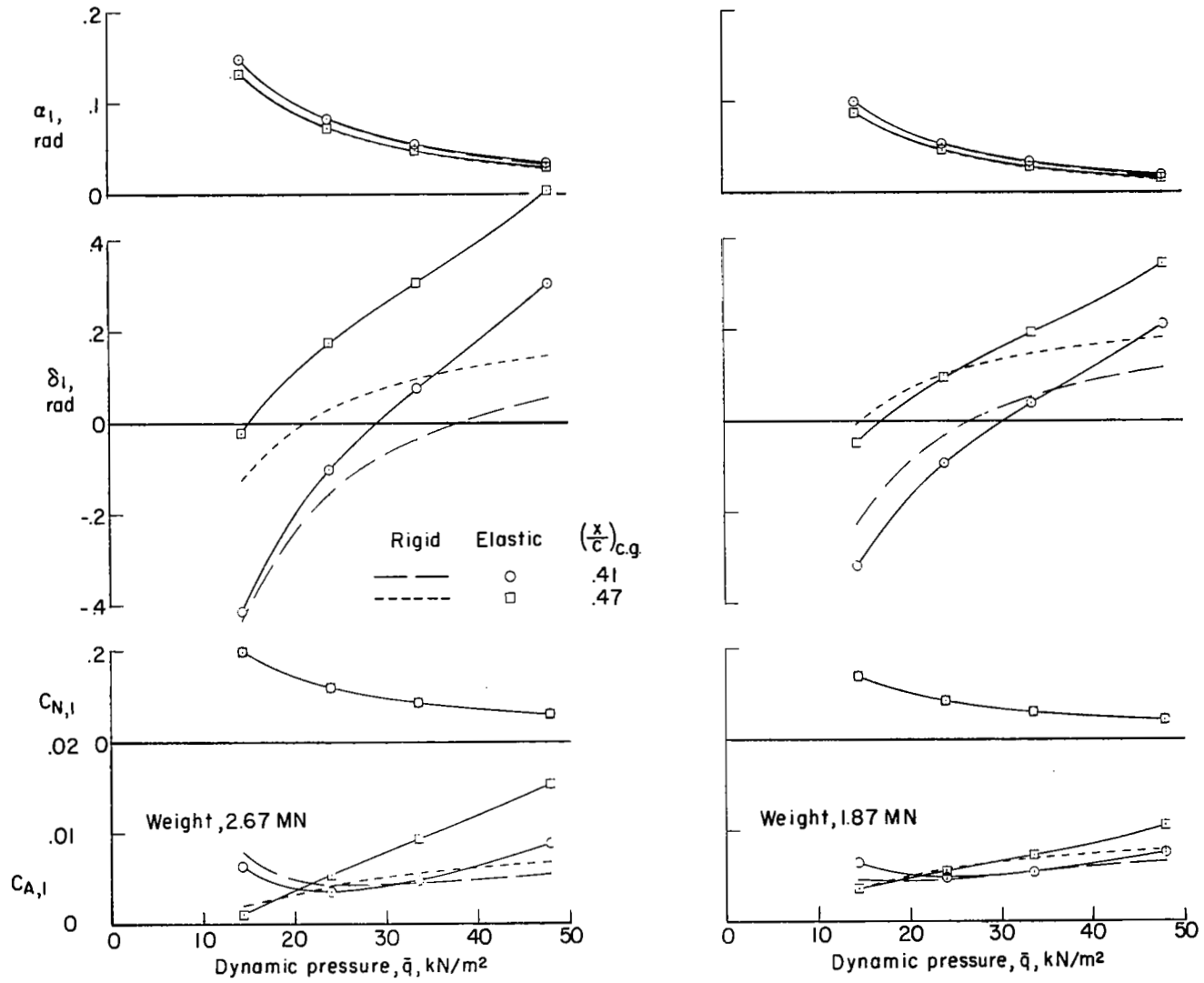


Figure 3.- Distribution of mean-camber-surface slopes for design shape and jig shape. $M_{des} = 2.7$;
 $C_{N,des} = 0.07914$; $\bar{q}_{des} = 28.6 \text{ kN/m}^2$.



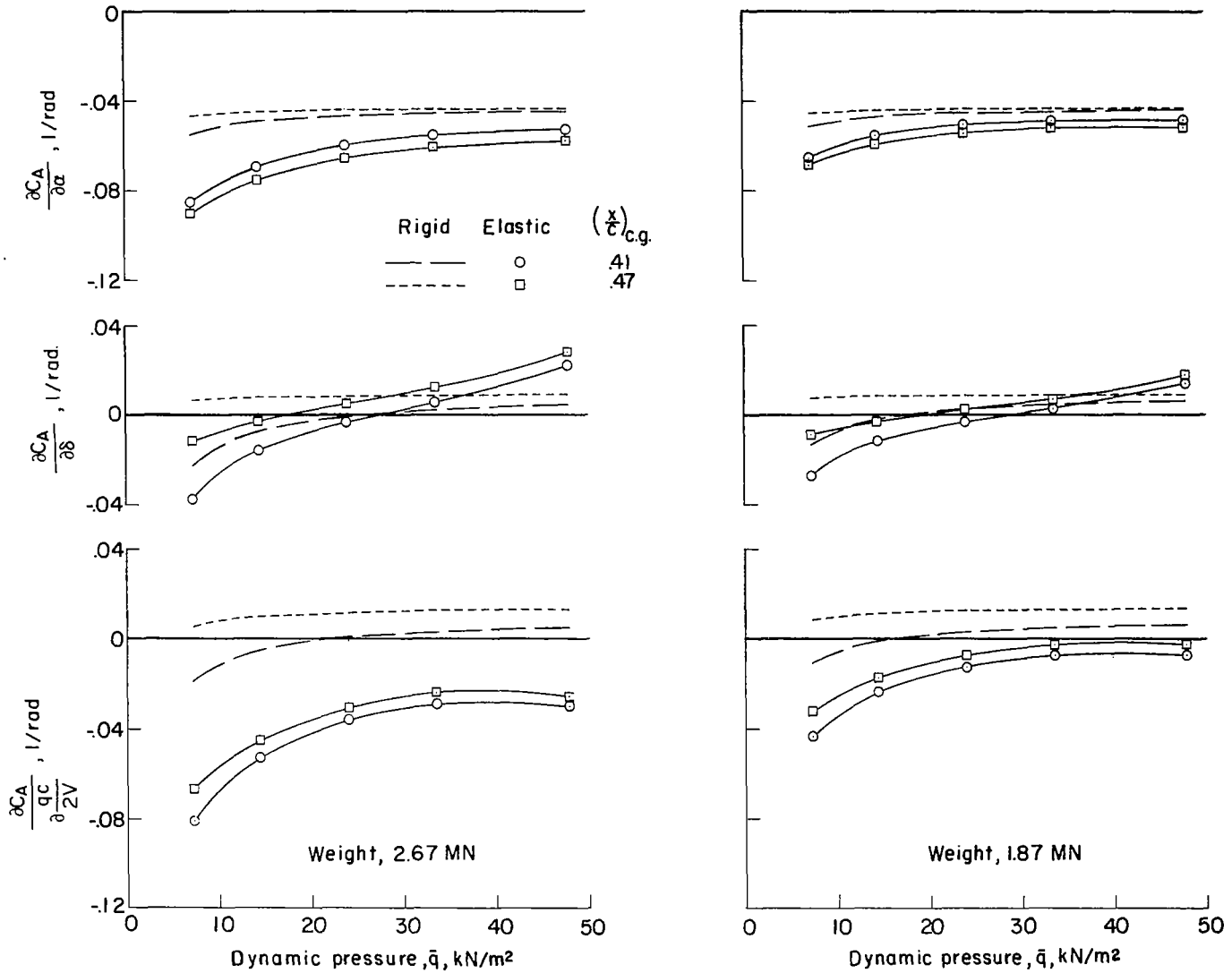
(a) $M = 0.8$.

Figure 4.- Parameters describing reference flight conditions.



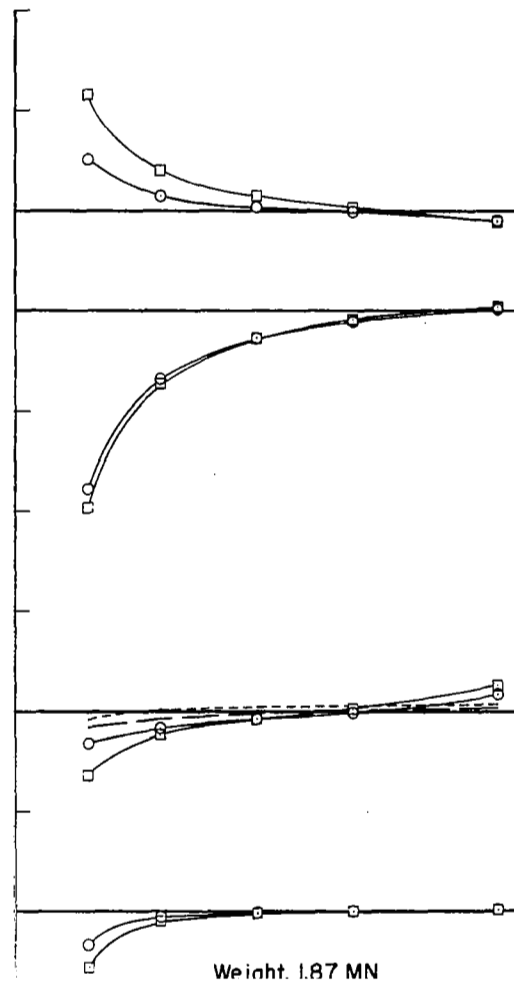
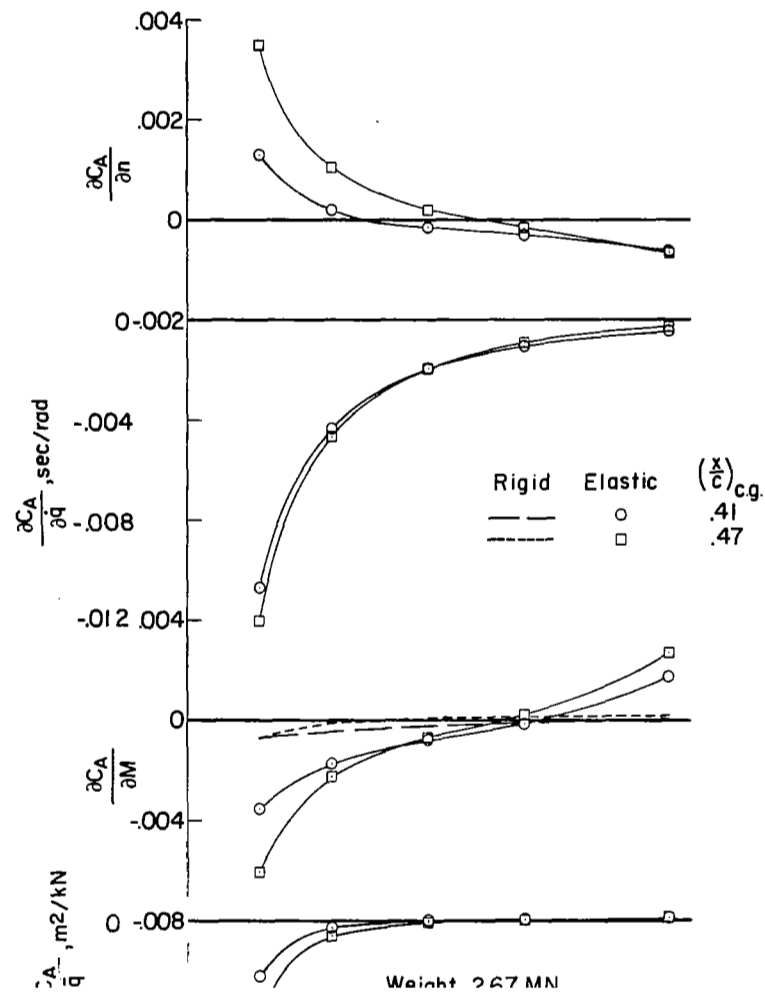
(b) $M = 2.7$.

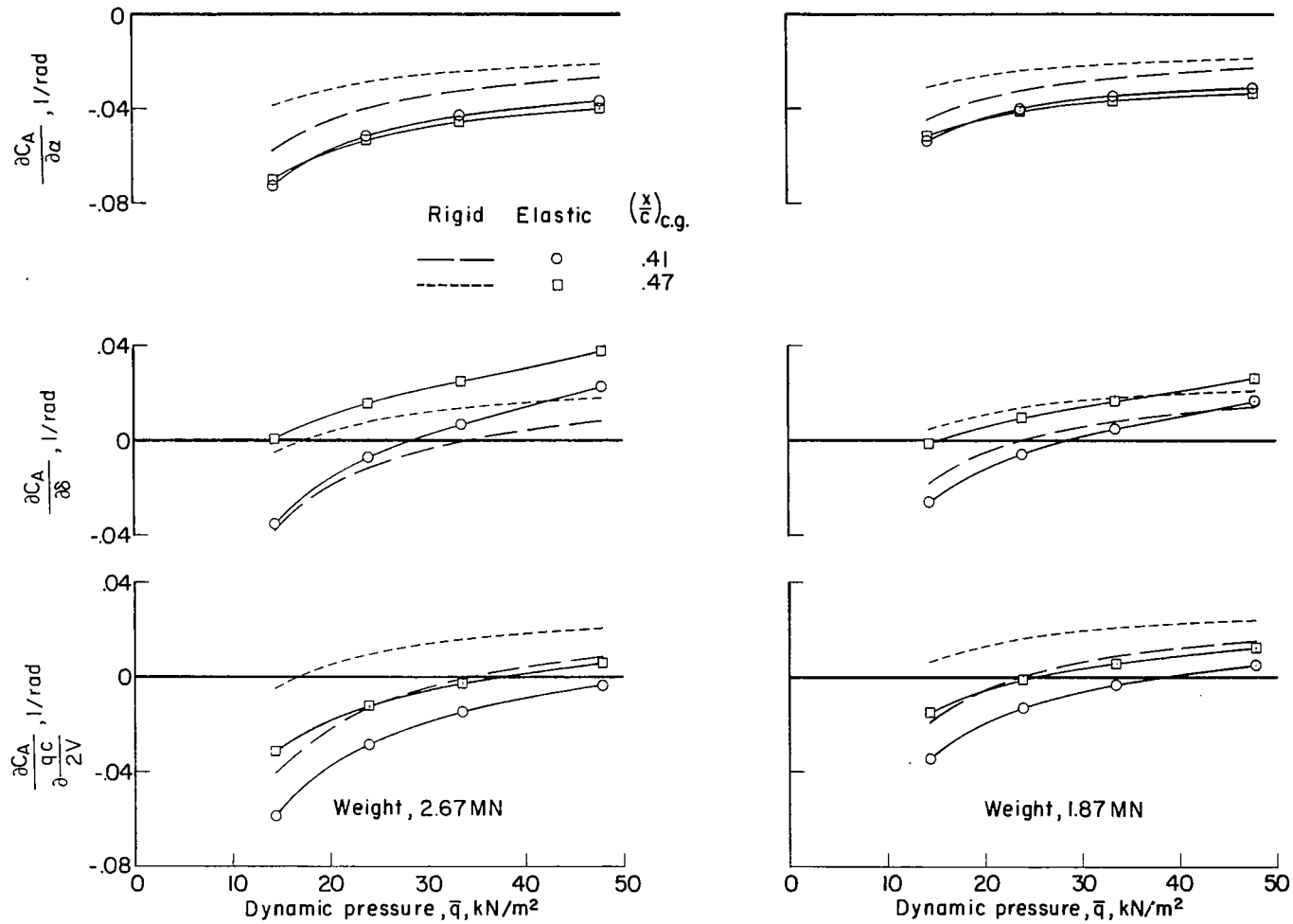
Figure 4. - Concluded.



(a) $M = 0.8$.

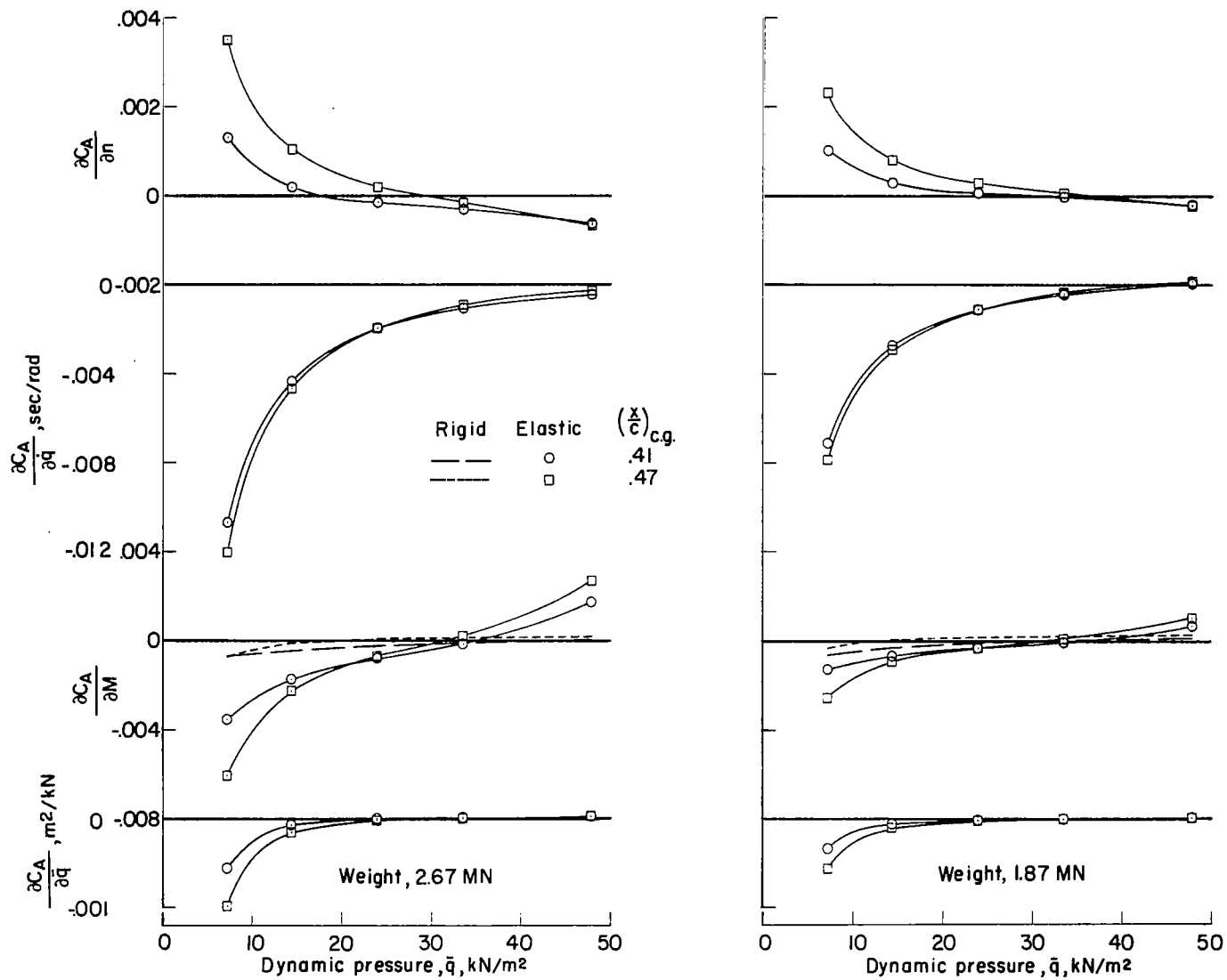
Figure 5.- Partial derivatives of C_A with respect to the physical variables.





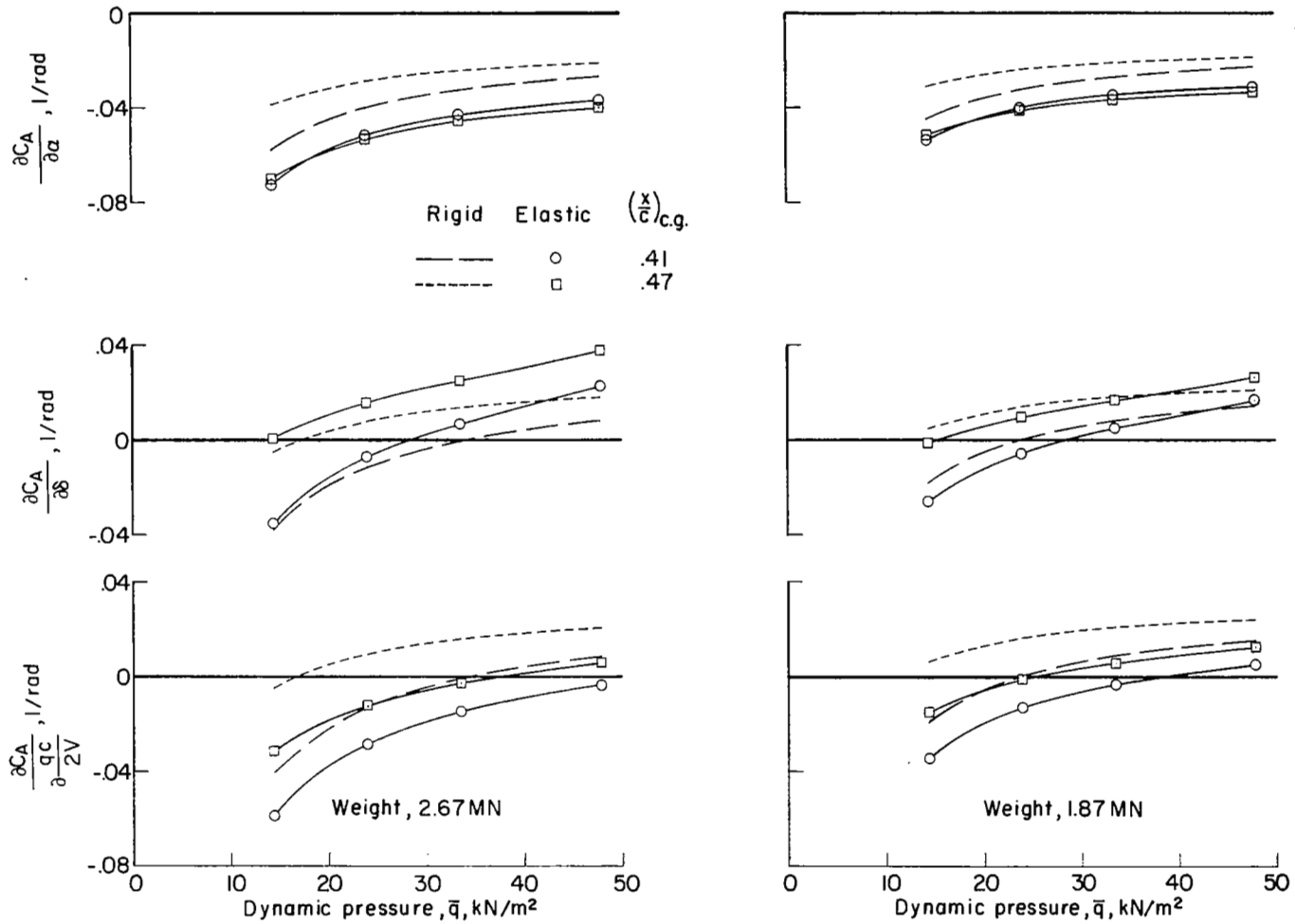
(b) $M = 2.7$.

Figure 5. - Continued.



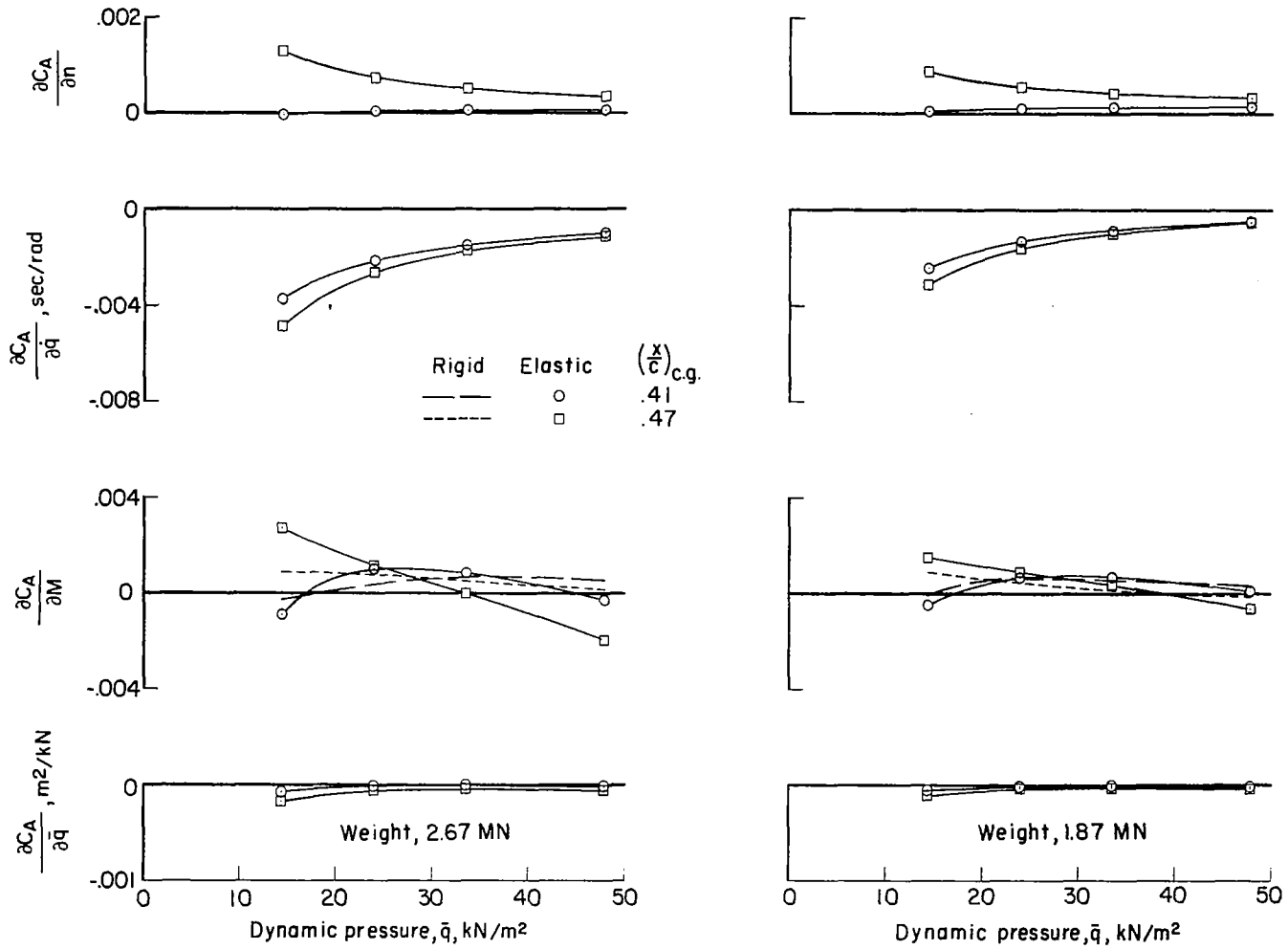
(a) Concluded.

Figure 5. - Continued.



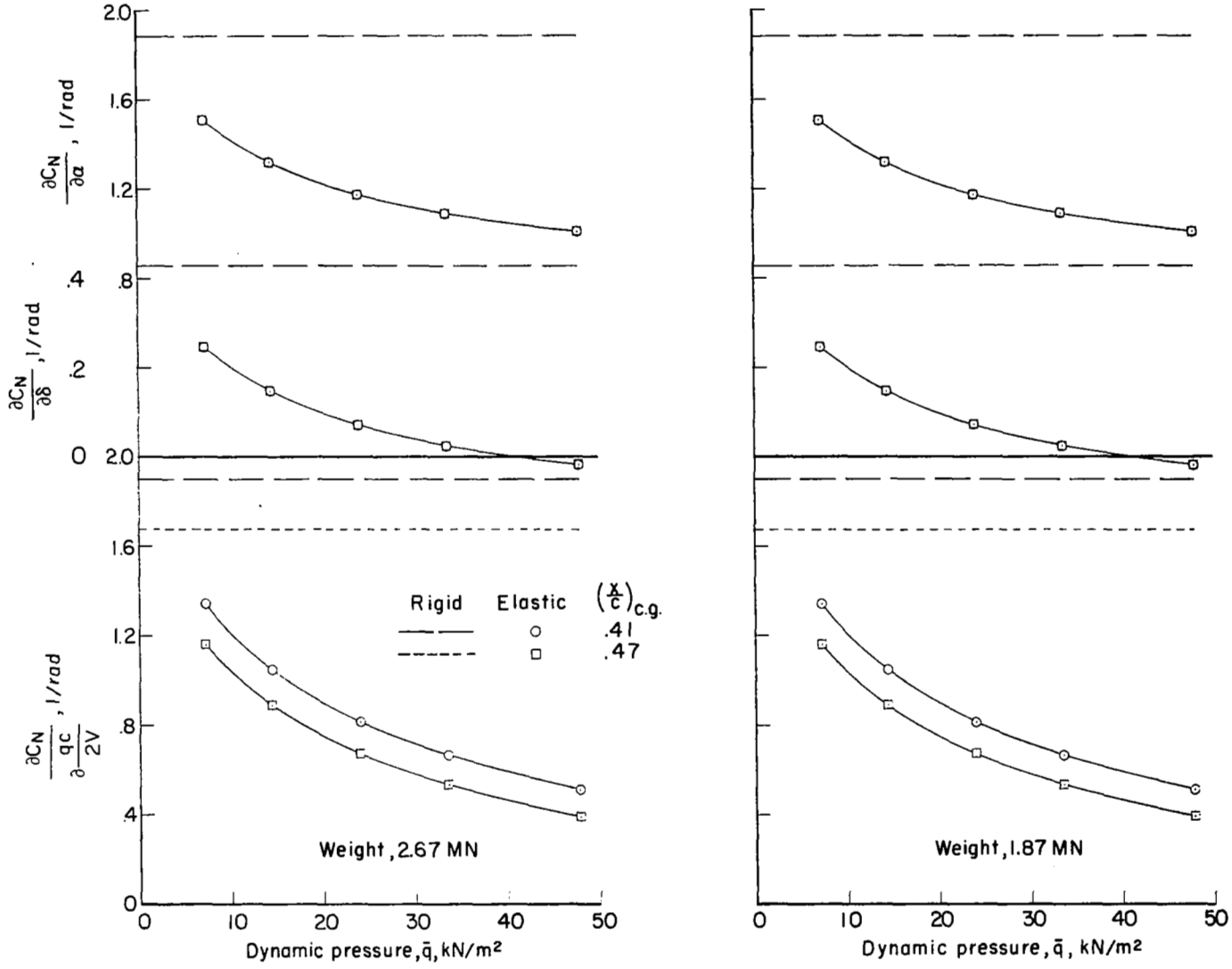
(b) $M = 2.7$.

Figure 5.- Continued.



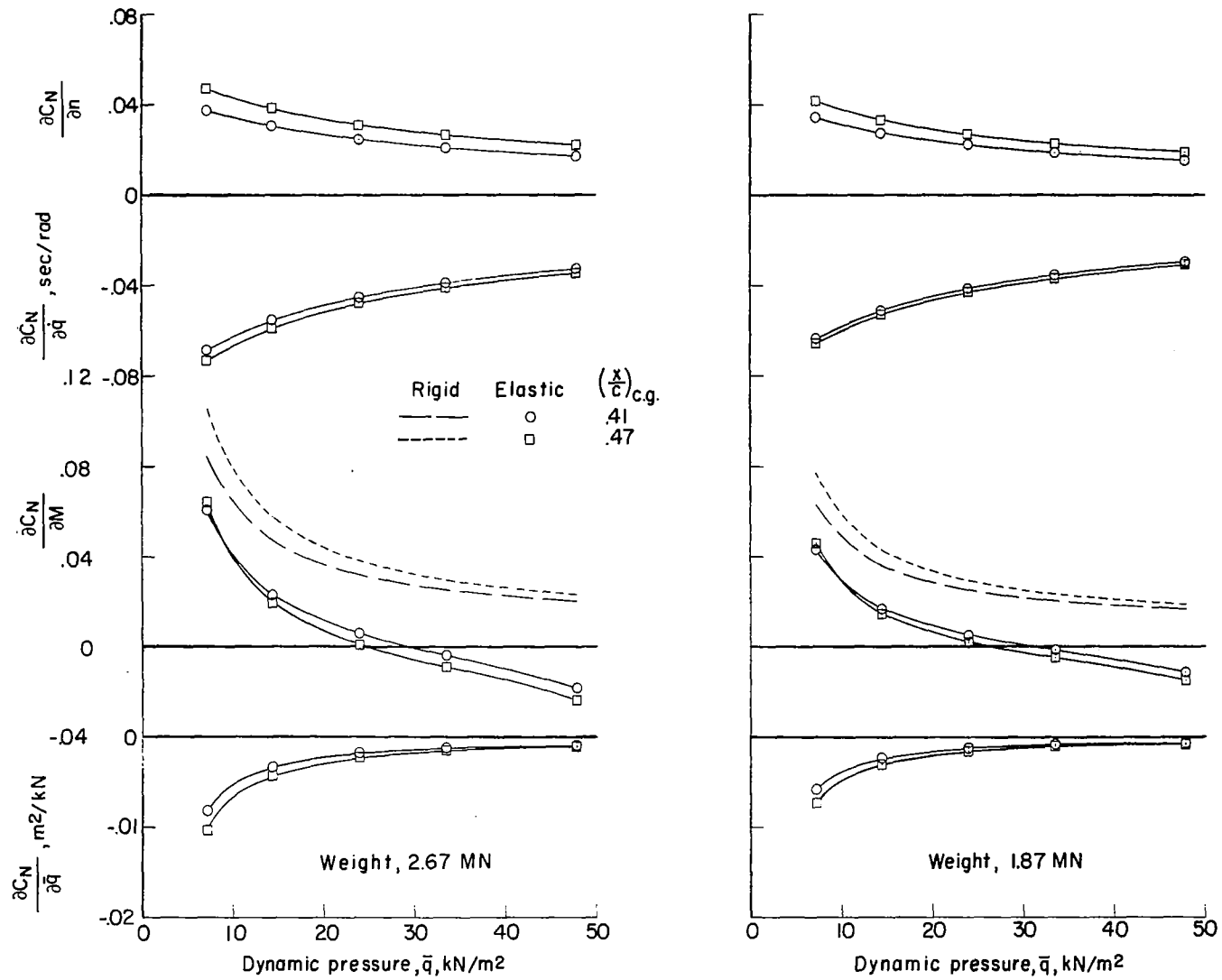
(b) Concluded.

Figure 5.- Concluded.



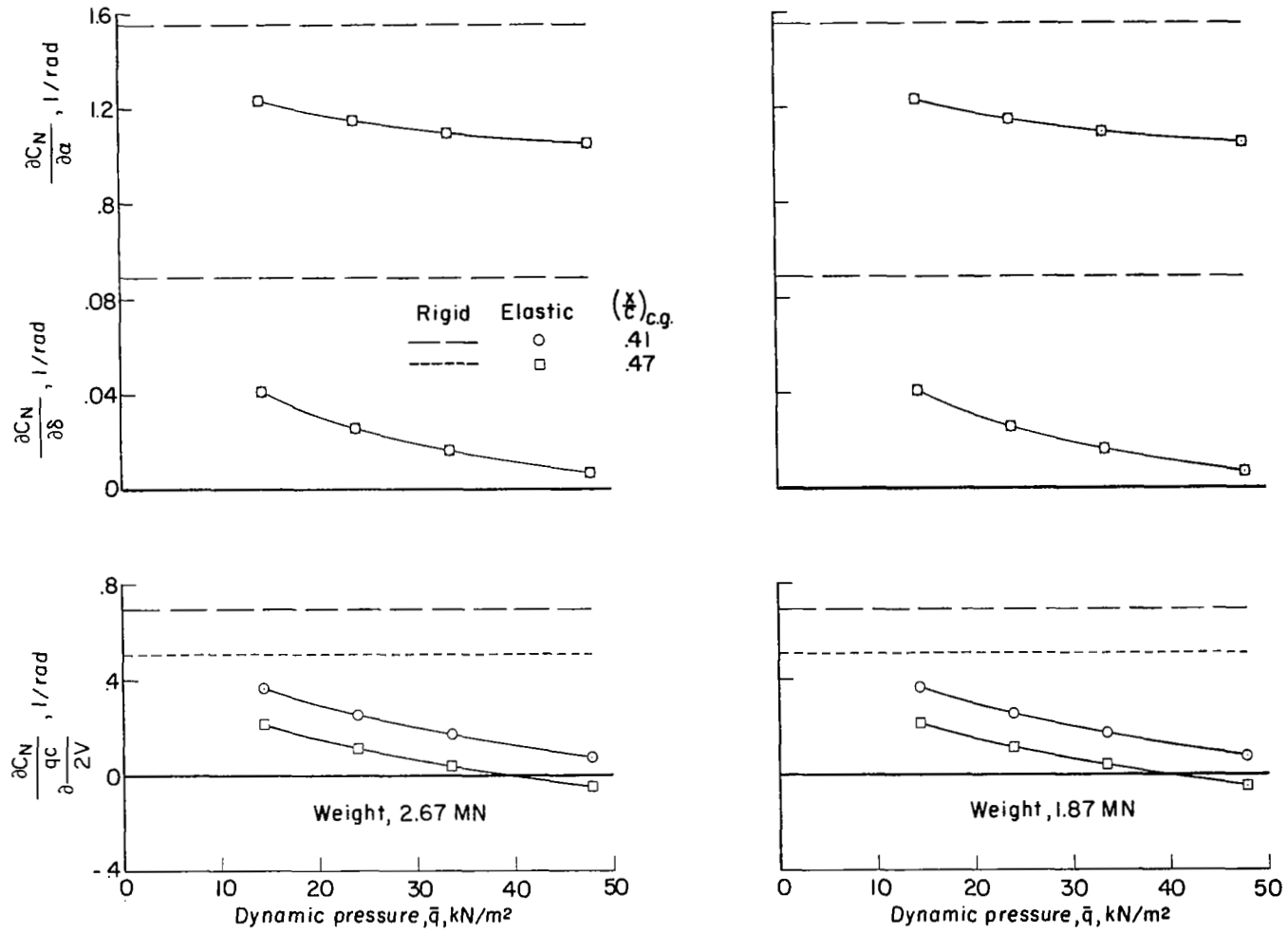
(a) M = 0.8.

Figure 6.- Partial derivatives of C_N with respect to the physical variables.



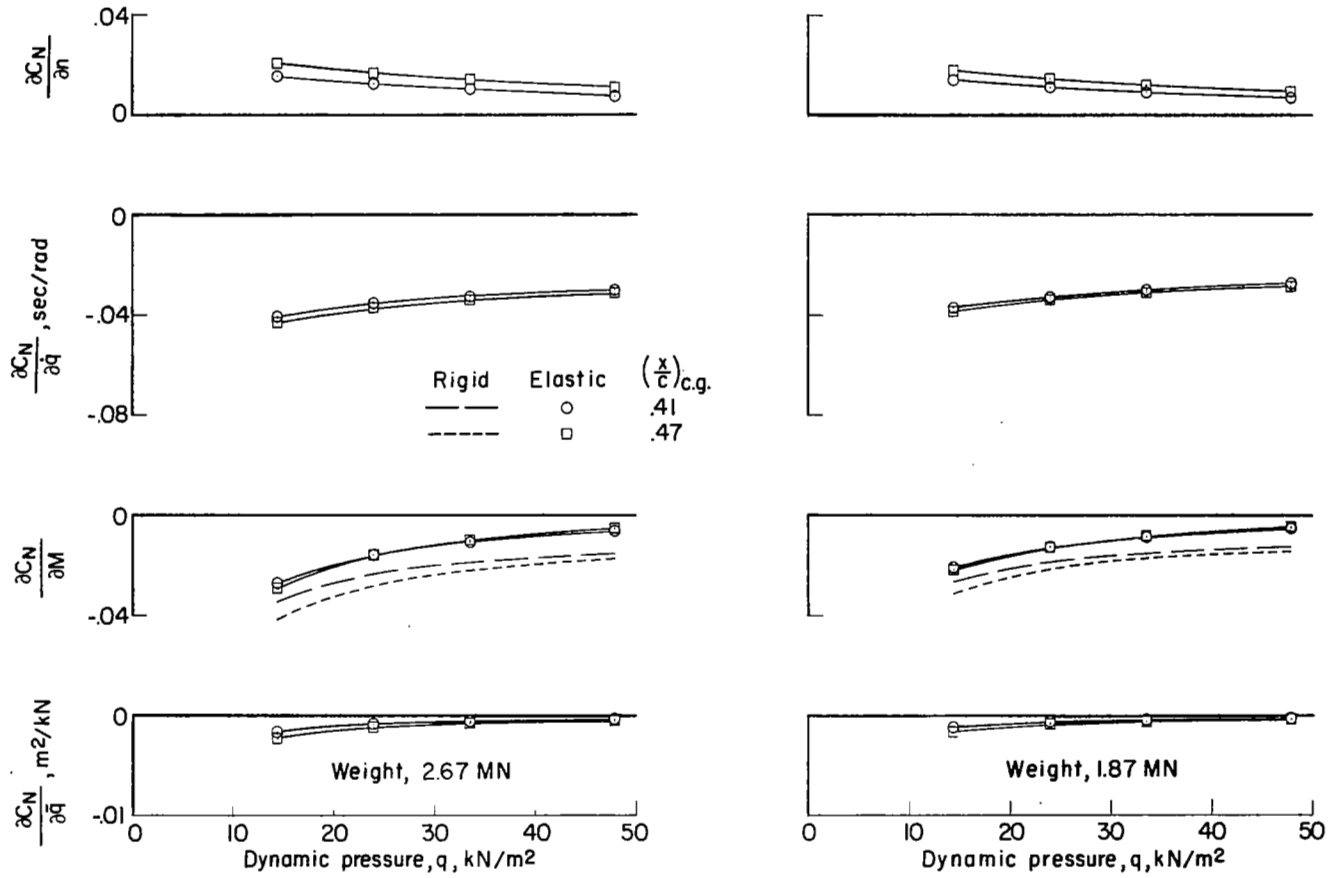
(a) Concluded.

Figure 6. - Continued.



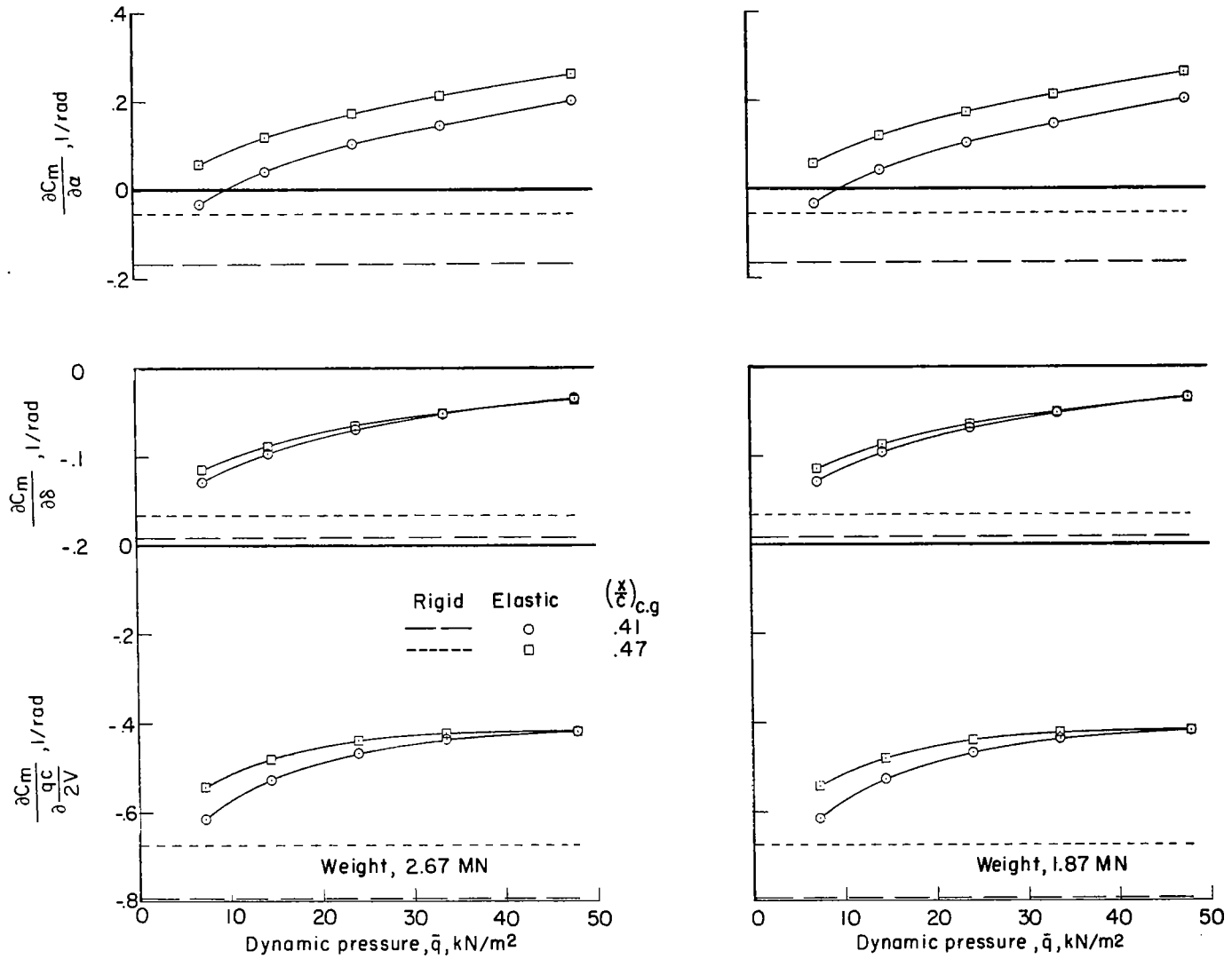
(b) M = 2.7.

Figure 6.- Continued.



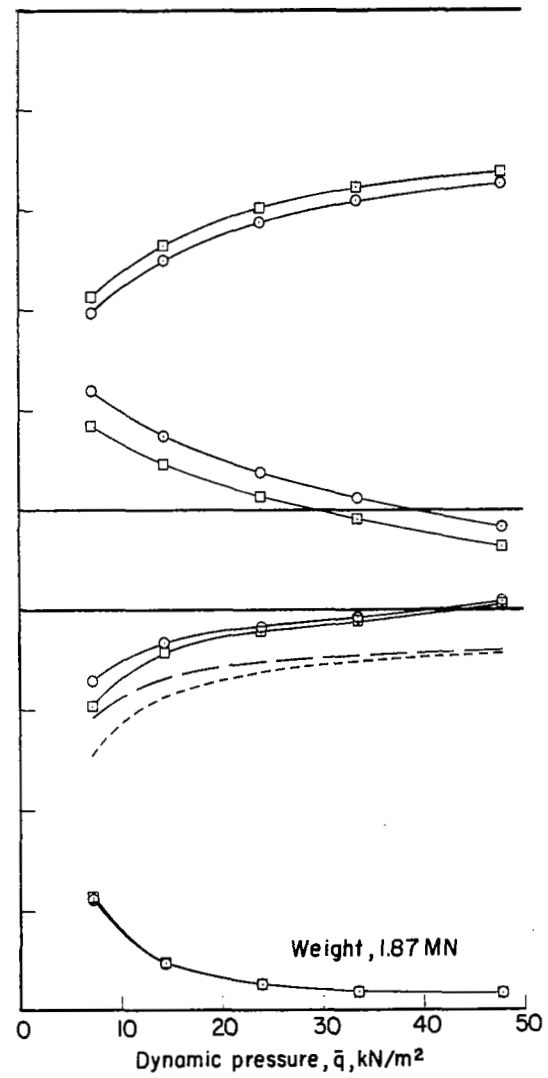
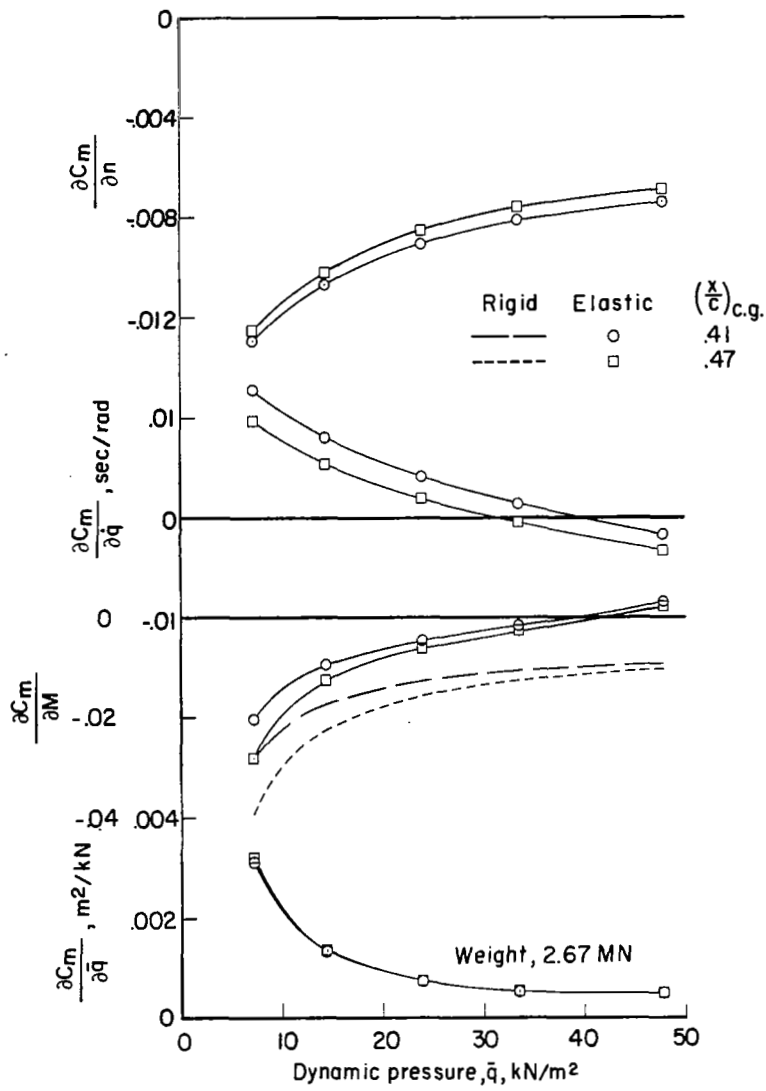
(b) Concluded.

Figure 6.- Concluded.



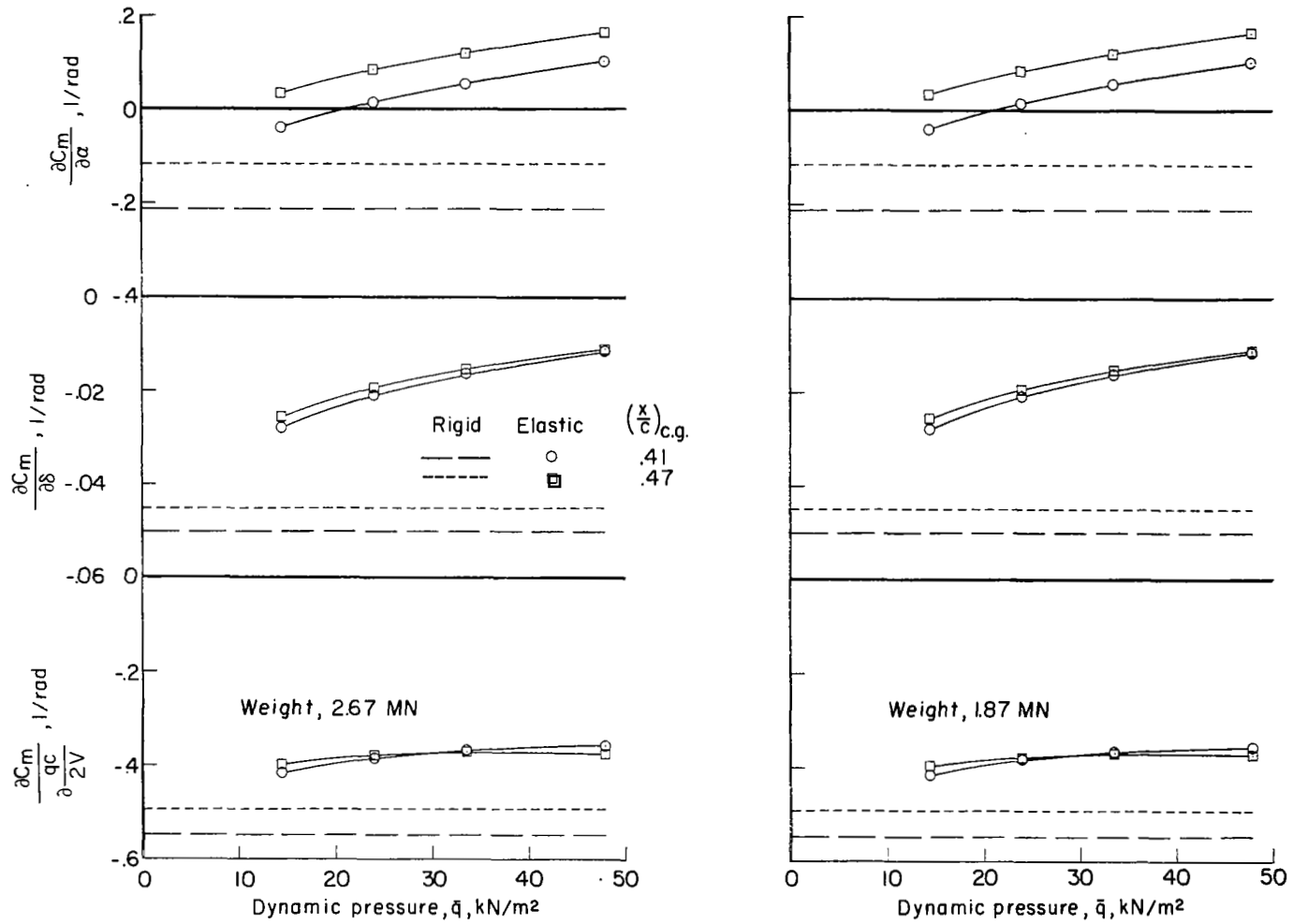
(a) $M = 0.8$.

Figure 7.- Partial derivatives of C_m with respect to the physical variables.



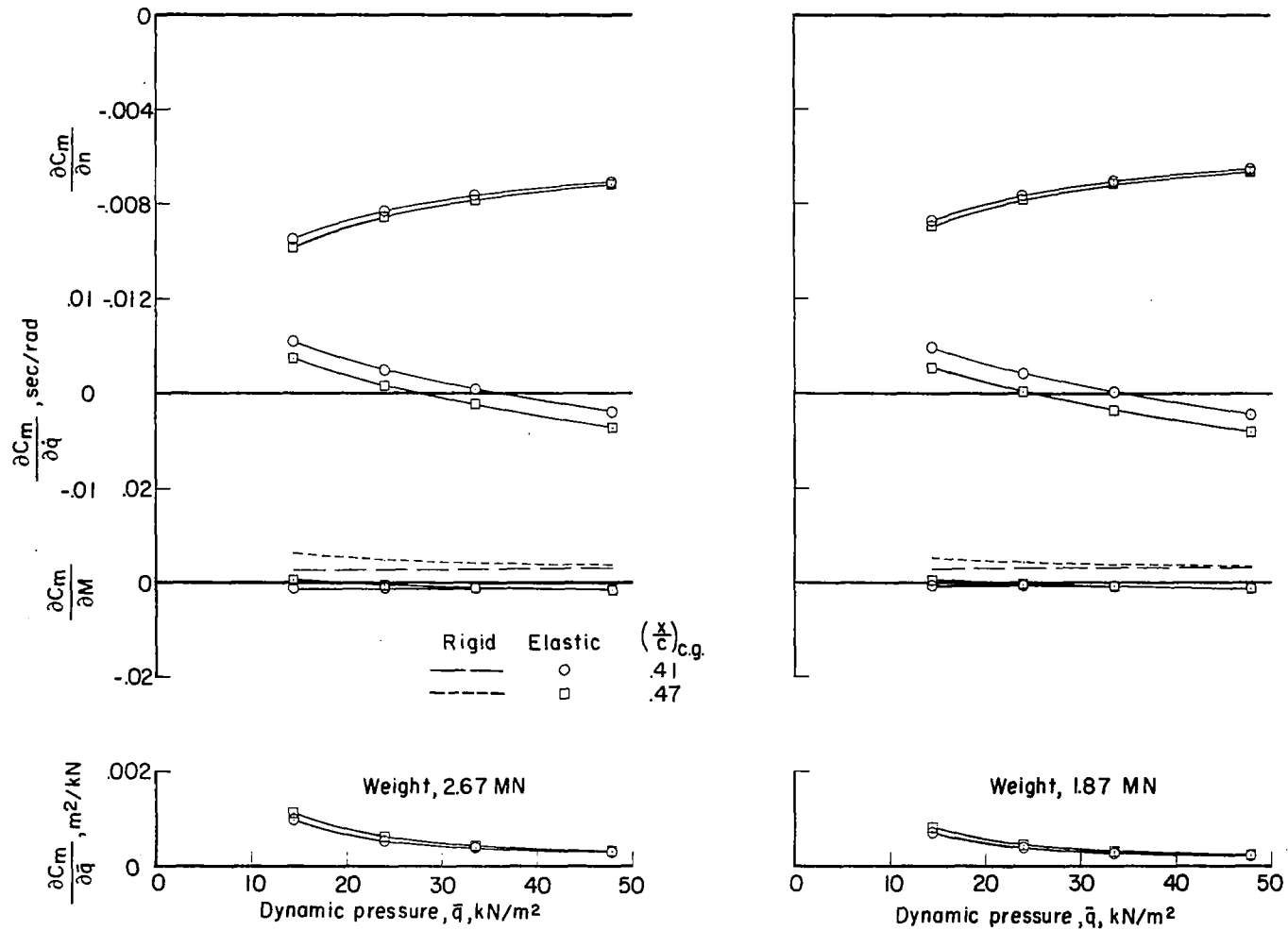
(a) Concluded.

Figure 7.- Continued.



(b) $M = 2.7$.

Figure 7.- Continued.



(b) Concluded.

Figure 7.- Concluded.

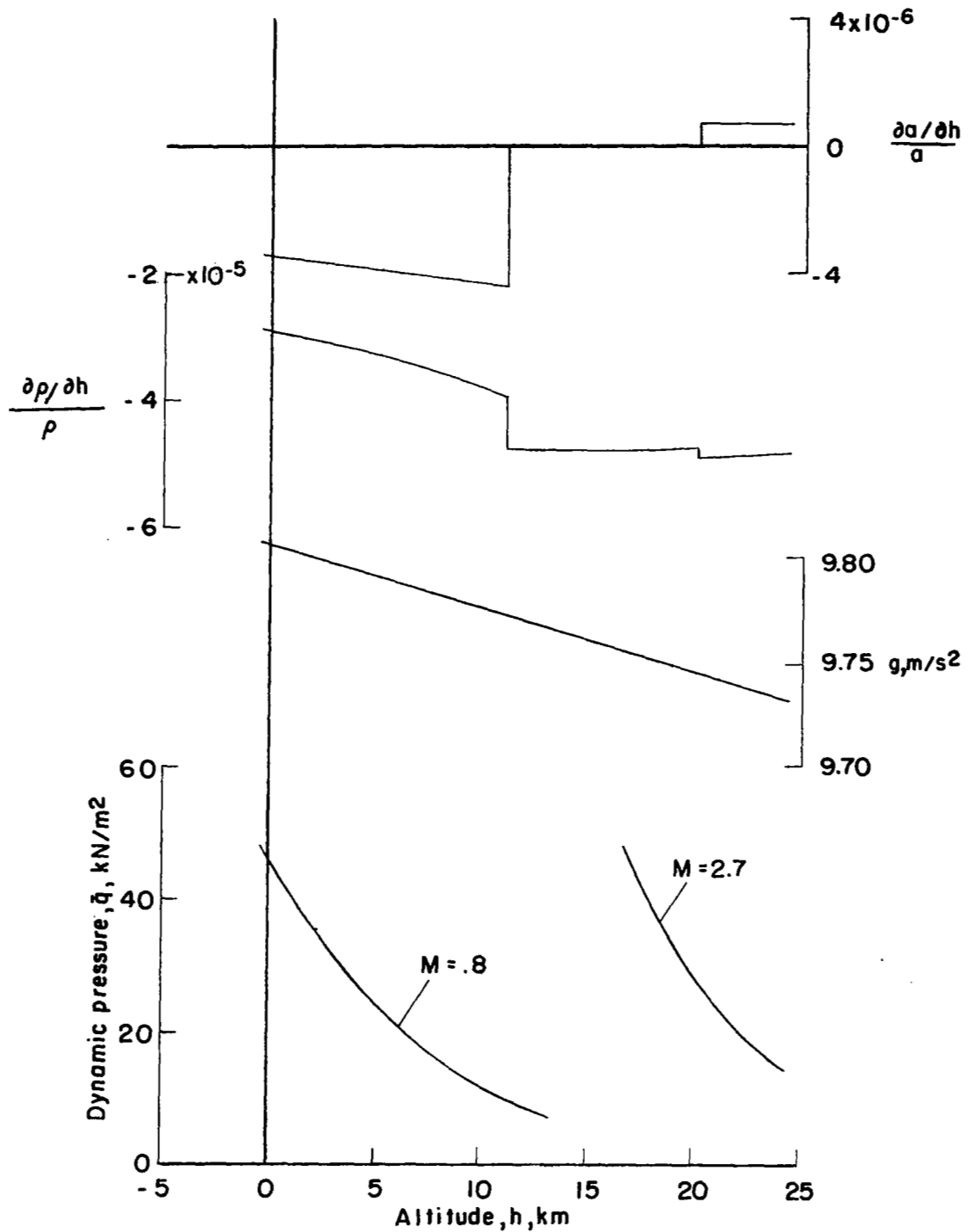
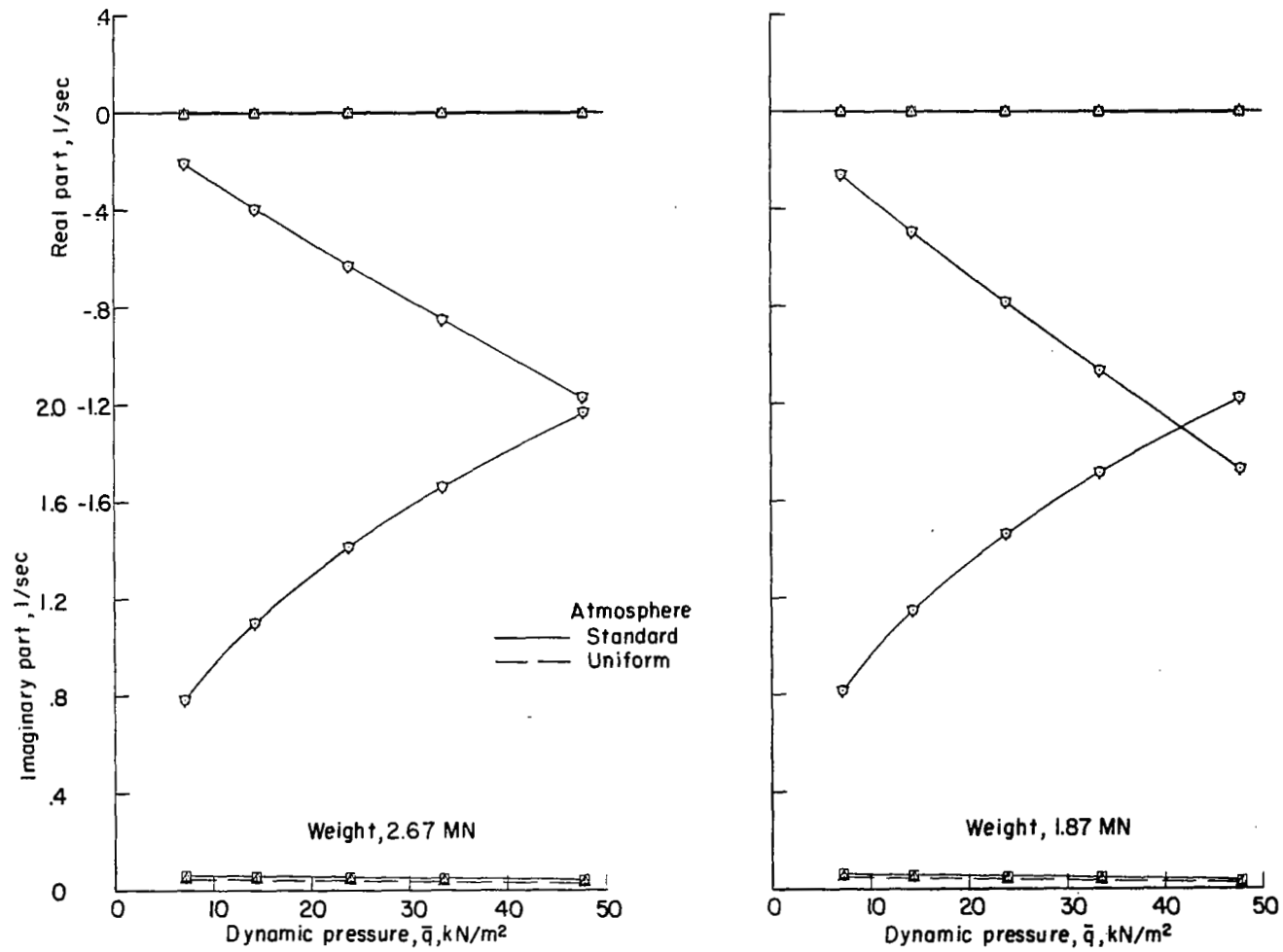
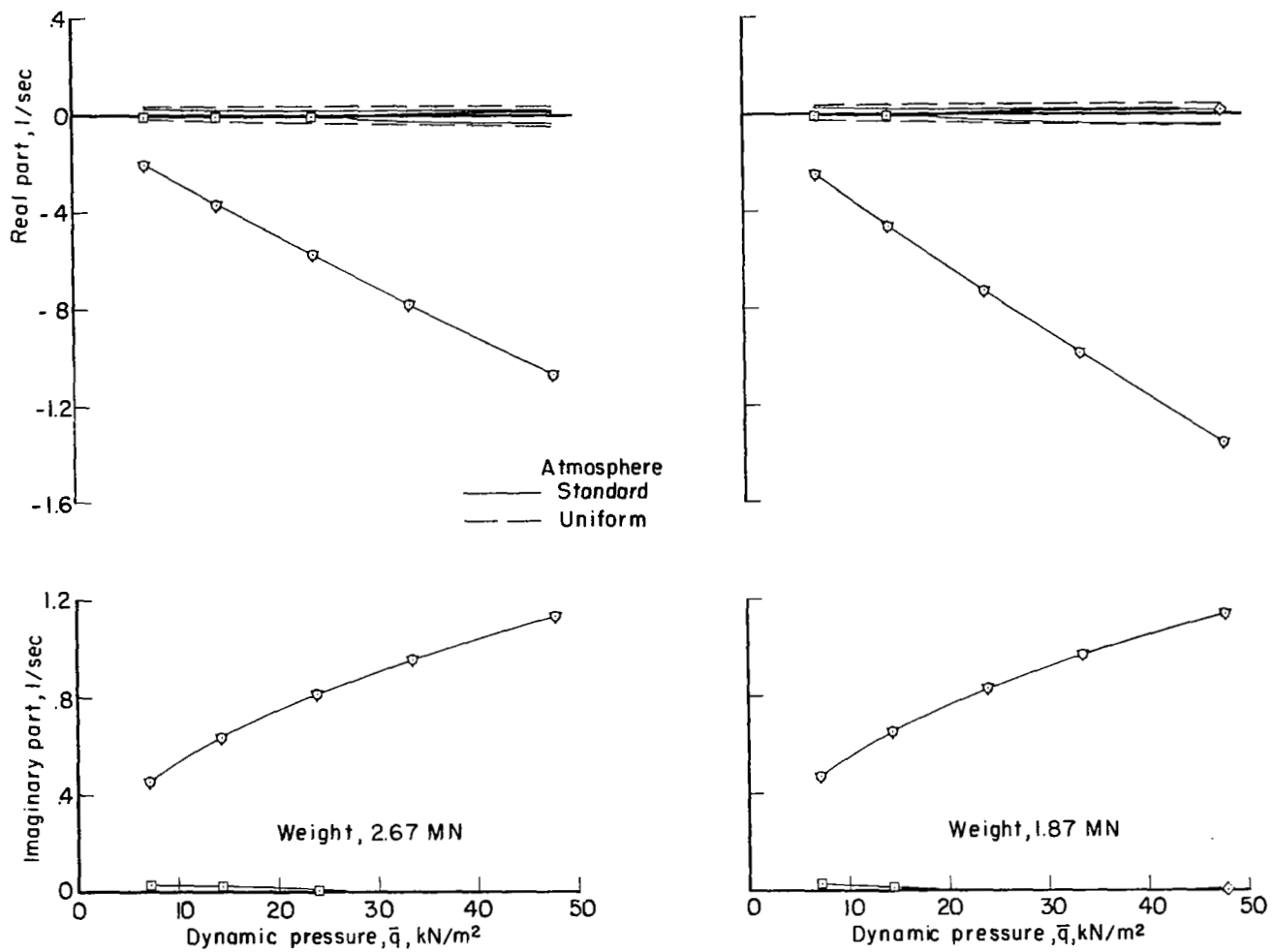


Figure 8.- Variation of sonic velocity gradient, density gradient, gravity acceleration, and dynamic pressure with altitude.



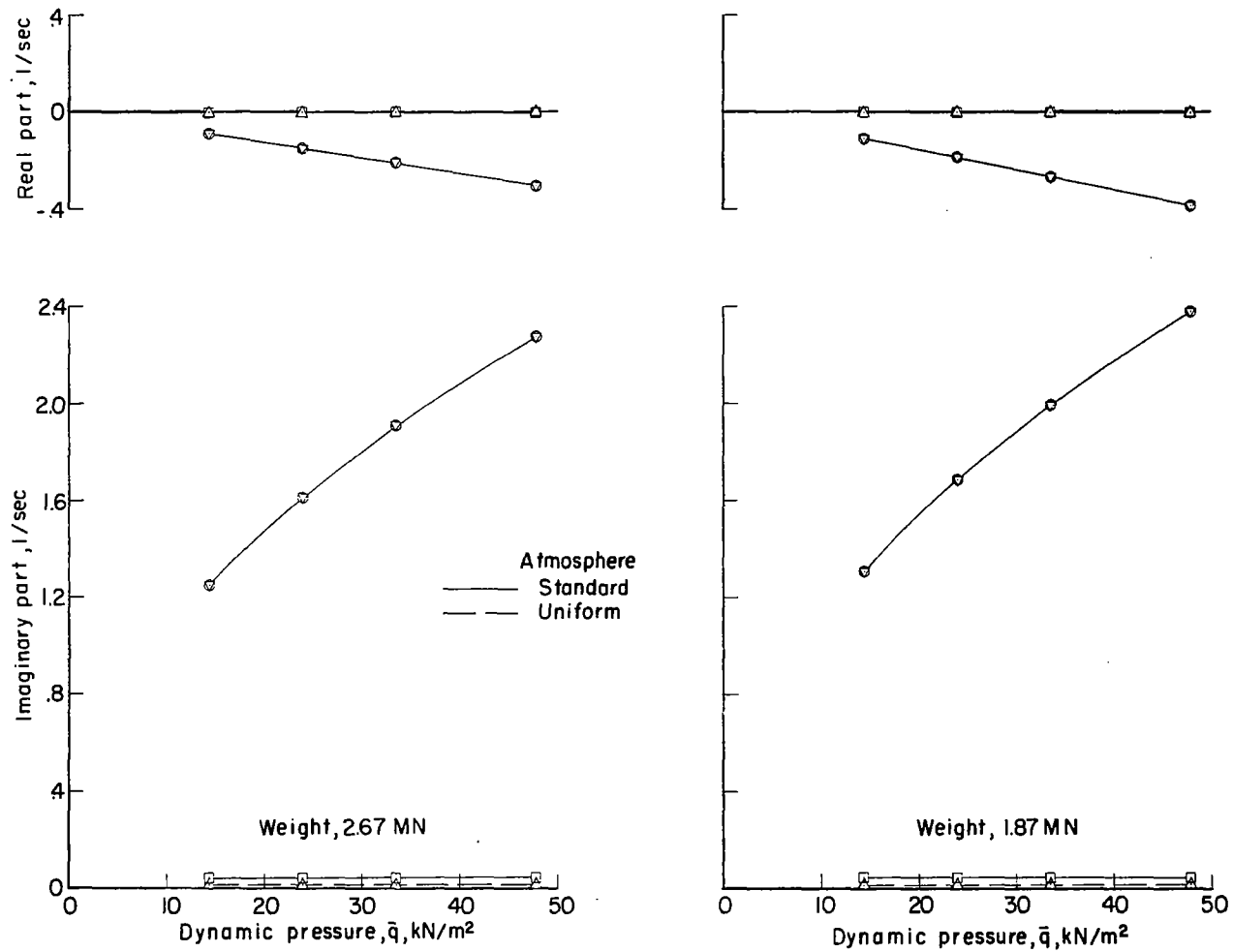
(a) $M = 0.8$; c.g. at 0.41c.

Figure 9.- Variation of characteristic roots with dynamic pressure. Rigid airplane.



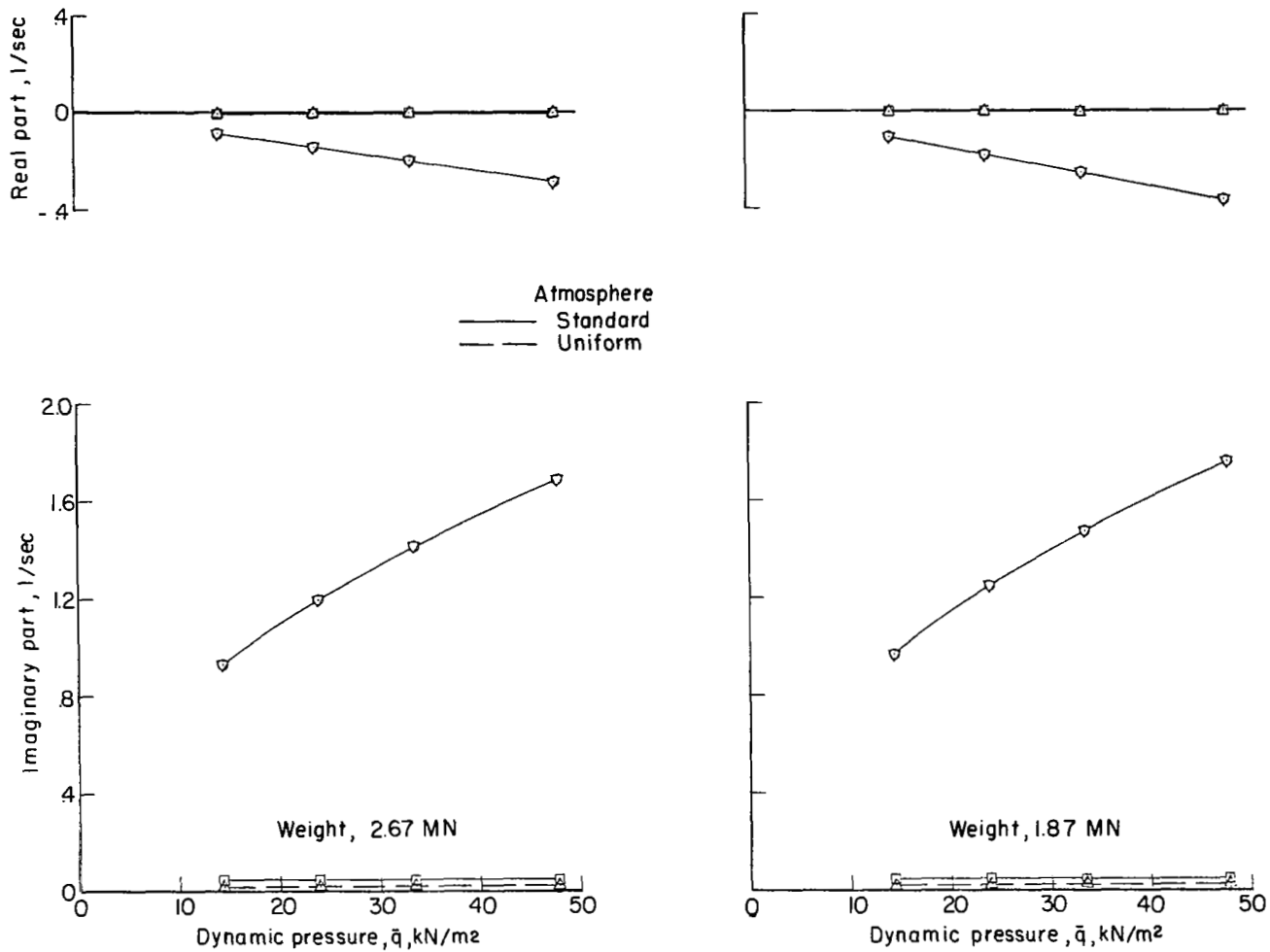
(b) $M = 0.8$; c.g. at $0.47c$.

Figure 9.- Continued.



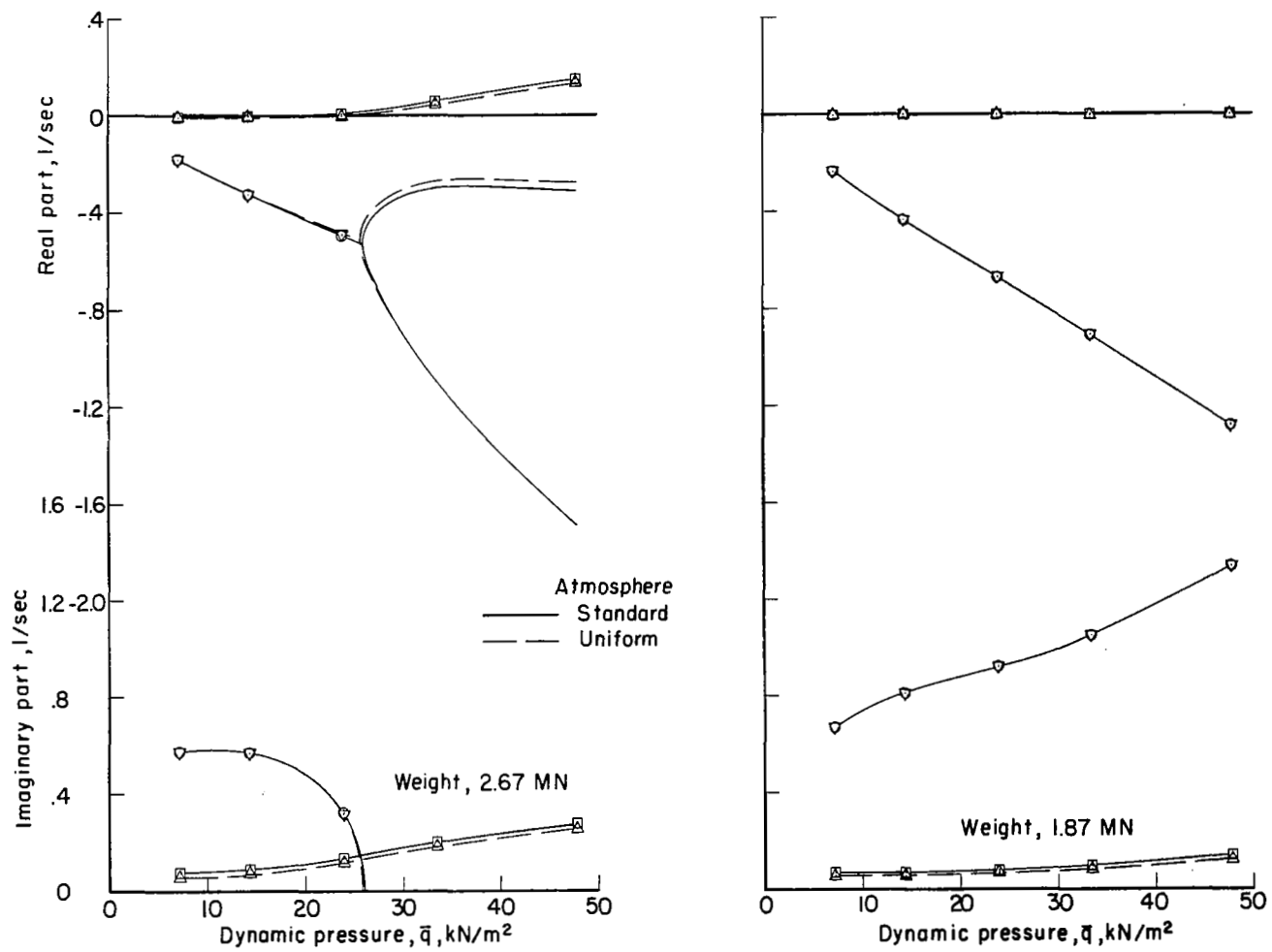
(c) $M = 2.7$; c.g. at $0.41c$.

Figure 9.- Continued.



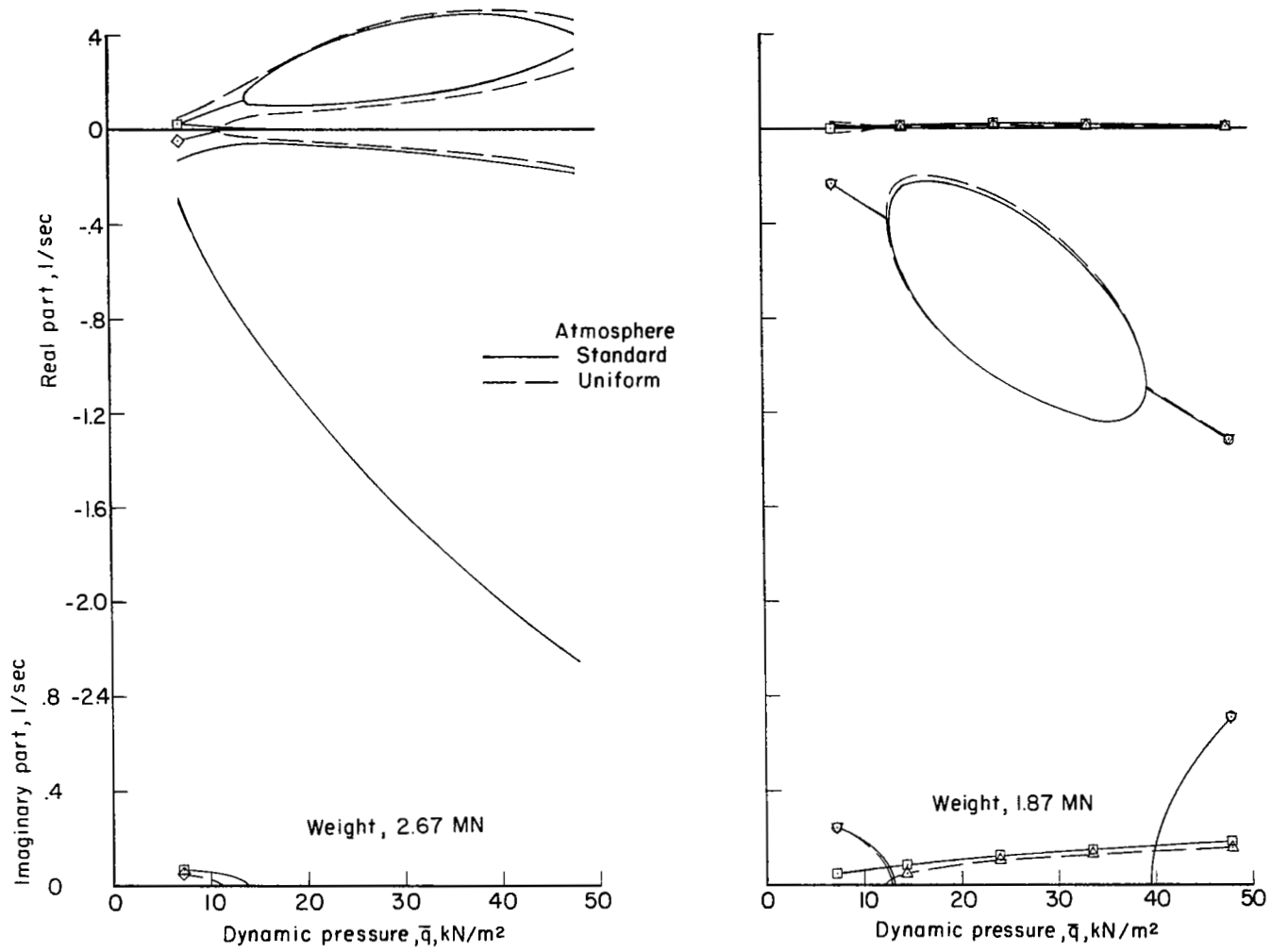
(d) $M = 2.7$; c.g. at $0.47c$.

Figure 9.- Concluded.



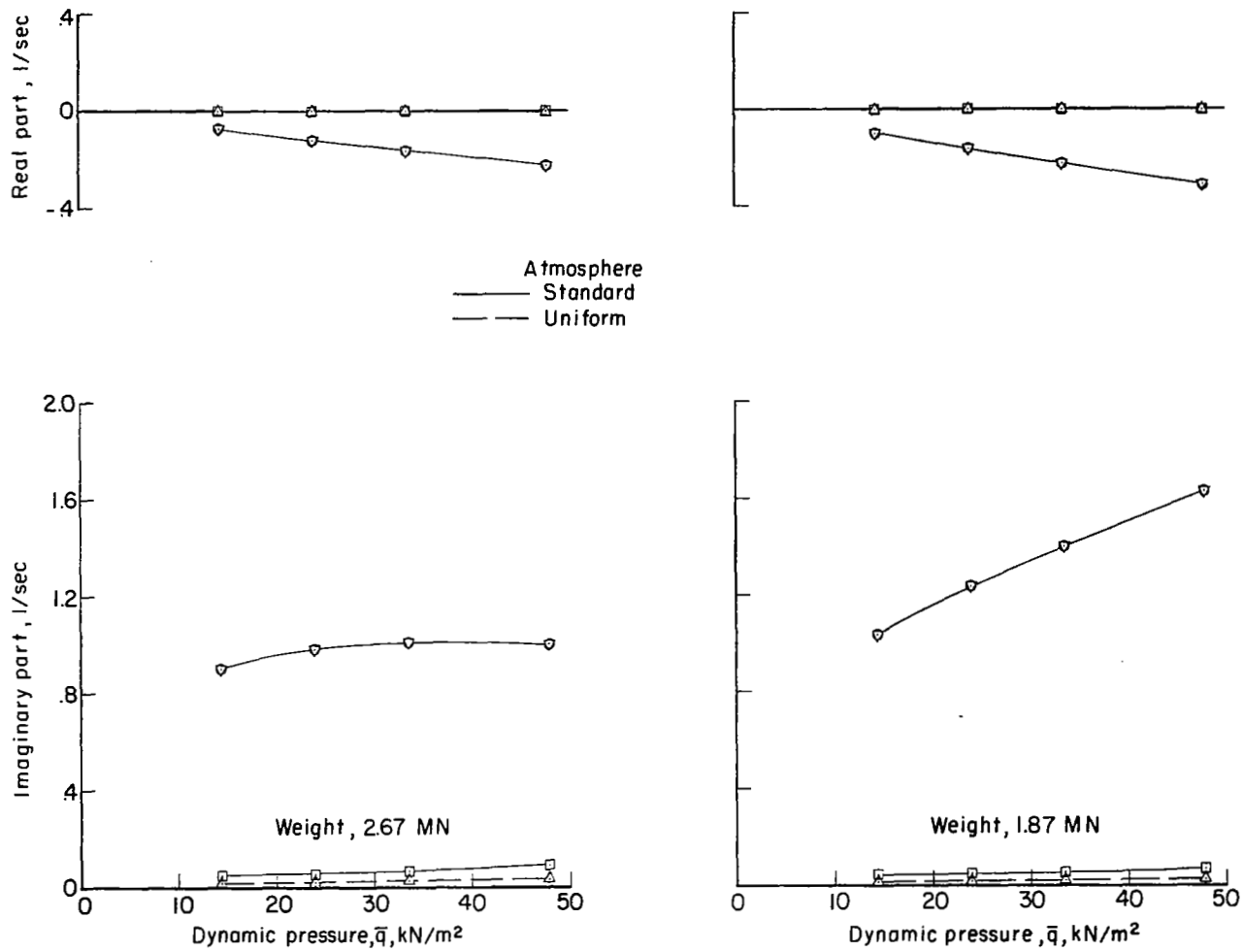
(a) $M = 0.8$; c.g. at 0.41c.

Figure 10.- Variation of characteristic roots with dynamic pressure. Elastic airplane.



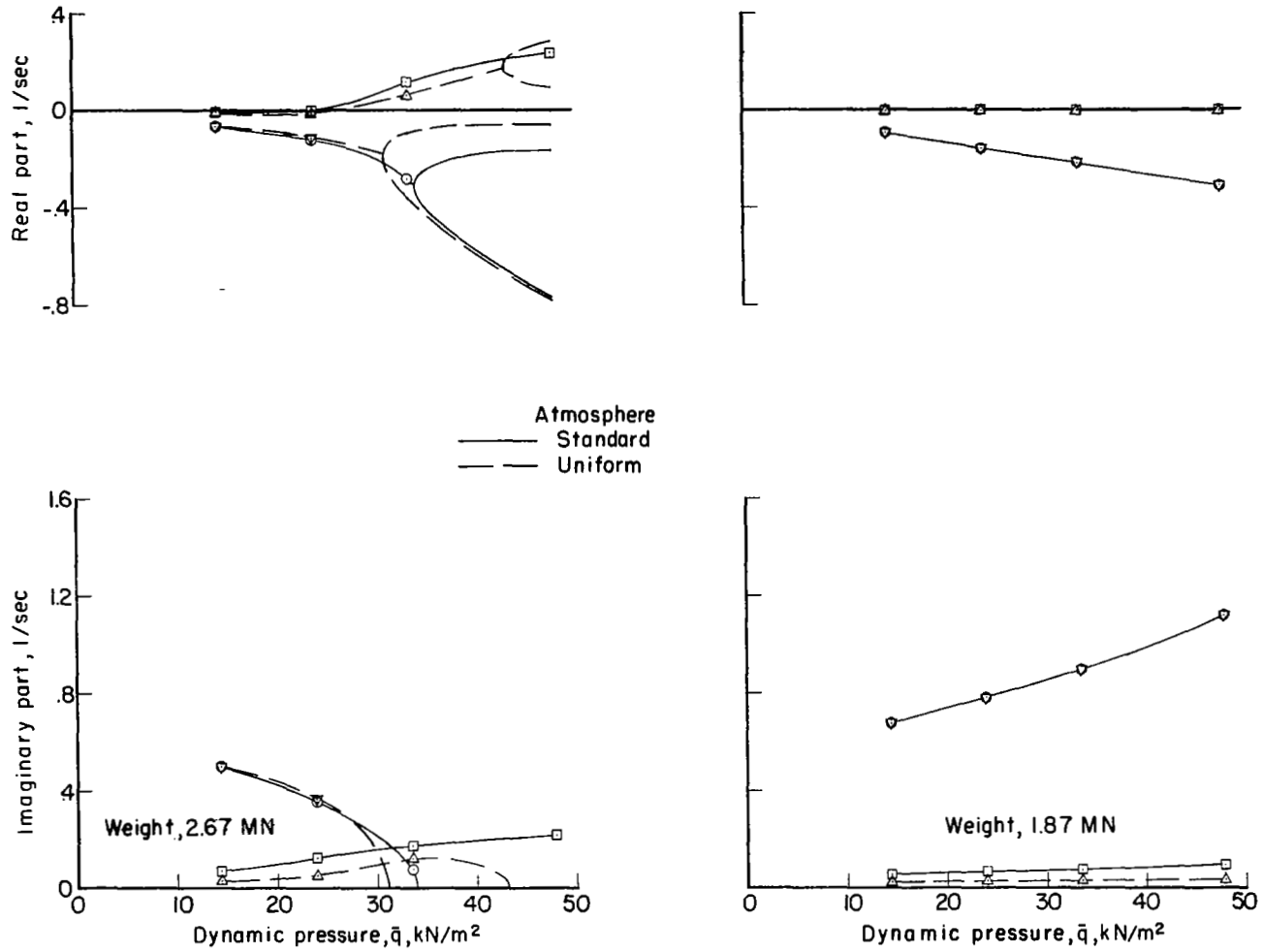
(b) $M = 0.8$; c.g. at $0.47c$.

Figure 10. - Continued.



(c) $M = 2.7$; c.g. at 0.41c.

Figure 10.- Continued.



(d) $M = 2.7$; c.g. at $0.47c$.

Figure 10.- Concluded.

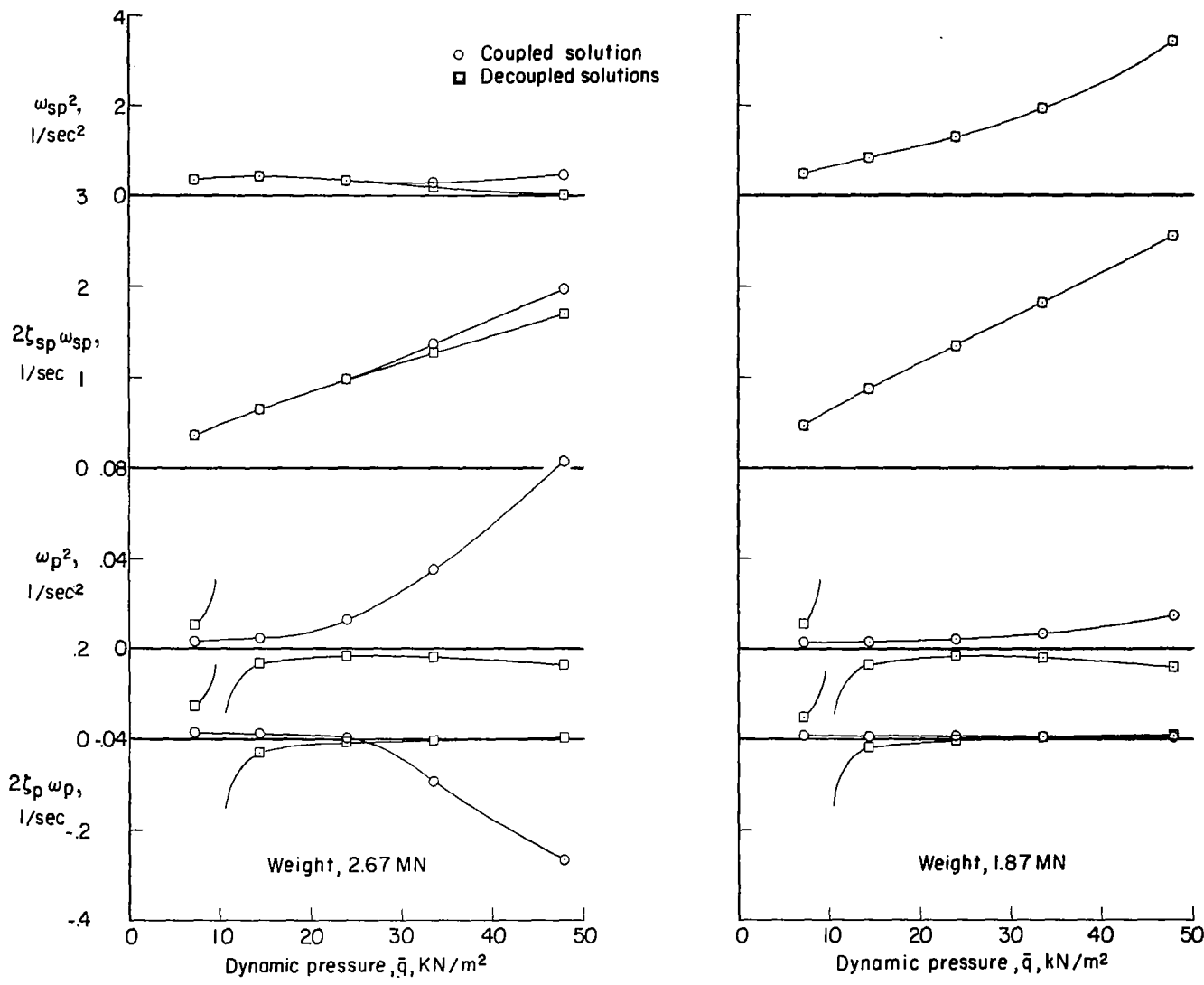


Figure 11.- Effect of root coupling on frequency and damping of short-period and phugoid modes. Elastic airplane; $M = 0.8$; c.g. at $0.41c$; uniform atmosphere.

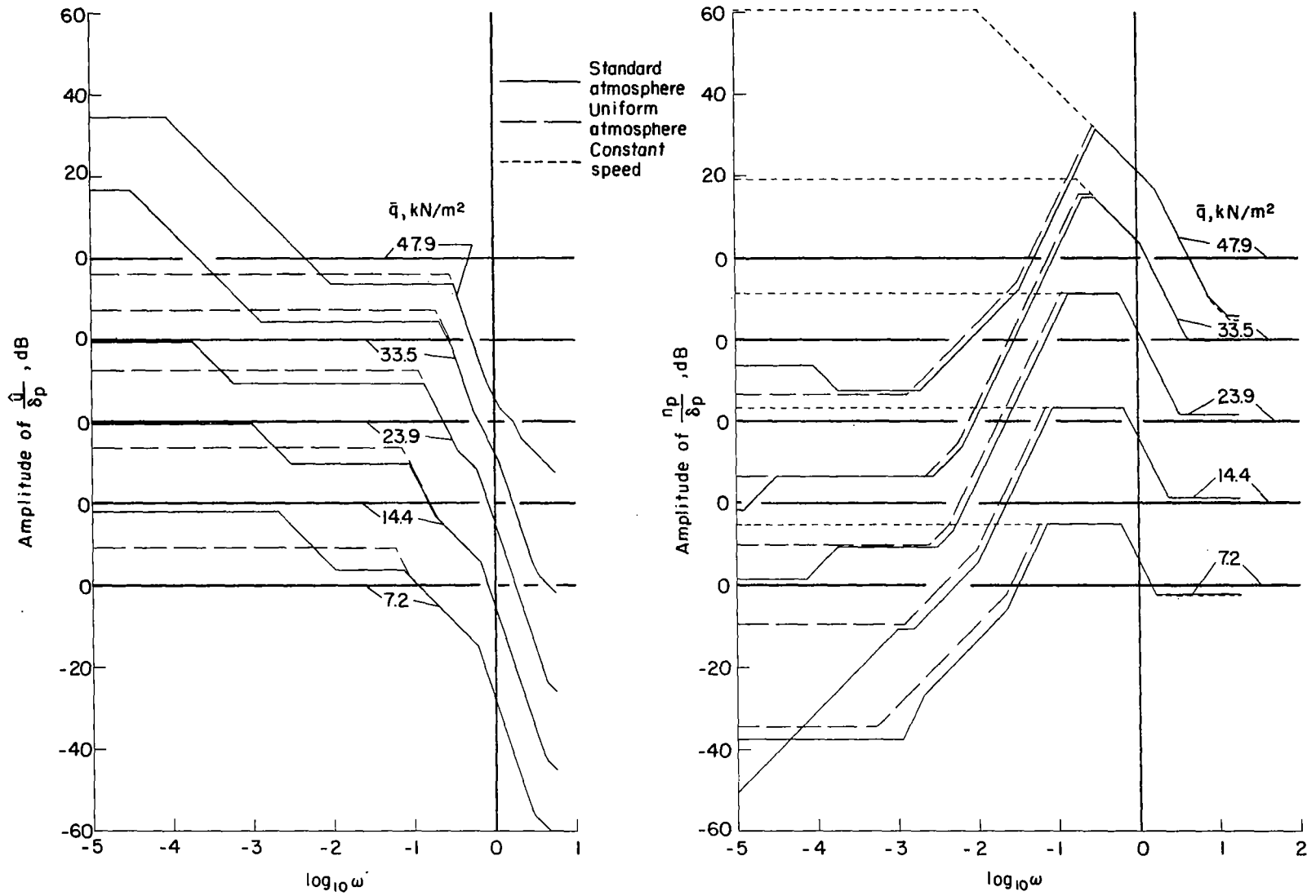
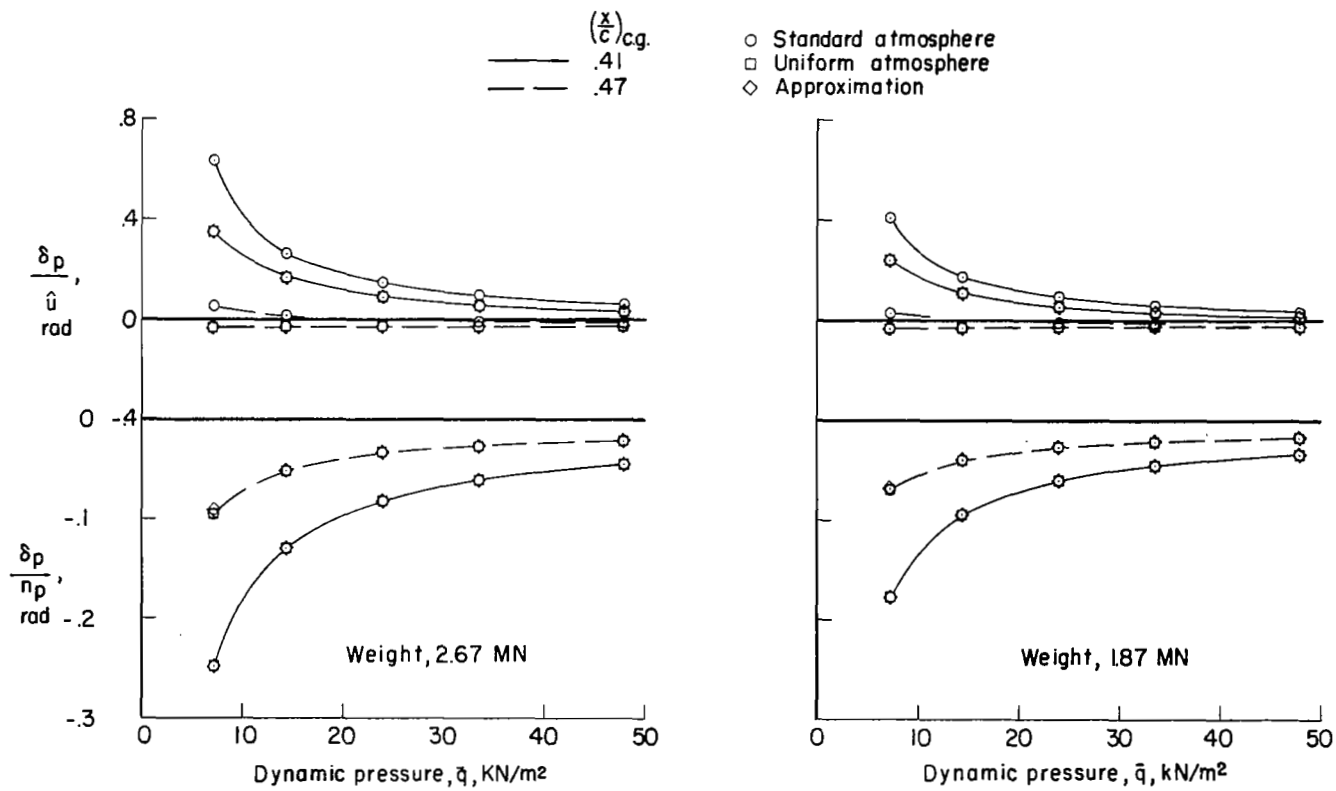
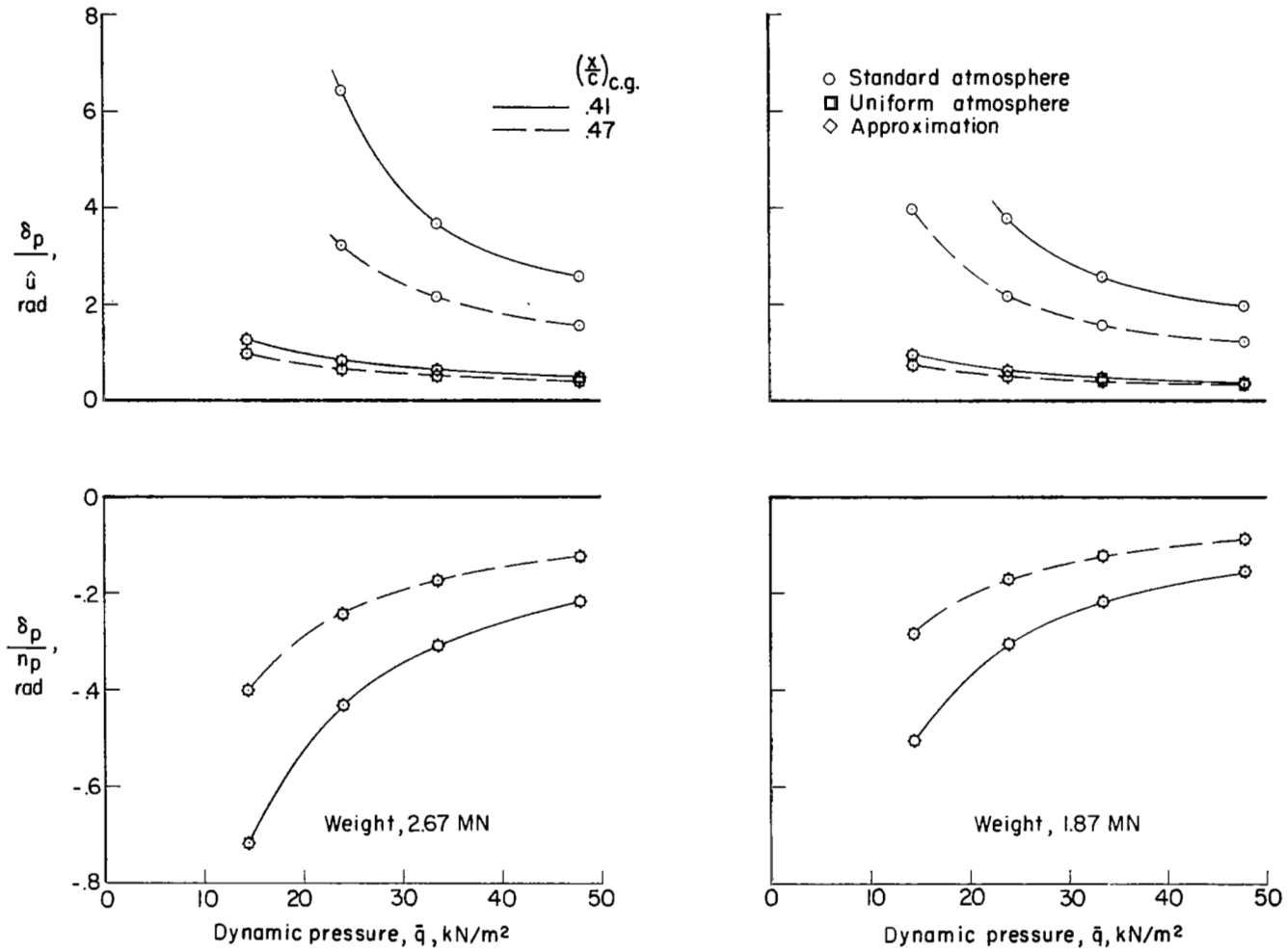


Figure 12.- Bode plots of frequency response amplitude of \hat{u}/δ_p and n_p/δ_p . Elastic airplane; $M = 0.8$; c.g. at $0.41c$; weight, 2.67 MN.



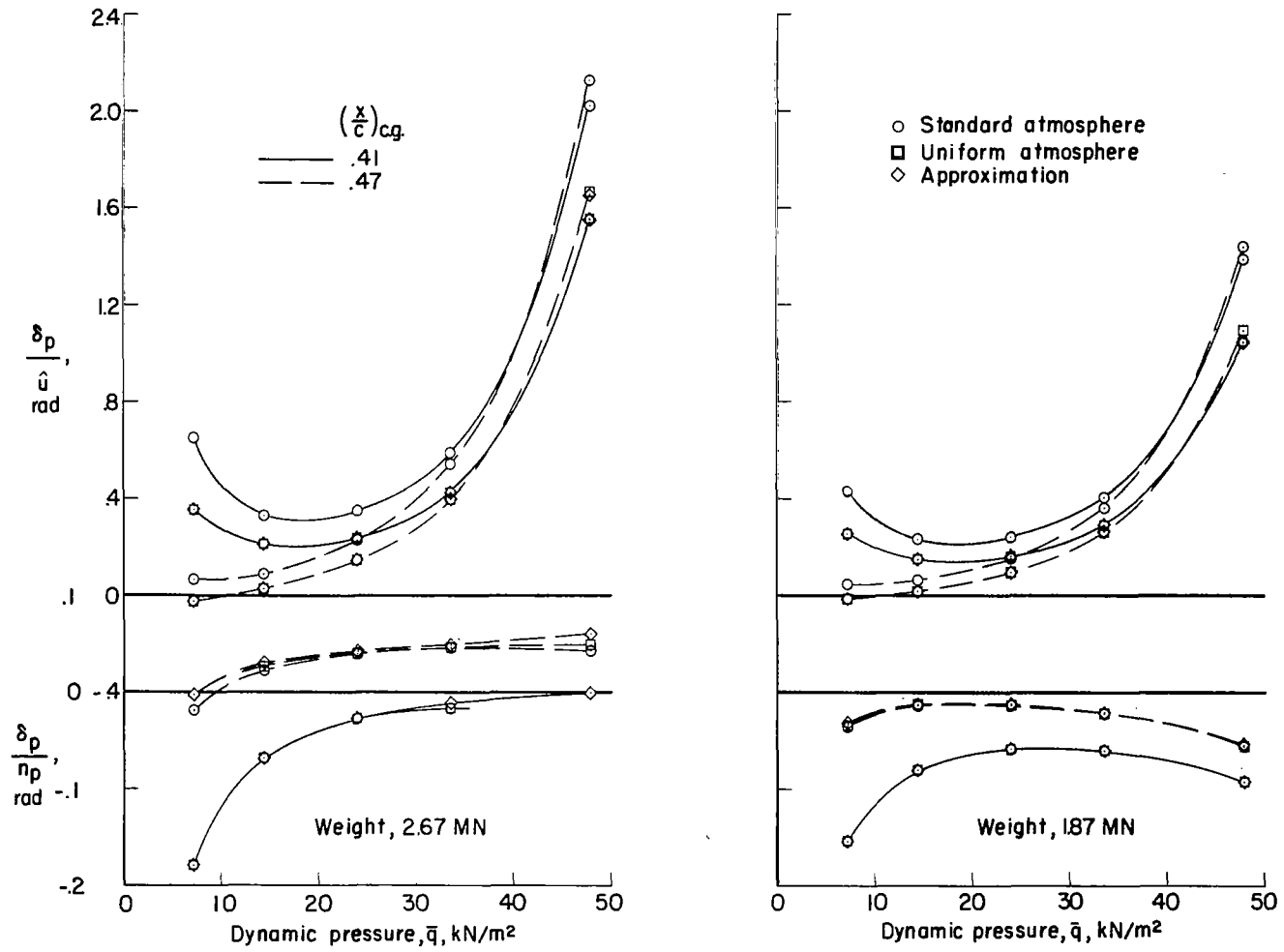
(a) $M = 0.8$.

Figure 13.- Variation of static control parameters with dynamic pressure. Rigid airplane.



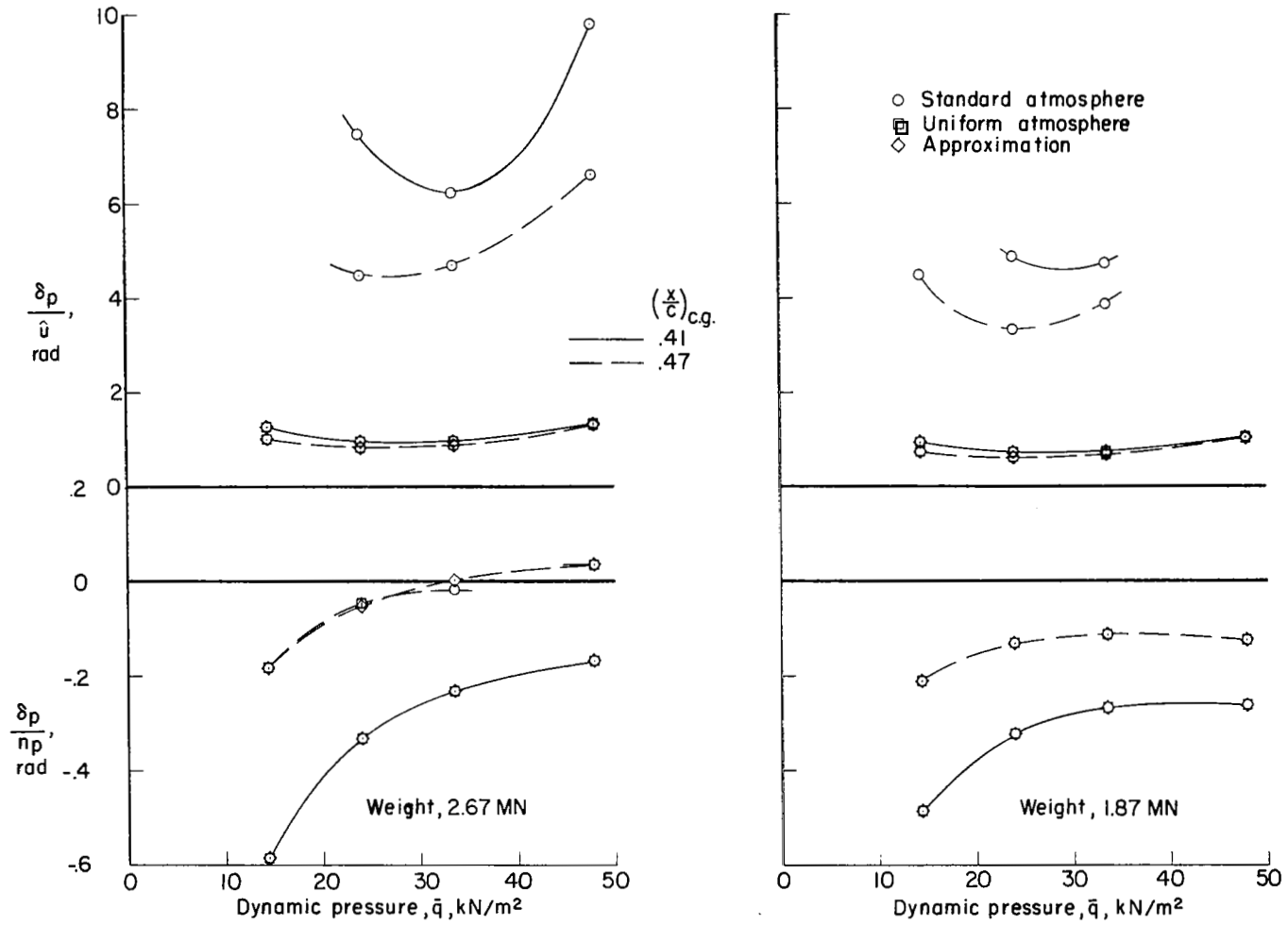
(b) $M = 2.7$.

Figure 13.- Concluded.



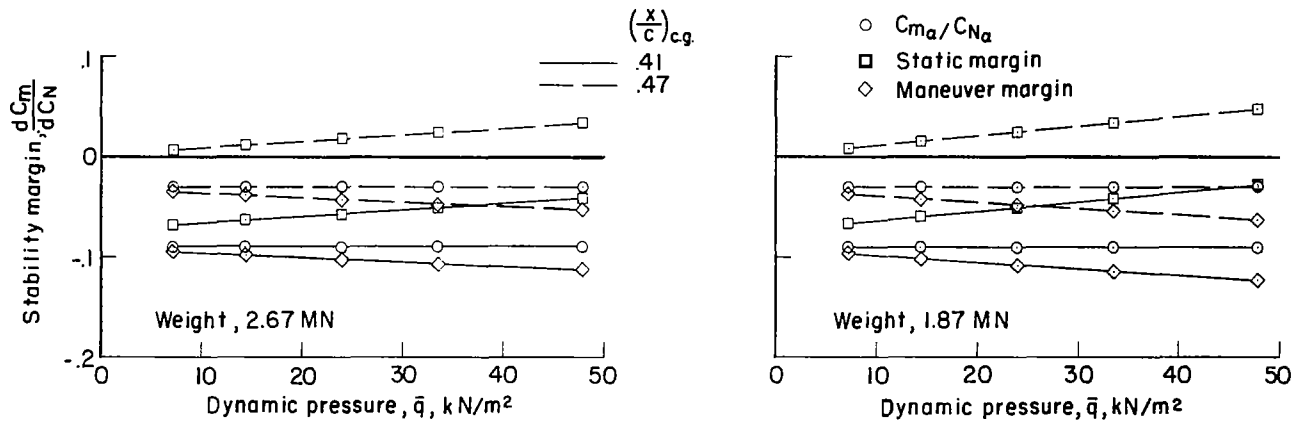
(a) $M = 0.8$.

Figure 14.- Variation of static control parameters with dynamic pressure. Elastic airplane.

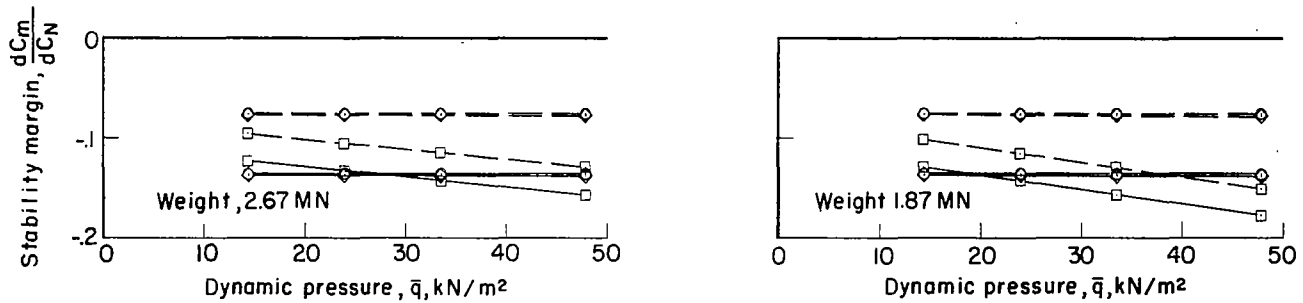


(b) $M = 2.7$.

Figure 14. - Concluded.



(a) $M = 0.8$.



(b) $M = 2.7$.

Figure 15.- Variation with dynamic pressure of approximations to static stability margins.
Rigid airplane; uniform atmosphere.

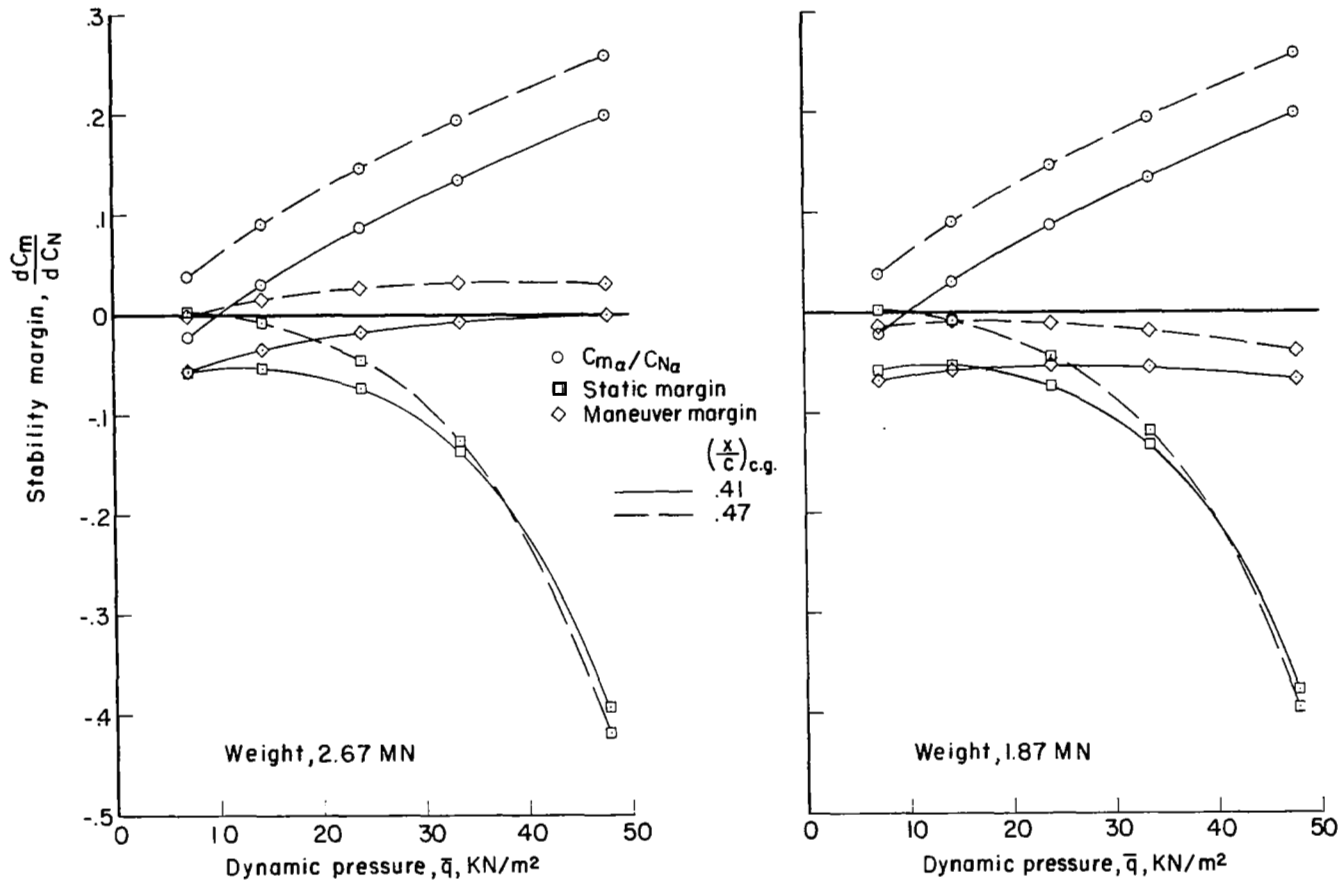
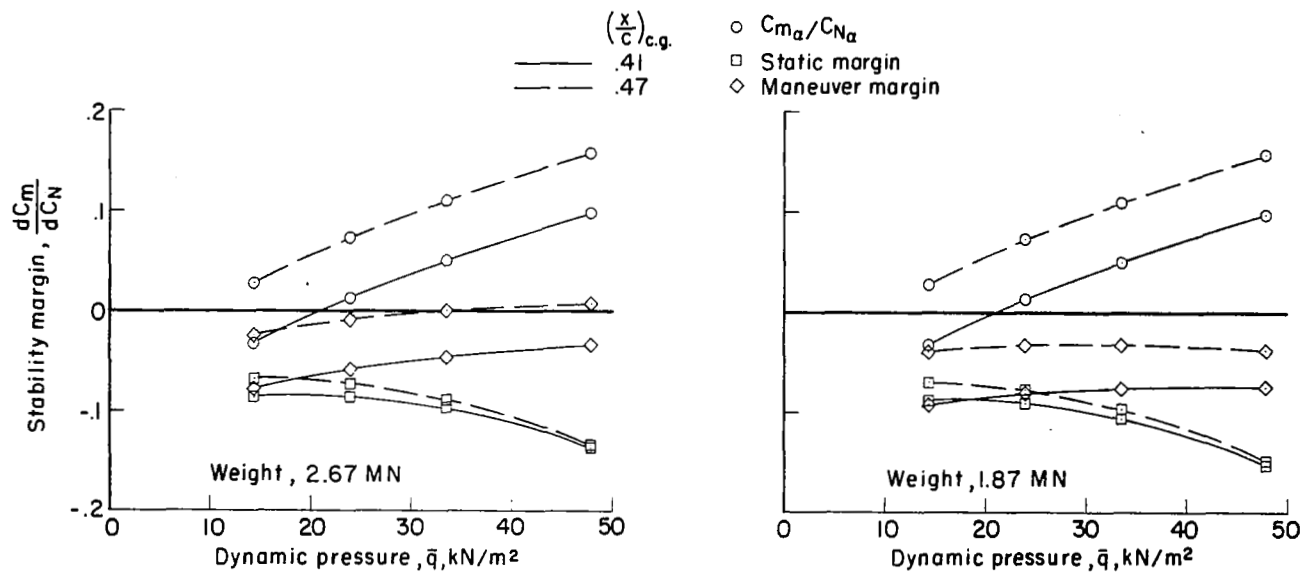
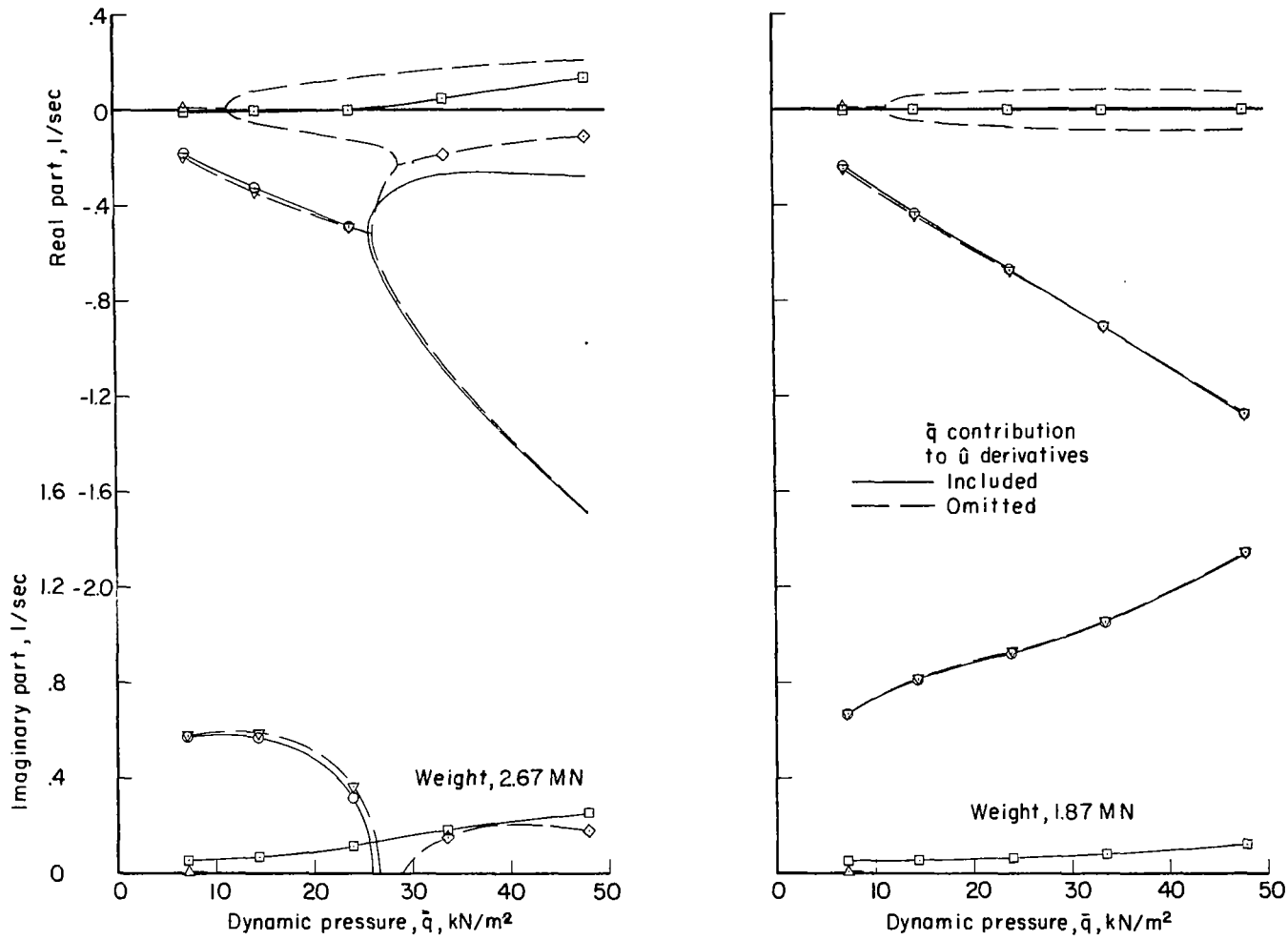
(a) $M = 0.8$.

Figure 16.- Variation with dynamic pressure of approximations to static stability margins.
 Elastic airplane; uniform atmosphere.



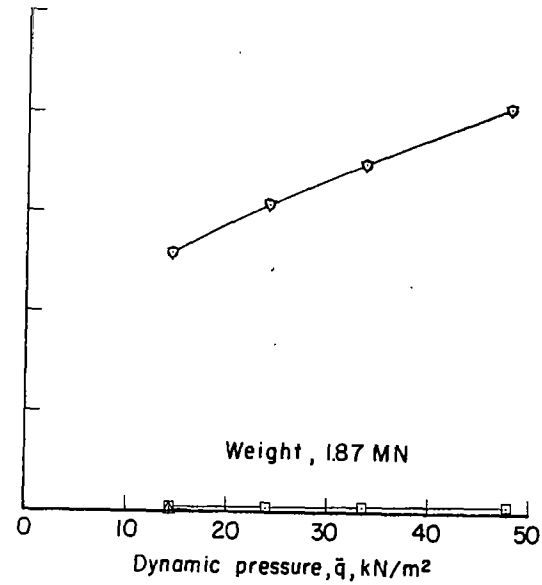
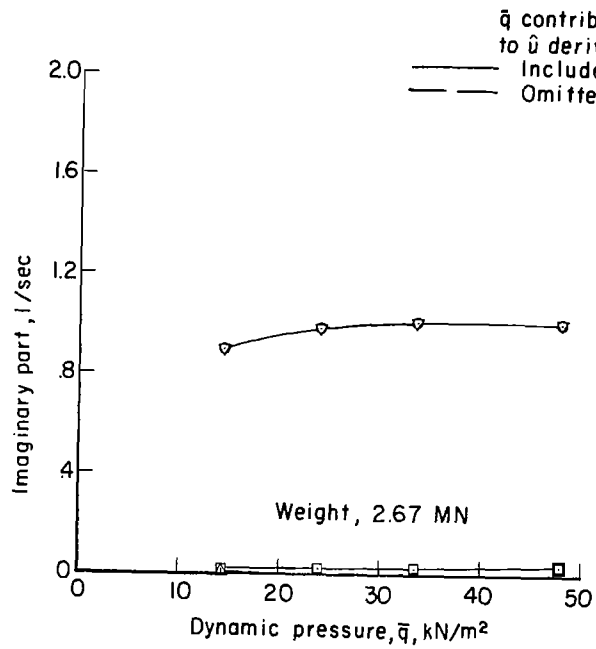
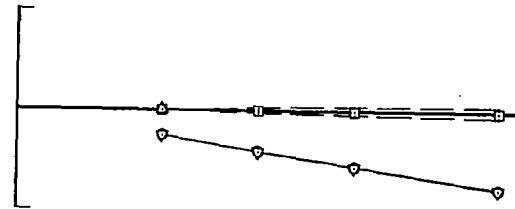
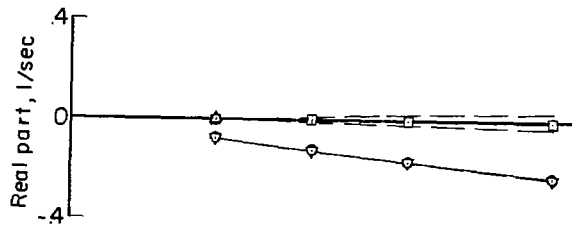
(b) $M = 2.7$.

Figure 16. - Concluded.



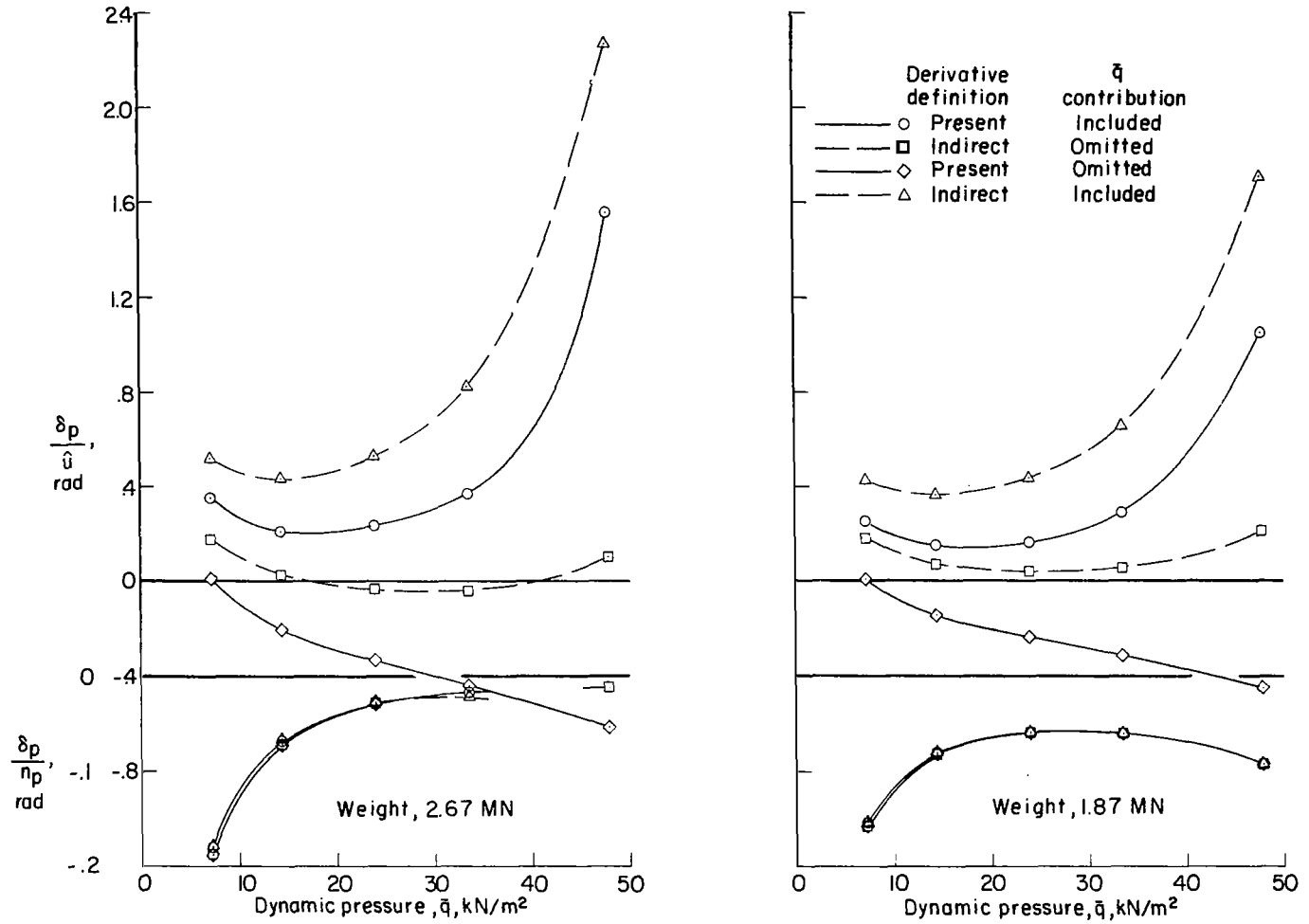
(a) $M = 0.8$.

Figure 17.- Effect of dynamic-pressure contribution to stability derivatives with respect to \hat{u} on characteristic roots. Elastic airplane; c.g. at 0.41c; uniform atmosphere.



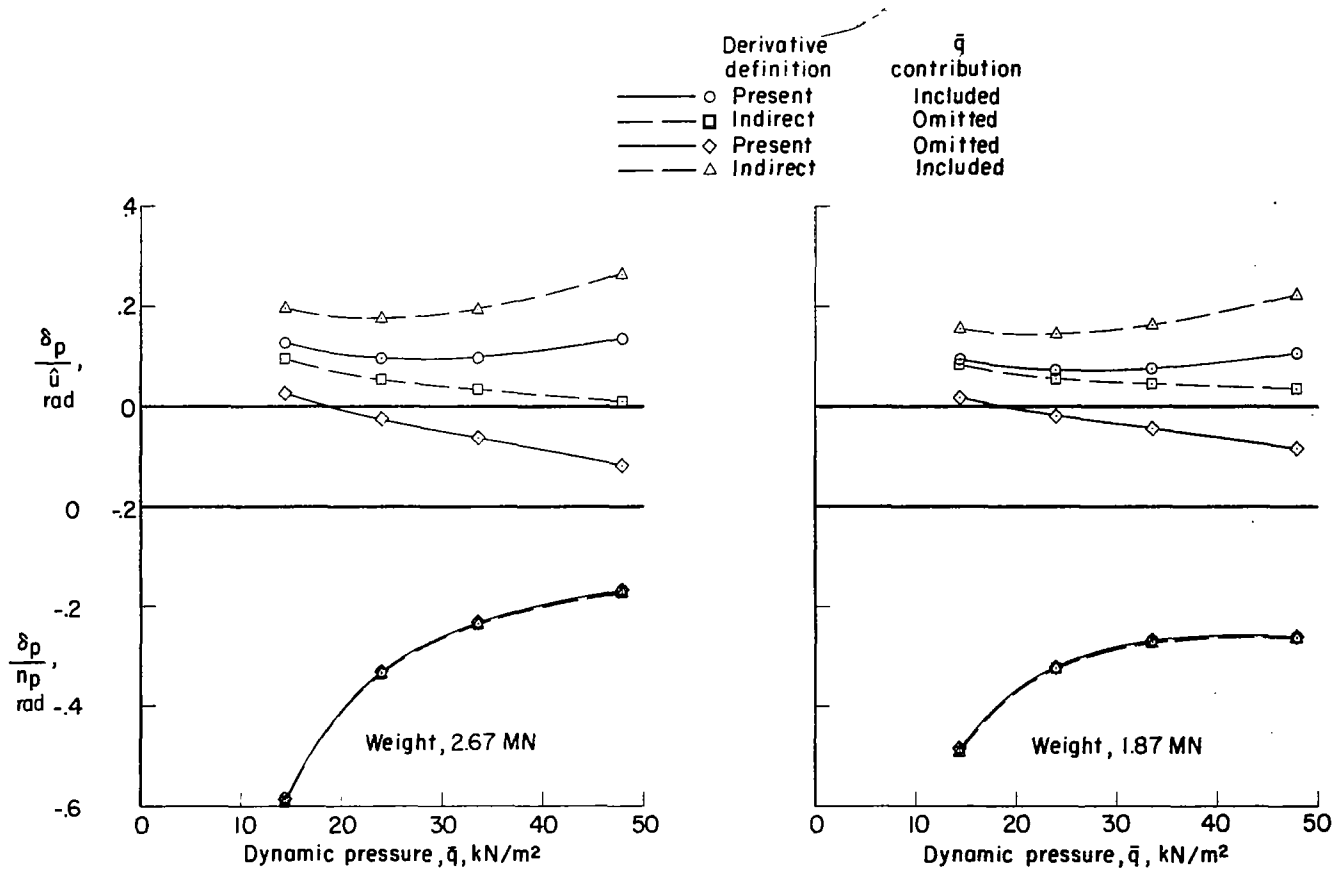
(b) $M = 2.7$.

Figure 17.- Concluded.



(a) $M = 0.8$.

Figure 18.- Effect of dynamic-pressure contribution to stability derivatives with respect to \hat{u} on static control parameters as calculated by using the present formulation and an indirect formulation. Elastic airplane; c.g. at 0.41c; uniform atmosphere.



(b) $M = 2.7$.

Figure 18.- Concluded.

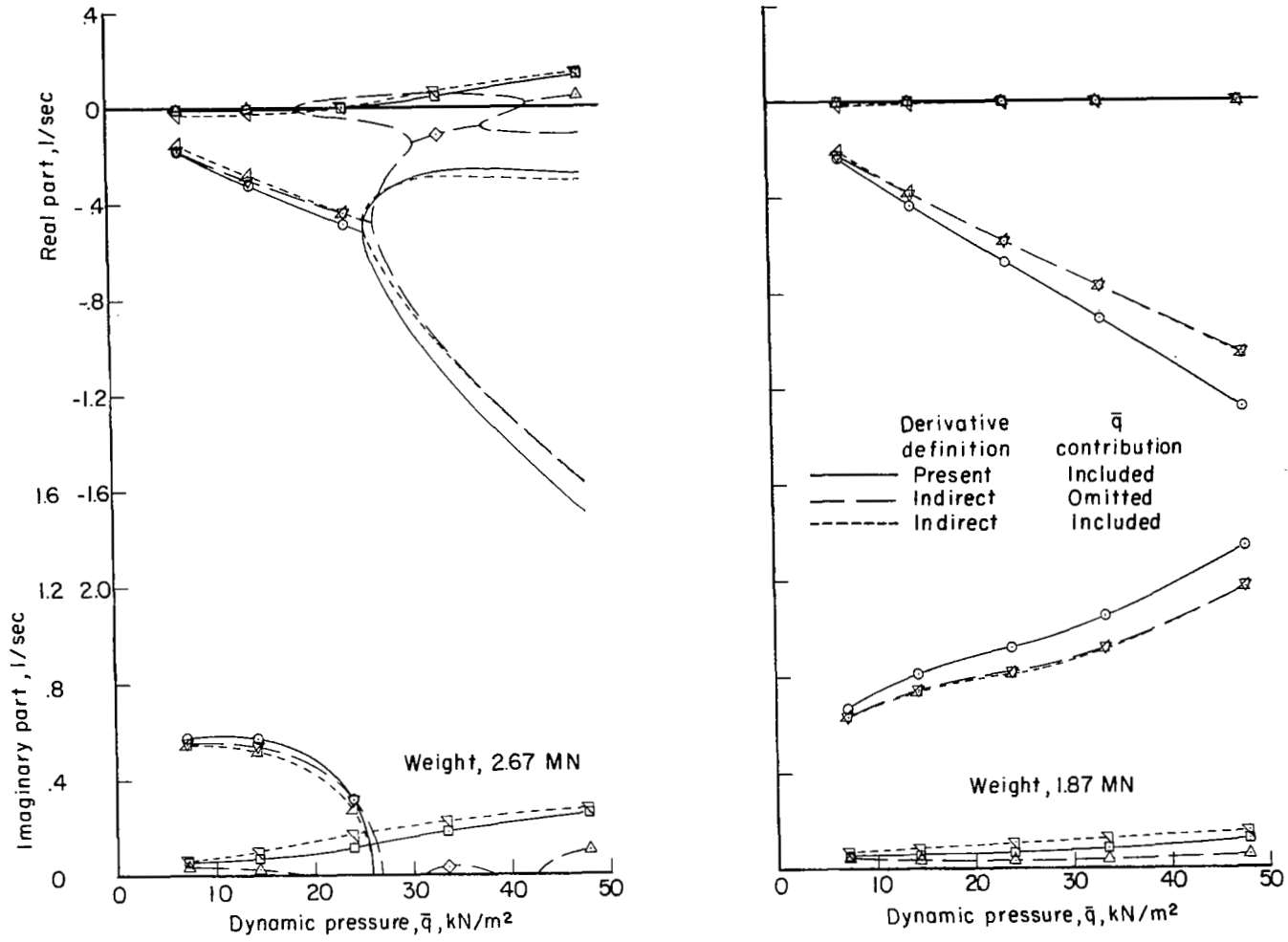
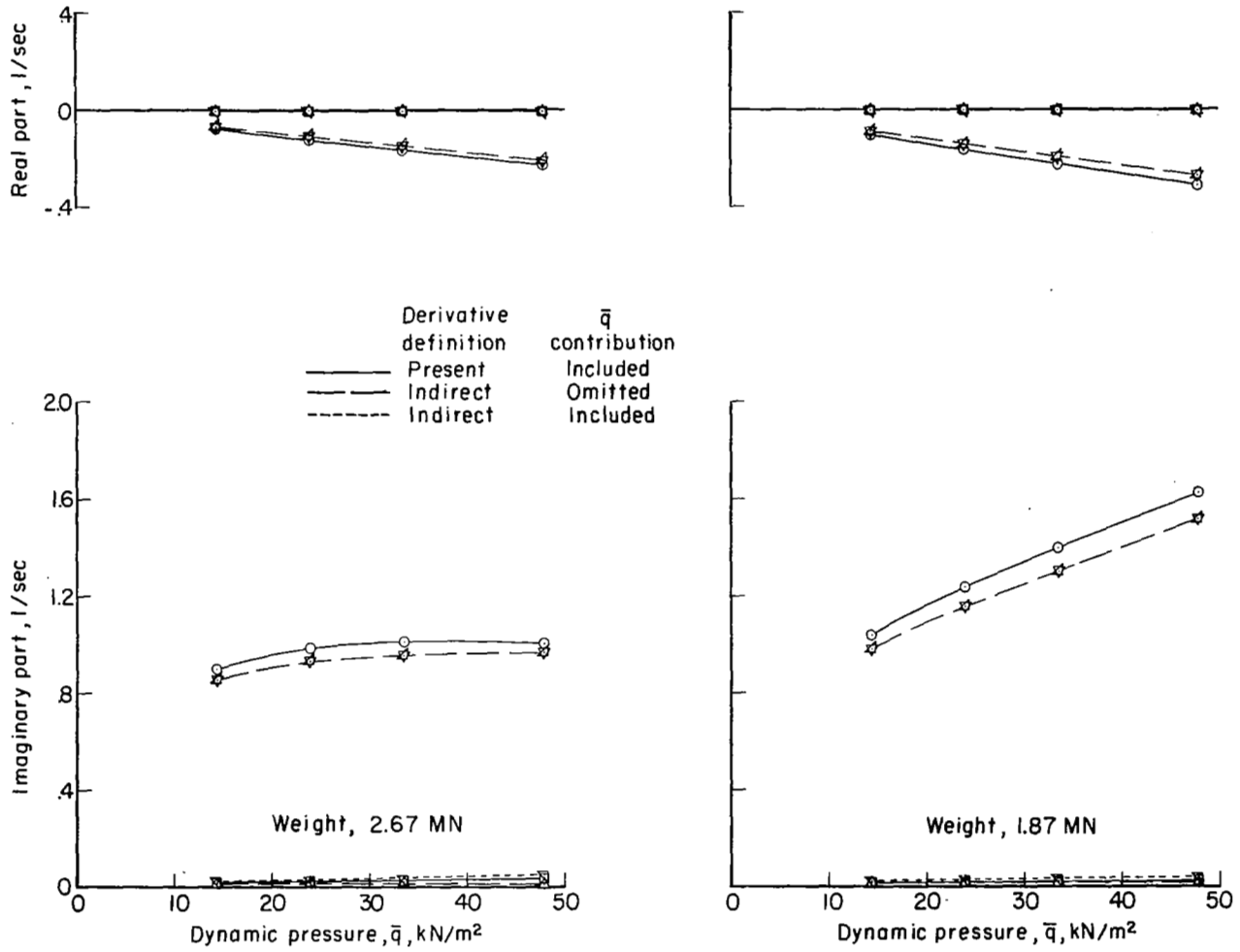
(a) $M = 0.8$.

Figure 19.- Comparison of the characteristic roots calculated by using the present formulation with those calculated by using an indirect formulation. Elastic airplane; c.g. at $0.41c$; uniform atmosphere.



(b) $M = 2.7$.

Figure 19. - Concluded.